

การศึกษากระบวนการดูซึมระหว่างเฟสก๊าซและของเหลวด้านพลศาสตร์ของฟองอากาศ-เฟสของ
ไหล และตัวแปรด้านการถ่ายเทมวลสาร: ด้านของเหลว และ ก๊าซ



บทคัดย่อและแฟ้มข้อมูลฉบับเต็มของวิทยานิพนธ์ตั้งแต่ปีการศึกษา 2554 ที่ให้บริการในคลังปัญญาจุฬาฯ (CUIR)
เป็นแฟ้มข้อมูลของนิสิตเจ้าของวิทยานิพนธ์ ที่ส่งผ่านทางบัณฑิตวิทยาลัย

The abstract and full text of theses from the academic year 2011 in Chulalongkorn University Intellectual Repository (CUIR)
are the thesis authors' files submitted through the University Graduate School.

วิทยานิพนธ์นี้เป็นส่วนหนึ่งของการศึกษาตามหลักสูตรปริญญาวิศวกรรมศาสตรดุษฎีบัณฑิต
สาขาวิชาวิศวกรรมสิ่งแวดล้อม ภาควิชาวิศวกรรมสิ่งแวดล้อม
คณะวิศวกรรมศาสตร์ จุฬาลงกรณ์มหาวิทยาลัย
ปีการศึกษา 2560
ลิขสิทธิ์ของจุฬาลงกรณ์มหาวิทยาลัย

STUDY OF GAS-LIQUID ABSORPTION IN TERMS OF BUBBLE-
FLUID HYDRODYNAMIC AND MASS TRANSFER PARAMETER: LIQUID PHASE AND
GAS PHASE



A Dissertation Submitted in Partial Fulfillment of the Requirements
for the Degree of Doctor of Philosophy Program in Environmental Engineering

Department of Environmental Engineering

Faculty of Engineering

Chulalongkorn University

Academic Year 2017

Copyright of Chulalongkorn University

ประจักษ์ ศาสตร์เวช : การศึกษากระบวนการดูดซึมระหว่างเฟสก๊าซและของเหลวด้านพลศาสตร์ของฟองอากาศ-เฟสของไหล และตัวแปรด้านการถ่ายเทมวลสาร: ด้านของเหลวและ ก๊าซ (STUDY OF GAS-LIQUID ABSORPTION IN TERMS OF BUBBLE-FLUID HYDRODYNAMIC AND MASS TRANSFER PARAMETER: LIQUID PHASE AND GAS PHASE) อ.ที่ปรึกษาวิทยานิพนธ์หลัก: รศ. ดร.พิสุทธิ์ เพ็ชรมนกุล, 148 หน้า.

งานวิจัยนี้ศึกษาผลกระทบในการเดินระบบแบบ Batch system และการเดินระบบแบบ Continuous system ในถังปฏิกรณ์แบบอากาศยก ต่อตัวแปรทางด้านอุทกพลศาสตร์ (Q_g , Q_L , D_{Bd} , U_{Bd} และ a) และตัวแปรทางด้านถ่ายเทมวลสาร (k_L and k_{La}) การทดลองออกแบบโดยใช้ถังปฏิกรณ์แบบอากาศยกทำด้วยพลาสติกอะคริลิก ขนาดเส้นผ่านศูนย์กลาง 0.15 เมตร สูง 1 เมตร ซึ่งด้านในของถังปฏิกรณ์แบบอากาศยกใส่แผ่นพลาสติกอะคริลิกเพื่อควบคุมทำให้เกิดการไหลวนกลับของอากาศและของเหลวในระบบ สำหรับการตรวจวัดตัวแปรด้านการถ่ายเทมวลสาร ใช้วิธีการลดปริมาณออกซิเจนด้วย sodium sulphite (Na_2SO_3) จากนั้นทำการเติมอากาศทำการการวัดค่าการเปลี่ยนแปลงออกซิเจนที่เกิดขึ้น สำหรับการตรวจวัดตัวแปรทางด้านอุทกพลศาสตร์ ทำได้โดยใช้วิธีการถ่ายภาพด้วยกล้องถ่ายภาพความเร็วสูง ที่ความเร็ว 100 ต่อวินาที จากนั้นทำการวิเคราะห์ภาพถ่ายด้วยโปรแกรม ImageJ เพื่อคำนวณหาความสัมพันธ์ของตัวแปรด้านอุทกพลศาสตร์ สำหรับตัวแปรที่ทำการศึกษาร่วมกับถังปฏิกรณ์แบบอากาศยก ได้แก่ รูปร่างและปริมาณของพลาสติกตัวกลาง 2% 5% 10% และ 15% (v/v) โดยปริมาตร อัตราเติมอากาศที่ 2.5 ถึง 15.0 ลิตรต่อนาทีและอัตราการไหลน้ำ 0 ถึง 10 ลิตรต่อนาที สำหรับการทดลองแบบ Batch system และแบบ Continuous system ตามลำดับ จากผลการทดลองพบว่าค่า k_{La} เพิ่มสูงขึ้นสอดคล้องกับการเพิ่มปริมาณของพลาสติกตัวกลางจาก 2% ถึง 15% (v/v) และอัตราการเติมอากาศ 2.5 ถึง 15 ลิตรต่อนาที โดยที่ค่า k_{La} สูงสุด (1.1×10^{-2} ถึง $3.23 \times 10^{-2} s^{-1}$) ที่ปริมาณ 10% ของตัวกลางรูปร่างวงแหวน นอกจากนี้ขนาดของฟองอากาศในระบบเพิ่มขึ้นอยู่ในช่วง 2.55 ถึง 3.97 มิลลิเมตร และค่าพื้นที่ผิวสัมผัสจำเพาะเพิ่มขึ้นอยู่ในช่วง 0 - 547.87 m^{-1} โดยที่การเพิ่มขึ้นของขนาดฟองอากาศ และค่าพื้นที่ผิวสัมผัสจำเพาะมีการความสอดคล้องกับการเพิ่มขึ้นของอัตราการไหลของอากาศจาก 2.5 ถึง 15 ลิตรต่อนาที

ภาควิชา วิศวกรรมสิ่งแวดล้อม

ลายมือชื่อนิสิต

สาขาวิชา วิศวกรรมสิ่งแวดล้อม

ลายมือชื่อ อ.ที่ปรึกษาหลัก

ปีการศึกษา 2560

5571412421 : MAJOR ENVIRONMENTAL ENGINEERING

KEYWORDS: BUBBLE COLUMN, BUBBLE HYDRODYNAMIC PARAMETERS, MASS TRANSFER PARAMETERS, INTERNAL LOOP AIRLIFT REACTOR

PRAJAK SASTARAVET: STUDY OF GAS-LIQUID ABSORPTION IN TERMS OF BUBBLE-FLUID HYDRODYNAMIC AND MASS TRANSFER PARAMETER: LIQUID PHASE AND GAS PHASE. ADVISOR: ASSOC. PROF. PISUT PAINMANAKUL, Ph.D., 148 pp.

This research focus on study the effect of continuous system on the bubble hydrodynamic and mass transfer parameters (Q_g , Q_L , D_{Bd} , U_{Bd} , a , k_L and $k_L a$). The experiment were set up in a cylindrical acrylic column with 0.15 m inside diameter and 1 m in height. ILALR was setup an acrylic plate for liquid recirculation. Moreover, mass transfer determination, liquid phase was removed dissolved oxygen by using sodium sulphite (Na_2SO_3). The bubble hydrodynamic mechanisms are investigated by the high speed camera (100 images/sec) and image analysis program is used to determine the bubble hydrodynamic parameters. The bubbles are generated by rigid diffuser which located at the bottom of column. Plastic media were added into the bubble column at 2% 5% 10% and 15% (v/v), air flow rate from 2.5 to 15.0 l/min and liquid flow rate from 0-10 l/min. the result showed mass transfer ($k_L a$) relate to increase the concertation from 2% to 15% (v/v) and gas flow 2.5 to 15 l/min, at media concentration 10% (v/v) has the highest $k_L a$ value (1.1×10^{-2} to $3.23 \times 10^{-2} \text{ s}^{-1}$). The bubble diameter (D_b) increase from 2.55 to 3.97 mm with increase gas flow rate from 2.5 to 15 l/min. The bubble velocity (U_b) slightly decrease from 0.094 to 0.015 m/s with increase liquid flow rate from 0 - 10 l/min and Interfacial area (a) increase 0 - 547.87 m^{-1} with gas flow rate increase from 2.5 - 15 l/min.

Department: Environmental
Engineering

Student's Signature

Advisor's Signature

Field of Study: Environmental
Engineering

Academic Year: 2017

ACKNOWLEDGEMENTS

I wish to express my profound gratitude and sincerest appreciation to my advisor Assoc. Prof. Dr. Pisut Painmanakul for his precious guidance, shape advice,

helpful suggestions, and continuous encouragement throughout this research. He gave me the useful knowledge and systematic thinking for the environmental

application and management. He has always taught several important points to gain he completion to work without is creative ideas and devotion, this study would not been successful.

This research was financially supported by Environmental Engineering, Chulalongkorn University. Without this scholarships, this research would not been achieved. I would like to thank laboratory staffs and students in Environmental Engineering, Chulalongkorn University for their support, kindness, and friendship which give me relax and familiar workplace surrounding. Finally, deepest and most sincere appreciation is extended to my parents for their support and encouragement.



จุฬาลงกรณ์มหาวิทยาลัย
CHULALONGKORN UNIVERSITY

CONTENTS

	Page
THAI ABSTRACT	iv
ENGLISH ABSTRACT	v
ACKNOWLEDGEMENTS	vi
CONTENTS	vii
List of Table	1
List of Figure	1
CHAPTER 1 INTRODUCTION	7
1.1 Introduction	7
1.2 Objectives	8
1.3 Scope of Research	8
CHAPTER 2 EFFECTS OF FIXABLE AND RIGID DIFFUSED AERATOR ON OXYGEN TRANSFER EFFICIENCY AND BUBBLE HYDRODYNAMIC PARAMETERS	10
2.1 Introduction	10
2.2 Objectives	11
2.3 Literature Review	11
2.4 Materials and Methods	12
2.4.1 Experimental set-up	12
2.4.2 Analytical methods	15
2.5 Results and Discussion	19
2.5.1 Characterization of the membrane with a single orifice	19
2.5.2 Characterization of the bubble provided by a single orifice	22
2.5.3 Performances of the two membranes	25
2.6 Conclusions	30

CHAPTER 3 COMPARATIVE STUDY OF MASS TRANSFER AND BUBBLE HYDRODYNAMIC PARAMETERS IN BUBBLE COLUMN REACTOR: PHYSICAL CONFIGURATIONS AND OPERATING CONDITIONS.....	32
3.1 Introduction	32
3.2 Objectives.....	33
3.3 Literature Review	33
3.4 Materials and Methods.....	34
3.4.1. Experimental Setup.....	34
3.4.2. Gas Diffusers Used in This Study	35
3.4.3. Determination of Bubble Hydrodynamic Parameters	37
3.4.4. Determination of Mass Transfer Coefficients	37
3.5 Results and Discussion.....	39
3.5.1. Volumetric Mass Transfer Coefficient ($k_L a$).....	39
3.5.2. Bubble Diameter (D_B)	42
3.5.3 Interfacial Area (a).....	44
3.5.4 Liquid-side Mass Transfer Coefficient (k_L)	47
3.6 Conclusions.....	51
CHAPTER 4 STUDY OF ABSORPTION PROCESS IN BUBBLE COLUMN REACTOR (BC): MASS TRANSFER AND HYDRODYNAMIC	53
4.1 Introduction.....	53
4.2 Objective.....	54
4.3 Literature Review.....	54
4.4 Materials and Methods.....	56
4.4.1 Experimental Setup.....	56

	Page
4.4.2. Method for determining the mass transfer and bubble hydrodynamic parameter.....	57
4.5 Results and Discussion	61
4.5.1 Effect of plastic media on overall mass transfer coefficient in BC.	61
4.5.2 Effect of plastic media on bubble hydrodynamic parameter in BC.	66
4.6 Conclusions	82
CHAPTER 5 STUDY OF ABSORPTION PROCESS IN INTERNAL LOOP AIRLIFT REACTOR (ILALR): MASS TRANSFER AND HYDRODYNAMIC.....	
5.1 Introduction	84
5.2 Objectives.....	85
5.3 Literature Review.....	85
5.4 Materials and Methods.....	86
5.4.1 Experimental Setup.....	86
5.4.2. Method for determining the mass transfer and bubble hydrodynamic parameter.....	88
5.5 Results and Discussion.....	91
5.5.1 Study the oxygen mass transfer and bubble hydrodynamic parameters in ILALR.	91
5.5.2. Effect of plastic media on oxygen mass transfer and bubble hydrodynamic parameters in ILALR.....	95
5.5.3 Comparison the effect of best plastic media condition on mass transfer and bubble hydrodynamic parameters in BC and ILALR.	106
5.6 Conclusions	109
CHAPTER 6 STUDY THE EFFECT OF CONTINUOUS SYSTEM ON BUBBLE HYDRODYNAMIC AND VOCS MASS TRANSFER PARAMETER IN ILALR.....	
	110

	Page
6.1 Introduction	110
6.2 Objectives.....	110
6.3 Literature Review	111
6.4 Materials and Method.....	112
6.4.1 Experimental setup.....	112
6.4.2 Experimental procedure	116
6.5 Results and Discussion	118
6.5.1 Study the oxygen mass transfer and bubble hydrodynamic parameters in continuous ILALR.....	118
6.5.2 Application for benzene gas absorption.....	121
6.6 Conclusions	129
CHAPTER 7 CONCLUDESIONS AND RECOMMENDATION.....	130
7.1 Conclusions	130
7.2 Overall suitable operation condition and prediction model.....	131
7.3 Recommendations for future work.....	133
NOTATION	134
REFERENCES	140
APPENDIX.....	141
Appendix A.....	142
VITA.....	148

List of Table

Table 1 parameters were studied in this experiment.....	15
Table 2 physical Characteristic of Diffuser and Operating Conditions.....	36
Table 3 Variable of studying effect of bubble column dimension on mass transfer and Bubble hydrodynamic parameters in BC.....	39
Table 4 Prediction Model for Liquid-Side Mass Transfer Coefficient (k_L).....	49
Table 5 Plastic media characteristics	56
Table 6 Variable for oxygen mass transfer and bubble hydrodynamic parameters in BC.	60
Table 7 Variable for study the effect of plastic media in BC.....	61
Table 8 Plastic media characteristics	87
Table 9 Variable for oxygen mass transfer and bubble hydrodynamic parameters ILALR.....	90
Table 10 Variable for study the effect of plastic media in ILALR.....	91
Table 11 the relation between Q_g , ϵ_g , D_{Br} , D_{Bd} , U_{Br} and U_{Bd} in ILALR at 10% concentration.	102
Table 12 Characteristics of surfactant and water.	114
Table 13 the conditions of GC parameters.....	115
Table 14 Variable of study the effect of co- current operation in ILALR.	117
Table 15 variable of study the effect of co- current operation on simulated VOCs absorption.	118
Table 16 summary of $K_L a$ values for benzene absorption	125
Table 17 Table the overall suitable operation condition obtained in this experiment.....	132

List of Figure

Figure 1 Flow chart of the research.....	9
Figure 2 the experiment set up.....	13
Figure 3 a and b for rigid diffuser and fixable diffuser respectively.....	14
Figure 4 Methods of study the effect of diffuser (rigid and fixable diffuser) on overall mass transfer coefficient and bubble hydrodynamic parameter in BC.....	15
Figure 5 Force balance of force during bubble formation at a flexible nozzle.	16
Figure 6 Equivalent hole diameter versus applied pressure for the rubber membranes diffuser with a single orifice.....	20
Figure 7 Different pressure versus applied pressure for the rubber membrane diffusers (a) and rigid diffusers (b) with a single orifice	21
Figure 8 Relation of deflection versus applied pressure for rubber membrane diffuse.	22
Figure 9 the shape of a spherical cab.....	22
Figure 10 Bubble diameter versus applied pressure for the rubber membrane diffusers (a) and rigid diffusers (b) with a single orifice.....	24
Figure 11 Bubble frequency versus applied pressure for the rubber membrane diffusers (a) and rigid diffusers (b) with a single orifice.	25
Figure 12 Interfacial area versus applied pressure for the rubber membrane diffusers (a) and rigid diffusers (b) with a single orifice	26
Figure 13 Power consumption versus applied pressure for the rubber membrane diffusers (a) and rigid diffusers (b) with a single orifice	28
Figure 14 Volumetric mass transfer coefficient versus applied pressure for the rubber membrane diffusers (a) and rigid diffusers (b) with a single orifice.	29

Figure 15 Liquid-side mass transfer coefficient versus applied pressure for the rubber membrane diffusers (a) and rigid diffusers (b) with a single orifice.	30
Figure 16 Schematic diagram of the experimental setup.	35
Figure 17 Installation of flexible orifice in bubble column - Fixable (F1).....	35
Figure 18 different types of gas diffusers used in this study.	36
Figure 19 diagram of studying effect of bubble column dimension on mass transfer and Bubble hydrodynamic parameters in BC.....	38
Figure 20 volumetric mass transfer coefficients ($k_L a$) vs. superficial gas velocity (V_g) in (a) small bubble column, (b) medium bubble column, (c) large bubble column, and (d) summary.	41
Figure 21 (a) Bubble diameter (D_B) vs. superficial gas velocity (V_g) for small bubble column, (b) example of orifice size obtained with flexible diffuser with single orifice (F1) at different superficial gas velocities.	43
Figure 22 Bubble diameter (D_B) vs. superficial gas velocity (V_g) for (a) medium bubble column and (b) large bubble column.	44
Figure 23 Bubble velocity (U_B) vs. bubble diameter (D_B).	45
Figure 24 Interfacial area (a) vs. superficial gas velocity (V_g) for (b) small bubble column, (c) medium bubble column, and (d) large bubble column.....	47
Figure 25 Liquid-side mass transfer coefficient (k_L) vs. superficial gas velocity (V_g).....	48
Figure 26 Liquid-side mass transfer coefficient (k_L) vs. bubble diameter (D_B).	48
Figure 27 the experiment set up.....	57
Figure 28 Shape of plastic media (a)Ring, (b)Circle, (c)Rod and (d)Square.	57
Figure 29 Diagram of study oxygen mass transfer and bubble hydrodynamic parameters in BC.	59
Figure 30 Diagram of study the effect of plastic media in BC.....	60

Figure 31 presents the variation of overall mass transfer coefficient with gas flow rates obtained with three types of diffuser without plastic media.	61
Figure 32 overall mass transfer coefficient versus gas flow rate in BC, shape of plastic media and plastic media concentration 2% 5% and 10% v/v with small rigid diffuser respectively.	63
Figure 33 overall mass transfer coefficient versus gas flow rate in BC, shape of plastic media and plastic media concentration 2% 5% and 10% v/v with large rigid diffuser respectively.	64
Figure 34 overall mass transfer coefficient versus gas flow rate in BC, shape of plastic media and plastic media concentration 2% 5% and 10% v/v with wood diffuser respectively.	65
Figure 35 presents the variation of bubble diameter with gas flow rates obtained	67
Figure 36 bubble formation photographs in BC at gas velocity :(a) 2.6×10^{-3} m/s, (b) 1.0×10^{-2} m/s, and (c) 1.5×10^{-2} m/s of small rigid diffuser.	67
Figure 37 bubble diameter versus gas velocity in BC, shape of plastic media and plastic media concentration 2% 5% and 10% v/v with small rigid diffuser respectively.	68
Figure 38 bubble diameter versus gas velocity in BC, shape of plastic media and plastic media concentration 2% 5% and 10% v/v with large rigid diffuser respectively.	69
Figure 39 bubble diameter versus gas velocity in BC, shape of plastic media and plastic media concentration 2% 5% and 10% v/v with wood diffuser respectively.	70
Figure 40 the Bubble attach with Plastic media and brake down in the system.	71
Figure 41 bubble in BC without plastic media and bubble in BC with plastic media.	71
Figure 42 the bubble attachment and bubble abstraction with plastic media in BC.	72

Figure 43 the variation of terminal rising bubble velocity with gas velocity obtained with three types of diffuser without plastic media.	73
Figure 44 terminal rising bubble velocity versus gas velocity in BC., shape of plastic media and plastic media concentration 2% 5% and 10% v/v with small rigid diffuser respectively.	74
Figure 45 terminal rising bubble velocity versus gas velocity in BC., shape of plastic media and plastic media concentration 2% 5% and 10% v/v with large rigid diffuser respectively.	75
Figure 46 terminal rising bubble velocity versus gas flow rate in BC., shape of plastic media and plastic media concentration 2% 5% and 10% v/v with wood diffuser respectively.	76
Figure 47 the variation of interfacial area with gas flow rates obtained with three types of diffuser without plastic media.	78
Figure 48 Specific interfacial area versus gas velocity in BC, shape of plastic media and plastic media concentration 2% 5% and 10% v/v with small rigid diffuser respectively.	79
Figure 49 Specific interfacial area versus gas velocity in BC, shape of plastic media and plastic media concentration 2% 5% and 10% v/v with large rigid diffuser respectively.	80
Figure 50 Specific interfacial area versus gas velocity in BC, shape of plastic media and plastic media concentration 2% 5% and 10% v/v with wood diffuser respectively.	81
Figure 51 schematic diagram of the split-cylinder airlift reactor.	86
Figure 52 the experiment set up.	87
Figure 53 shape of plastic media (a)Ring, (b)Circle, (c)Rod and (d)Square.	87
Figure 54 Diagram of study oxygen mass transfer and bubble hydrodynamic parameters in ILALR.	89
Figure 55 diagram of study the effect of plastic media in ILALR.	90

Figure 56 overall mass transfer coefficient versus gas velocity in ILALR for different amount of ABS: (a) Riser zone, (b) Down-comer zone.....	91
Figure 57 Bubble diameter versus gas velocity in BC and ILALR.....	92
Figure 58 Bubble formation photographs in ILALR at gas flow rate: (a) 2.0×10^{-3} m/s, (b) 5×10^{-3} m/s, and (c) 1.5×10^{-2} m/s.....	93
Figure 59 Terminal rising bubble velocity versus gas velocity in ILALR.	93
Figure 60 Specific interfacial area versus gas flow rate in BC. and ILALR.	94
Figure 61 Overall mass transfer coefficient versus gas velocity for different amount and shape of plastic media: (a) circle, (b) Rod, (c) Square and (d) Ring respectively.....	96
Figure 62 Bubble formation photographs in ILALR (Riser zone) at gas velocity 1.5×10^{-2} m/s and 15% plastic media loading of ring shape: (a) Riser Zone and (b) Down comer Zone.	97
Figure 63 Bubble sizes versus gas velocity for different amount and shape of plastic media: (a) circle, (b) Rod, (c) Square and (d) Ring respectively.	98
Figure 64 bubble formation photographs in ILALR (Riser zone) at gas velocity 1.5×10^{-2} m/s for: (a) No plastic media and 15% loading of Rod (b), Circle (c) and (d) Ring shape respectively.....	99
Figure 65 Terminal rising bubble versus gas velocity for different amount and shape of plastic media: (a) circle, (b) Rod, (c) Square and (R) Ring respectively.	101
Figure 66 relation of Q_{gr} and air flow rate in ILALR.	103
Figure 67 specific interfacial area versus gas velocity for different amount and shape of plastic media: (a) Ring, (b) Circle, (c) Rod and (d) Ring respectively.	105
Figure 68 Comparison of experimental and predicted of k_L by using the different gas flow rates.....	106
Figure 69 overall mass transfer coefficient versus gas velocity in BC and ILALR.	107
Figure 70 Bubble diameter versus gas velocity in BC and ILALR.....	108

Figure 71 specific interfacial area versus gas velocity in BC. and ILALR.....	109
Figure 72 Schematic of the experimental setup.....	111
Figure 73 Schematic of Karman contactor.....	112
Figure 74 Internal loop airlift reactor (ILALR) in study of continuous system.	113
Figure 75 Benzene generator.....	113
Figure 76 diagram of study the effect of continuous system in IILALR.....	116
Figure 77 diagram of studying application for simulated VOCs absorption.	117
Figure 78 The variation of overall mass transfer coefficient obtained in the ILALR for amount of liquid velocity and plastic media 2%, 5%, 10% and 15% in ILALR respectively.....	120
Figure 79 the variation of overall mass transfer coefficient obtained by.....	121
Figure 80 Bubble diameters versus gas velocity for different liquid phases.....	122
Figure 81 Interfacial area versus superficial gas velocity for different liquid phases.	123
Figure 82 Absorbent versus time for benzene absorption.	124
Figure 83 Mechanism for benzene absorption and adsorption.....	127
Figure 84 Effect of surfactant (non-ionic) on GAC adsorption.....	128
Figure 85 Summary of $k_L a$ benzene removal efficiency.....	128

CHAPTER 1

INTRODUCTION

1.1 Introduction

Absorption process is commonly used as a raw material or product recovery techniques inspiration and purification of gases streams containing CO₂ such as biogas or air pollution contaminate with VOCs. However absorption is possibility used as an emission control technique. The absorption is a diffusional mass-transfer operation by which a soluble gaseous component, it is removed from a gas stream by dissolution in a solvent liquid. The driving force for mass transfer is the concentration difference of the solute between the gaseous and liquid phases. Generally, absorption technic is designed to improve the specific surface area and contact time between the gas phases and liquid phases. Conventional absorption process is general use in tray towers (plate columns), packed columns, spray towers, bubble columns, and centrifugal contactors. However, bubble column reactors are the most popular and commonly used for absorption in chemical, petrochemical, biochemical and separation industries.

In general, research with bubble columns usually focuses on the following topics: gas holdup studies, bubble characteristics, investigation of flow regime and fluid dynamics studies, local and average mass transfer coefficient, the effects of column dimensions, column internals design, operating conditions, i.e. pressure and temperature, the effect of superficial gas velocity, solid type and concentration. Although a tremendous number of studies exist in the literature, but bubble columns for VOCs absorption process are still not clearly understood due to the fact that most of these studies often focus on only one phase, such as liquid or gas phase.

To fill this gap, this research is mainly focus on VOCs absorption. Moreover, it study the effect of bubble hydrodynamic conditions (gas diffuser and gas flow rate) and also using non-ionic, cat-ionic and non-ionic surfactant as absorbents these are investigated in order to clearly understand the VOCs absorption. The methods for measuring the bubble hydrodynamic and mass transfer coefficient are applied to find the mass transfer efficiency to be effectively controlled and operating conditions.

1.2 Objectives

- To Study the effect of gas diffuser, bubble column dimensions, operating condition, aqueous solutions with surfactant and type of plastic media on the bubble hydrodynamic and the VOCs mass transfer parameters.
- To find the suitable operation parameters for Batch and Continuous-flow bubble column with co-current system.
- To propose the theoretical prediction model for predicting bubble hydrodynamic and VOCs mass transfer parameter.

1.3 Scope of Research

The objective of this research was to study the absorption mechanism for removing benzene from simulate Volatile Organic Compounds (VOCs) in absorption process. The experiment can be divided into three part (Figure 1.16) such as small size bubble column (BC), middle size bubble column (MBC) and continuous bubble column reactor (BC).

First part, small bubble column part focus on physical property of rigid and fixable diffuser (inside diameter and thickness) and type of absorbent these effect to mass transfer parameters ($k_L a$ and k_L) and the bubble hydrodynamic parameters (bubble size, D_B ; terminal bubble rising velocity, U_B ; and specific interfacial area, a).

Secondary part middle size bubble column part study type of bubble column (bubble column and airlift reactor), bubble column dimension, type of absorbent and diffuser and operation parameter these effect to mass transfer and the bubble hydrodynamic parameters.

The Last part, continuous bubble column mainly focus on the effect of continuous operation (co-current and counter-current system), type of bubble column (bubble column and airlift reactor) type of absorbent and diffuser. Then, the data from each part of experiment will be applied to produce empirical prediction model for predicting bubble hydrodynamic and VOCs mass transfer parameters, then the prediction parameters can be used as a primary data for bubble column and airlift reactor process operation.

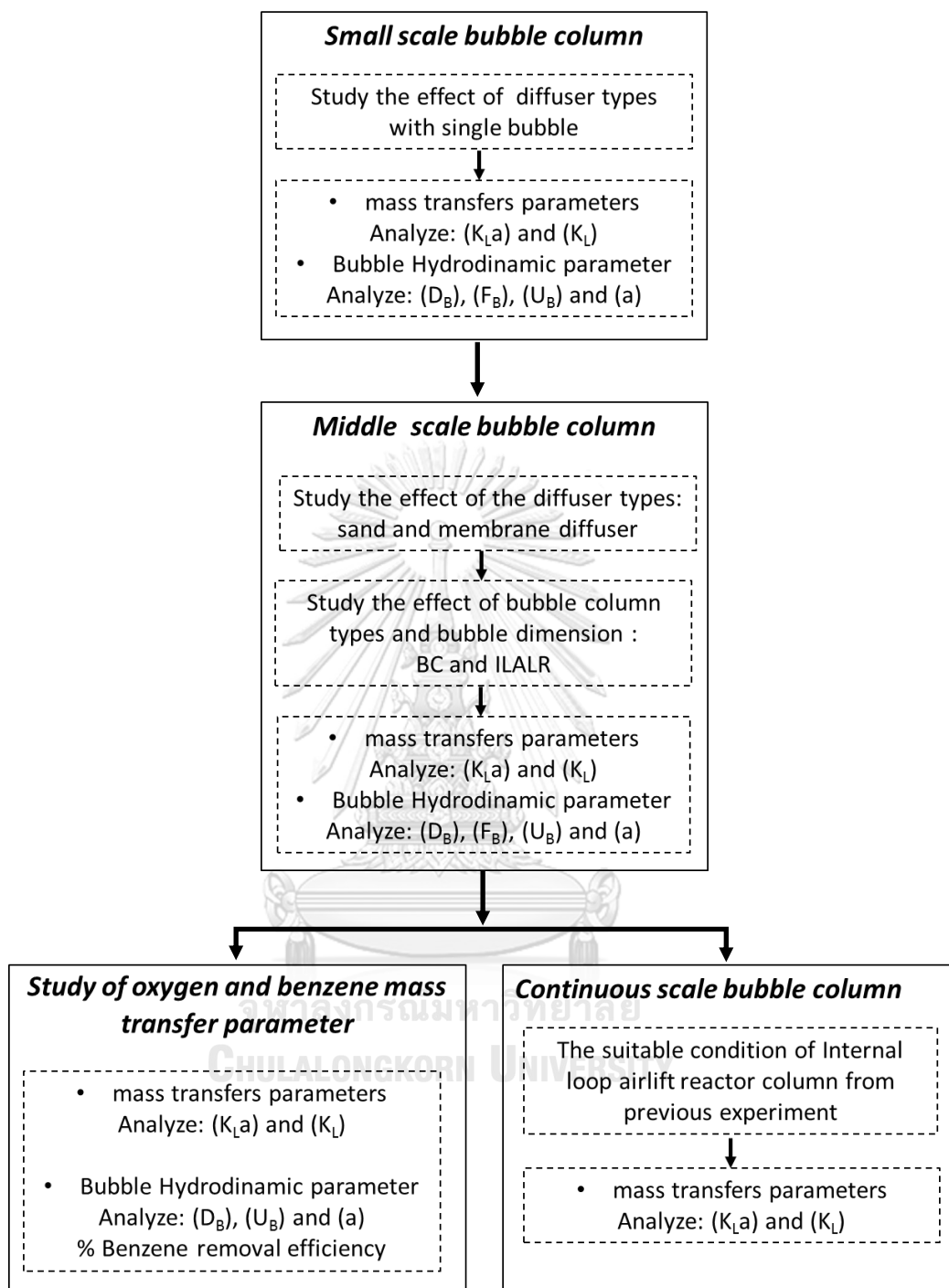


Figure 1 Flow chart of the research

CHAPTER 2

EFFECTS OF FIXABLE AND RIGID DIFFUSED AERATOR ON OXYGEN TRANSFER EFFICIENCY AND BUBBLE HYDRODYNAMIC PARAMETERS

2.1 Introduction

Bubble column reactors belong to the general class of multiphase reactors which consist of three main categories namely, the trickle bed reactor (fixed or packed bed), fluidized bed reactor, and the bubble column reactor. A bubble column reactor is basically a cylindrical vessel with a gas distributor at the bottom. The gas is sparged in the form of bubbles into either a liquid phase or a liquid–solid suspension. These reactors are generally referred to as slurry bubble column reactors when a solid phase exists. Bubble columns are intensively utilized as multiphase contactors and reactors in chemical, petrochemical, biochemical and metallurgical industries. They are used especially in chemical processes involving reactions such as oxidation, chlorination, alkylation, polymerization and hydrogenation, in the manufacture of synthetic fuels by gas conversion processes and in biochemical processes such as fermentation and biological wastewater treatment. Some very well-known chemical applications are the famous Fischer–Tropsch process which is the indirect coal liquefaction process to produce transportation fuels, methanol synthesis, and manufacture of other synthetic fuels which are environmentally much more advantageous over petroleum-derived fuels

Recent research with bubble columns frequently focuses on the following topics: gas holdup studies, bubble characteristics, flow regime investigations and computational fluid dynamics studies, local and average heat transfer measurements, and mass transfer studies. The effects of column dimensions, column internals design, operating conditions, i.e. pressure and temperature, the effect of superficial gas velocity, solid type and concentration are commonly investigated in these studies. Many experimental studies have been directed towards the quantification of the effects that operating conditions, slurry physical properties and column dimensions have on performance of bubble columns. Although a tremendous number of studies exist in the literature, bubble columns are still not well understood the basic of hole size diameter and physical property of rubber membrane and rigid diffuser which effect to bubble generation, bubble hydrodynamic and mass transfer parameter. The main point of this study focus on Small-scale bubble columns (SBC), it is a basic tool for process development. SBC were investigated the on the bubble hydrodynamic (D_B , f_B

and U_B), the mass transfer parameters (a , $k_L a$ and k_L) and also the best operating condition in SBC.

2.2 Objectives

- Study the effects of the hole size diameter of rigid and fixable diffuser on the bubble hydrodynamic (D_B , f_B and U_B) and the mass transfer parameters (a , $k_L a$ and k_L).
- Study the power consumption which relate the interfacial area provided by rigid and fixable diffuser. Note that this applied method enables the mass transfer efficiency to be effectively operating controlled.

2.3 Literature Review

Painmanakul et al., (2004) studied to compare the physical property of two flexible membranes (the new membrane and the old membrane) used in waste water treatment. In this study focus on the physical properties of membrane (hole diameter, pressure drop, critical pressure, deflection at the centerline and elasticity). Moreover, the bubble generation from diffusers with a single orifice and with four orifices have been studied and have been compared in terms of interfacial area and power consumption. The result was showed with a single orifice, the bubble diameter generated from the new membrane still constant in every gas flow rate, whereas bubble frequency increases with an increase in UG. Moreover, the new membrane has a behavior comparable to a rigid orifice. The four orifice and the multi orifice, the hole size diameters of the membranes with four orifices are lower than the membranes with a single orifice. The variation in hole diameter with the gas flow rate is less pronounced than with a single orifice membrane. It does not has the effect of coalescence at bubble formation is observed under these operating conditions, can be explained by the inter-orifice distance being greater than the detached bubble diameters.

Muroyama et al., (2014) studied to investigate the gas holdup, bubble size distribution, and Sauter mean diameter for oxygen micro-bubble dispersions in water

in an acrylic-acid resin column with an inner diameter of 0.15 m, and with a working liquid height varying from 0.500 to 1.850 m. The result showed that the $k_L a$ values for the degassed water were represented well by the complete absorption model, and generally increased with increasing gas flow rate. It was found that the oxygen absorption efficiency, which was defined by the ratio of the absorption rate to the supply rate of oxygen, decreased with increasing gas flow rate and increased with increasing liquid depth. It could be described well by an empirical correlation in terms of the ratio of the liquid height to the superficial gas velocity, h/U_G or in terms of the ratio of the liquid height to the linear gas velocity, $h/(U_G/\epsilon g)$.

2.4 Materials and Methods

2.4.1 Experimental set-up

The experiment set up in this section was schematically represented in Figure 2 the experiments were studied with a small bubble column 5 cm in diameter and 30 cm in height. Tap water and aqueous solution. Air is generated by air pump, pass through gas inlet. The flow of air is regulated by a gas flow meter, Pressure gage and diffuser. Air pass through the bubble column. The average gas flow rate from air tank was measured by using the soap film meter. The equipment used in this study contains: 1) Ball valve 2) Pressure gage 3) Gas flow meter 4) Rigid orifice gas diffuser 6) Bubble column reactor and Benzene generator.

For the bubble hydrodynamic mechanisms are investigated by the high speed camera (100 images/sec) and image analysis program is used to determine the bubble hydrodynamic parameters. The bubbles are generated by a diffuser located at the center of column in Figure 3 for rigid diffuser and rubber diffuser

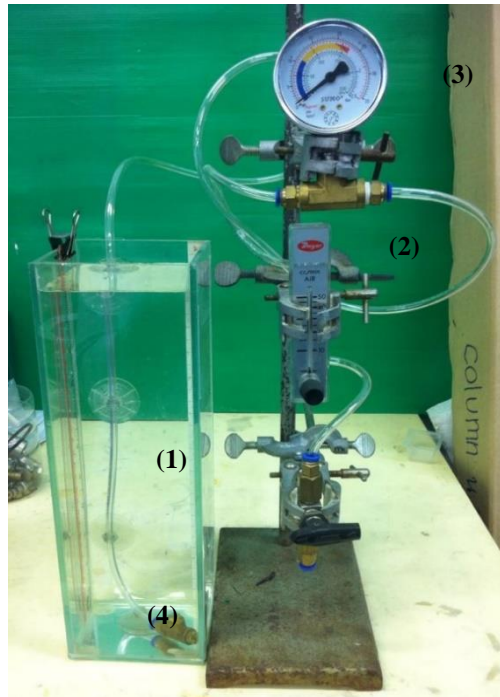


Figure 2 the experiment set up

In this work, the diffusers were used two types of rigid (inside diameter 0.3, 0.4, 0.5, 0.6, 0.7, 0.8, 0.9 and 1.1 mm) and flexible membrane (thickness 0.5, 1.0, 1.5, 2 and 3 mm) as show in Figure 3. The bubbles were generated by a diffuser that located at the center of membrane and needle by Figure 3a and 3b respectively. In order to analyze the bubble hydrodynamic mechanism, in this study use the high speed camera (100 images/second) and imageJ program were used to determine the bubble hydrodynamic parameters.

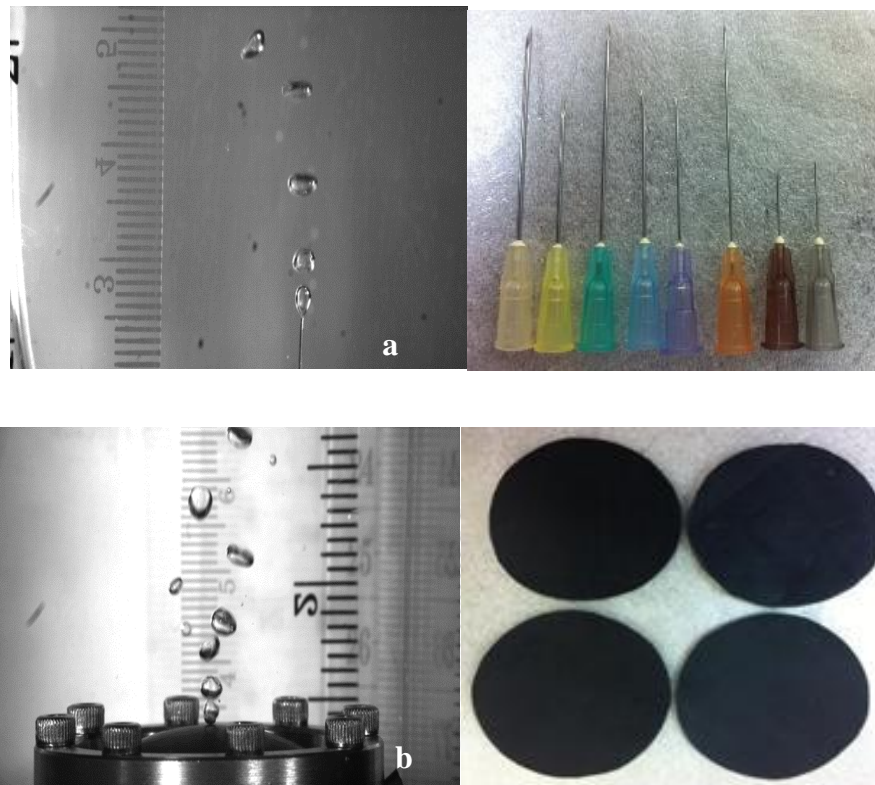


Figure 3 a and b for rigid diffuser and fixable diffuser respectively

In this part of research study the effects of the physical property of rigid and fixable diffuser (inside diameter and thickness) and operating conditions, i.e. pressure, gas flow rate on the bubble hydrodynamics (D_B , f_B and a). The parameters were studied in this experiment, these were showed in the figure 4 and table 1

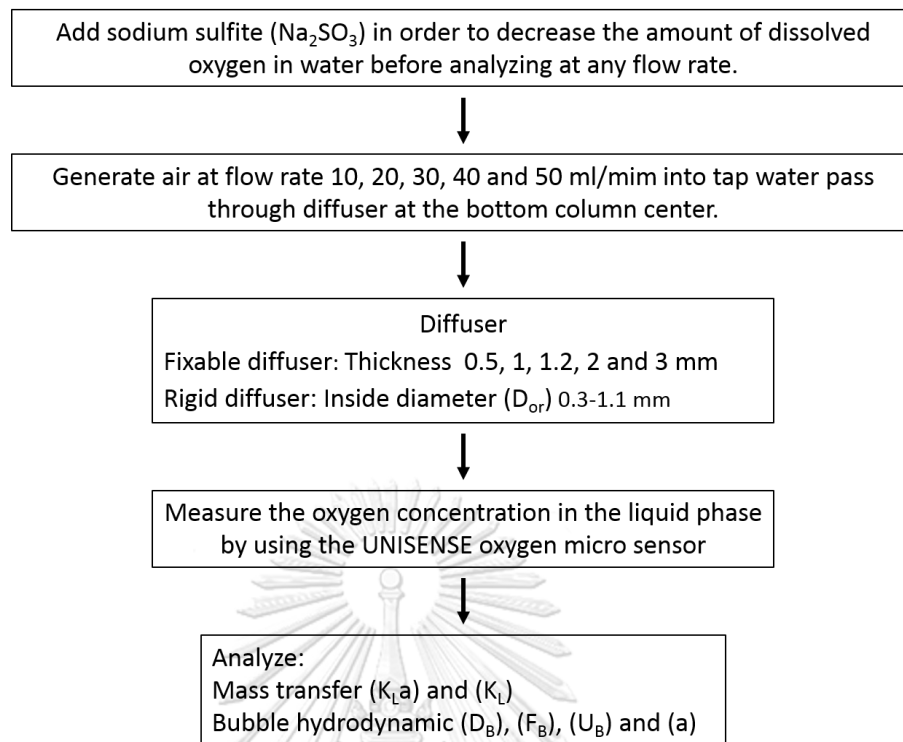


Figure 4 Methods of study the effect of diffuser (rigid and fixable diffuser) on overall mass transfer coefficient and bubble hydrodynamic parameter in BC.

Table 1 parameters were studied in this experiment.

Fixed Variables	Parameter
Gas phase (absorbate)	Oxygen
Liquid phase (absorbent)	Tap water
Independent Variables	Parameter
Gas flow rate	10, 20, 30, 40 and 50 ml/mim
Fixable diffuser	
Thickness	0.5, 1, 1.2, 2 and 3 mm
Rigid diffuser	
Inside diameter (D _{or})	0.3-1.1 mm
Dependent Variables	Parameter
Mass transfer parameters	k _L a, k _L
Bubble hydrodynamic parameters	a, D _B , f _B , U _B

2.4.2 Analytical methods

Membrane sparger characterization

- Equivalent hole diameter

The dynamic rubber membrane behavior was studied experimentally. Using the image acquisition system previously described, hole diameters are measured. They correspond to the equivalent diameters defined from the area assuming a circular hole, given by:

$$D_{OR} = \left[\frac{4(\text{Hole area})}{\pi} \right]^{1/2} \quad (2.1)$$

- Critical pressure and “elastic” pressure

Rice & Howell., (1986) and Bischof & Sommerfeld., (1991) have proposed the force balance described in Fig. 5 for a bubble formed at a fixable nozzle. In contrast to a rigid nozzle, the force due to the elasticity of the material has also to be taken into consideration. The required pressure which allows the formation of a bubble is given by

$$\Delta p > p_c - p_H - p_{HB} - p_\sigma - p_o \quad (2.2)$$

Where the capillary pressure p_o is equal to $4\sigma/D_{OR}$, assuming no bubble spreading on the membrane. The hydrostatic correction for bubble height ($p_{HB} = \rho g r$) is negligible. The “elastic” pressure p_o which depends on the properties of the flexible membrane is unknown and has to be determined experimentally. The present authors decided to define the critical pressure p to just initiate bubbling as

$$\Delta p_c = \frac{4\sigma_L}{d_{OR}} + p_o \quad (2.3)$$

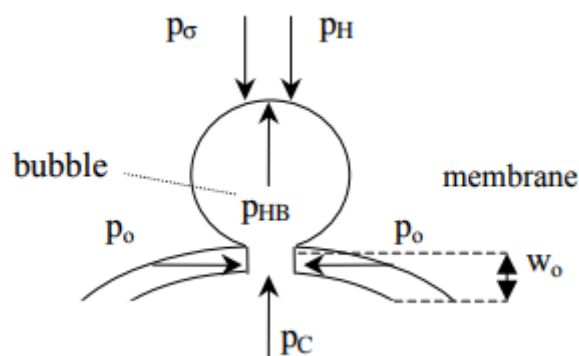


Figure 5 Force balance of force during bubble formation at a flexible nozzle.

- Pressure balance on gas–liquid interface

This motion equation describes the radial expansion of the bubble. The conservation of momentum for liquid around a spherical bubble in the radial direction

(axisymmetric geometry) is applied and coupled with the continuity equation for the purely extensional, incompressible and irrotational flow. The continuities of the normal stress vector and of the velocity at the interface are considered as boundary conditions. The effect of gas momentum is neglected. It leads to the modified Rayleigh equation given by

$$p_b - p_h = \rho_L \left[R \frac{d^2 R}{dt^2} + \frac{3}{2} \left(\frac{dR}{dt} \right)^2 \right] + \frac{2\sigma_L}{R} + \frac{4\mu_L}{R} \frac{dR}{dt} \quad (2.4)$$

The three terms on the right-hand side of Eq. (2) represent inertial, surface tension and viscous forces, respectively. This equation is assumed to be valid for any point i on a non-spherical bubble interface by replacing the global spherical radius R with the local radius of curvature R

- Pressure change in the gas chamber

The thermodynamic system is defined as the sum of the gas in the bubble, in the chamber and the gas that enters the chamber during the time interval dt . Assuming a polytropic behavior of gas in the gas chamber and no pressure drop at the level of gas supply, the mass conservation equation is expressed as

$$\frac{dp_c}{dt} = \frac{xp_c}{v_c} (Q_g - q) = \frac{xp_c}{v_c} \left(Q_g - \frac{dV_B}{dt} \right) \quad (2.5)$$

The gas chamber volume V is measured experimentally. In the known literature, the polytropic coefficient X define between 1 for isothermal change (Terasaka & Tsuge, 1990) and 1.4 for adiabatic change (Mc Cann & Prince, 1971 and Li, 1999). Even though the thermodynamic behavior of the membrane gas chamber is not usual, the polytropic coefficient assumed to be equal to 1.4.

- Calculation of the power consumption, P_g

Total specific power consumption (P_g/V_{Total}) of aeration system is the relation of gas flow (Q_g) rate and pressure drop (ΔP) which can be calculated by the equation below;

$$\frac{P_g}{V_{Total}} = Q \times \frac{\Delta P_{Total}}{V_{Total}} = Q \times \frac{\rho_L g H_L + \Delta P}{V_{Total}} \quad (2.6)$$

The total gas pressure drop (ΔP_{Total}), total volume in reactor (V) m^3 and pressure drop created by the membrane sparger (ΔP)

- Membrane deflection at the pole (W_0)

This model has been developed to show the connection between elastic and fluid mechanics in order to describe the membrane behavior when it is subjected to pressure from below. The authors have shown that the excess tension T can be related to the applied pressure by Eq. (14):

$$T = K.\Delta TP^n \quad (2.7)$$

T is a function of the applied pressure, the deflection and the membrane radius and is given by the following equation:

$$T = \frac{\Delta P.Z^2}{4W_0} \quad (2.8)$$

When $W_0 \ll Z$

$$T = \frac{\Delta P.Z^2}{4W_0} + \frac{\Delta P.W_0}{4W_0} \quad (2.9)$$

Bubble hydrodynamic and mass transfer coefficient parameters determination

- Bubble diameter (D_B)

The measurement of bubble diameter at any flow rate (Q_g) can be determined by image analysis technique. The observed bubbles have mainly ellipsoidal shapes characterized by the major axis, E , which represents the largest distance between two points on a bubble, and the minor axis, e , which represents the smallest length of the bubble. Both axis were measured using ImageJ software and the bubble as the ellipsoid was calculated as follows:

$$D_B = \sqrt[3]{E^2 e} \quad (2.10)$$

- Local interfacial area (a)

The local interfacial area is defined as the ratio between the bubble surfaces (S_B) and the total volume in the reactor (V_{Total}), N_B is number of bubbles that can be deduced from the bubble rising velocities (U_B) and the bubble formation frequency (f_B). In this work, the interfacial area is expressed as Eq.(1). (Painmanakul et al., 2005);

$$a = N_B \times \frac{S_B}{V_{total}} = f_B \times \frac{H_L}{U_B} \times \frac{\pi D_B^2}{4H_L + N_B V_B} \quad (2.12)$$

A and H_L are the cross-sectional area and the liquid height, respectively.

- Terminal rising bubble velocity (U_B)

The bubble rising velocity were calculated by taking picture of bubble in reactor to analyze its distance (D) at any time frame (t_{frame}). Thus, the U_B were calculated from equation (3). (Painmanakul et al., 2005),

$$U_B = \frac{D}{t_{frame}} \quad (2.13)$$

- The overall mass transfer coefficient ($K_L a$)

The overall mass transfer coefficient ($K_L a$) is used in order to analyses the absorption process. According to the Non-stationary or dynamic method (Deckwer, 1992), the $K_L a$ is given by the following equation:

$$\frac{dC}{dt} = K_L a (C^* - C) \quad (2.14)$$

or in its integral form by:

$$\frac{\ln [C^* - C]}{\ln C^*} = - K_L a (t) \quad (2.15)$$

where C and C^* are the concentration of contaminant and the saturated concentration of contaminant in the liquid phase, respectively. The slope of this equation gives $- K_L a$

- Liquid film mass transfer coefficient (k_L)

The liquid film mass transfer coefficient (k_L) was the proportions of the overall mass transfer coefficient and interfacial area (a) obtained experimentally in this study. Therefore, the value of K_L can be determined by Sardeing *et al.* (2006);

$$K_L = \frac{k_L a}{a} \quad (2.16)$$

2.5 Results and Discussion

2.5.1 Characterization of the membrane with a single orifice

- Equivalent hole diameter

In this study focus on study 2 types of diffuser (rubber membrane and rigid diffuser) properties were studied in the experimentally. For the study of rubber membrane diffuser, the image system was used to measure the hole diameter which

were calculated to the equivalent diameters defined from the area assuming a circular hole, given by equation (2.1).

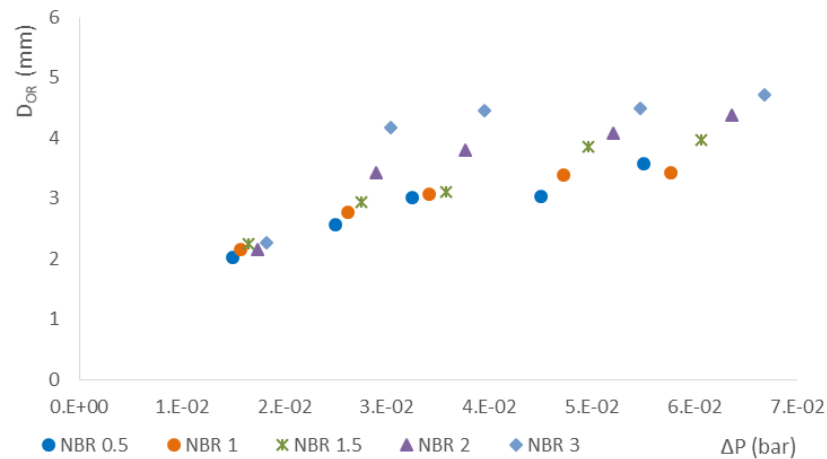


Figure 6 Equivalent hole diameter versus applied pressure for the rubber membranes diffuser with a single orifice.

Figure 6 shows that for a given ΔP , the membrane thickness of the NBR 0.5, 1, 1.5, 2 and 3 mm. The result show that for all the membranes, the apparent equivalent hole diameter increases with the applied pressure: when the pressure increases, the hole expands owing to the membrane's elastic nature.

All the rigid diffuser, the apparent equivalent hole diameter increases with the applied pressure: when the pressure increases, the hole expands owing to the membrane's elastic nature. The orifice varies in shape: at low applied pressures, the orifice appears as a slit and as the pressure increases, the slit expands to form a more circular shape.

- **Pressure drop and the gas flow rate**

According to the data as Figure 7(a) and 7(b) showed the relation of pressure drop and gas flow rate for the rigid and fixable diffuse. The pressure drop increases linearly from 0.192 to 0.725 bar with increasing gas velocity from 8.4×10^{-5} to 4.2×10^{-4} m/s respectively. Moreover, some appearance in the rigid diffuser that the pressure drop increased directly with decreasing the hole diameter (D_{or}) of rigid diffuser. Besides, fixable diffuser also had the similar effect with rigid diffuser; increasing thickness of membrane related to increase the pressure drop.

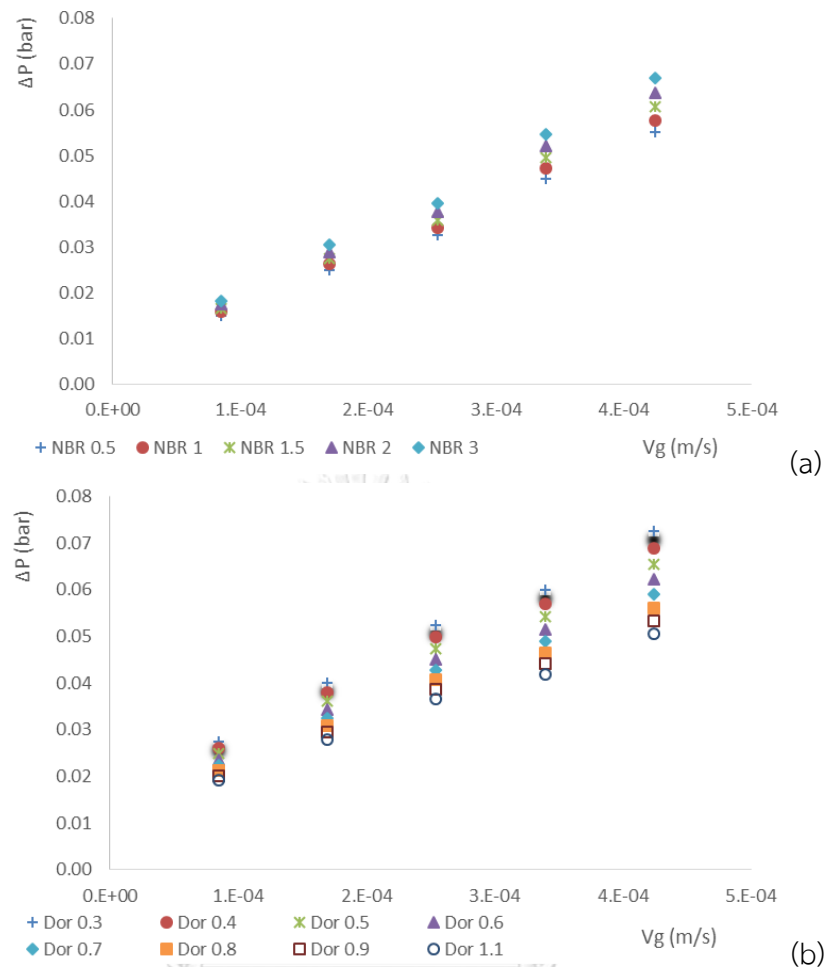


Figure 7 Different pressure versus applied pressure for the rubber membrane diffusers (a) and rigid diffusers (b) with a single orifice

- **Deflection and flexibility.**

As an increasing pressure was applied, it caused the membrane to enlarge. Thus membrane took on the shape of a spherical cap (Figure 9). Figure 8 presents the curves relating the membrane deflection at the pole W_0 to the pressure drop. It can be observed that the deflection at the pole increased with pressure for all membranes. However, the deflection at the pole for NBR 0.5 was smallest around 0.019 - 0.40 cm for 8.4×10^{-5} to 4.2×10^{-4} m/s respectively. So the bubbles were produced from NBR 0.5. These are smaller than other membrane.

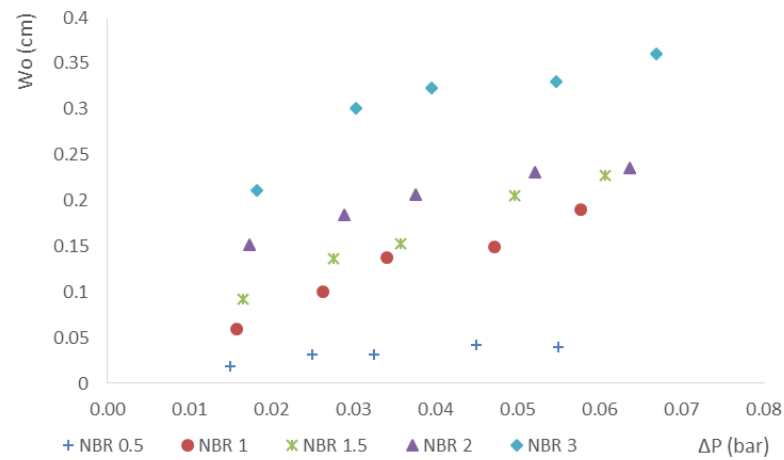


Figure 8 Relation of deflection versus applied pressure for rubber membrane diffuse.

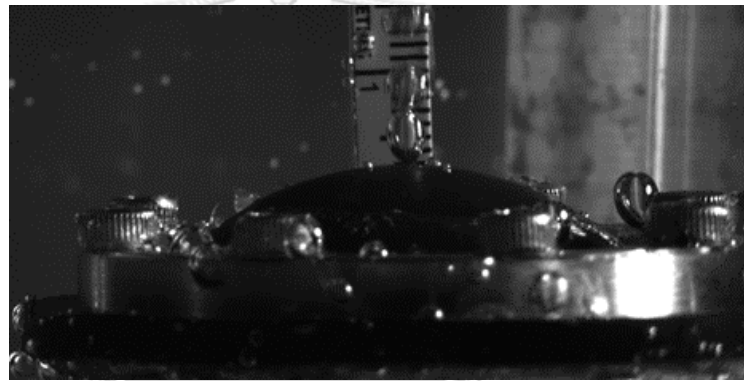


Figure 9 the shape of a spherical cap.

2.5.2 Characterization of the bubble provided by a single orifice

In this part of study use 2 types of sample such as rubber membrane (thickness 0.5, 1, 1.5, 2 and 3 mm) and rigid diffuser (0.3, 0.4, 0.5, 0.6, 0.7, 0.8, 0.9 1.0 and 1.1 mm) were chosen in order to analyze the related physical characteristics such as bubble diameter and bubble frequency. Table 1 shows the summary of the experimental results in terms of tube wall thickness, tensile strength, hardness and elongation.

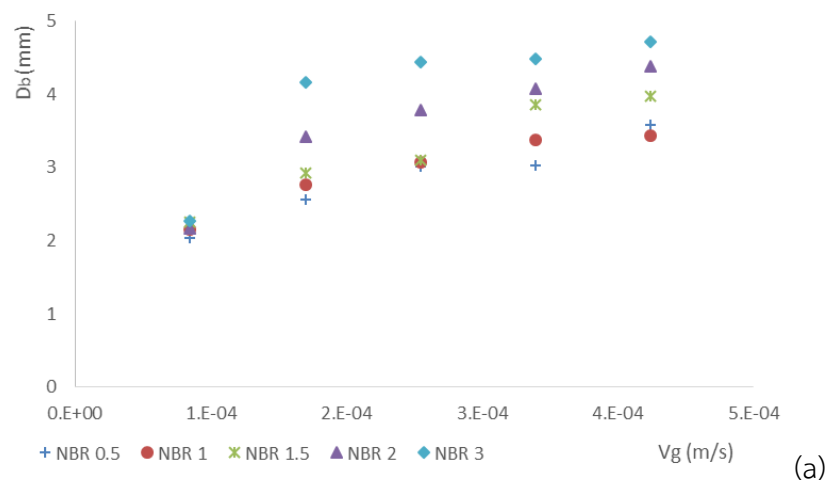
- **Bubble diameter**

Figure 10(a) shows the relation between the bubble diameter of rubber membrane and the gas flow rate. For different thickness (0.5, 1, 1.5, 2 and 3 mm) of rubber membrane, the bubble diameter slightly increase around 0.2464 to 0.3919 cm which correspond to increase gas flow rate in the system. It can be confirm that the bubble diameter of rubber membrane depend on the gas flow rate. Moreover, the thickness of rubber membrane also have an effect to the bubble diameter. The result

show that the increasing of rubber membrane thickness directly match with the advancing of bubble diameter around 0.2464 to 0.3919 cm.

The explanation in the effect of increasing bubble diameter relate to the advancing of gas flow rate and thickness of rubber membrane, Due to increasing of gas flow correspond to increase D_{or} of rubber membrane and pressure in the systems which relate to the result form previous experiment. And the effect of membrane thickness, the result show that high thickness of rubber membrane correspond the bubble diameter due to the fist bubble that produce from high thickness rubber membrane highly use gas pressure and volume of gas when compare to lower thickness rubber membrane.

Figure 10(b) shows the relation between the bubble diameter and the gas flow rate for the two kind of diffusers. For rigid diffuse, the bubble diameter (0.2464 - 0.3919 cm) did not depend on the gas flow rate and stilled constant for every gas flow rate whereas the bubble directly depend on the D_{or} of rigid diffuser. Thus, can be explain that the bubble diameter directly relate with increasing D_{or} of rigid diffuser and gas velocity.



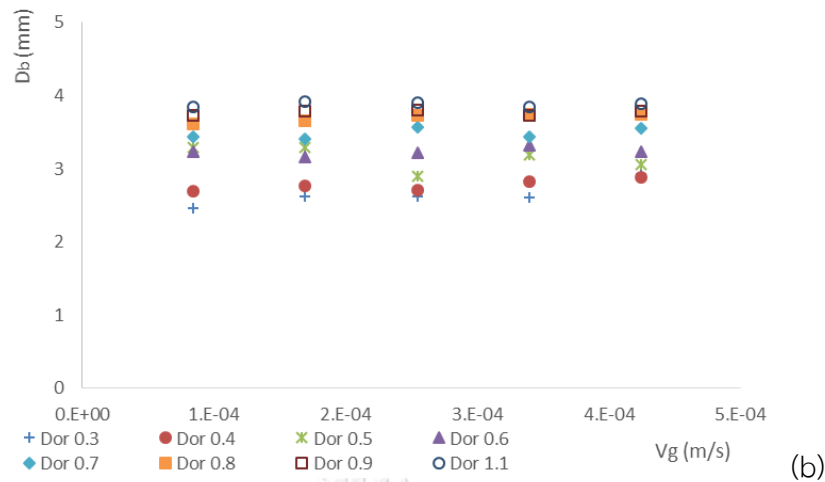


Figure 10 Bubble diameter versus applied pressure for the rubber membrane diffusers (a) and rigid diffusers (b) with a single orifice.

- **Bubble frequency**

The bubble frequency curves as a function of the gas flow rate were given in Fig.11 for the two membranes. Figure 11(a) and 11(b) shows that the bubble formation frequencies of rigid and fixable diffuse.

For rubber membrane diffuser, the result is showed in Figure A the bubble frequency in rubber membrane thickness form 0.5 to 3 mm clearly increases with the gas flow rate through the orifice. Whereas the same gas flow rate, the bubble frequency of thin rubber membrane is higher than high thickness rubber membrane. These results agree with the previous result, high membrane thickness relate to produce high bubble diameter which correspond the decreasing of bubble frequency.

For the rigid diffuser, the result show that the bubble frequency increased continuously with an increase gas flow rate. Which the same gas flow rate, the bubble frequency slightly increase with D_{or} of rigid diffuser. Comparing the result rubber membrane and rigid diffuser found that bubble frequency of rigid diffuse is higher than rubber membrane diffuser at high gas flow rate, due to high gas flow rate of rubber membrane diffuser. The bubble diameter of membrane diffuser higher than rigid diffuser which correspond to report lower bubble frequency in the experiment. The relation of bubble diameter and bubble diameter can be explained by the equation below;

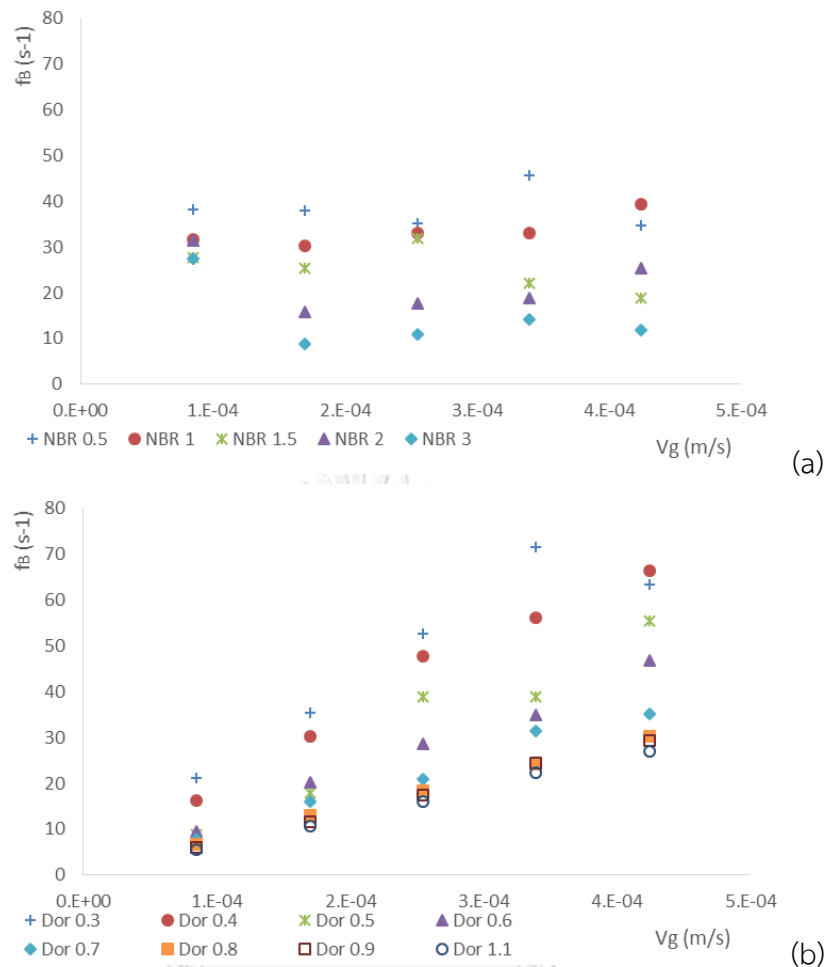


Figure 11 Bubble frequency versus applied pressure for the rubber membrane diffusers (a) and rigid diffusers (b) with a single orifice.

2.5.3 Performances of the two membranes

- Interfacial area

To study the interfacial area of rigid and fixable diffuser, the variations in the bubble diameter, the bubble frequency and terminal bubble rising velocity. These parameter were used to calculate the interfacial by equation (2.6).

For this purpose, Figure 12(a) presented the study of rubber membrane on the variation of the interfacial area with the gas flow rate with a single orifice. The figures showed that the interfacial area continuously increased with gas flow rate. Whereas, the similar gas flow rate, the result show that NBR 1 show the highest interfacial area and slightly decrease with increased the membrane thickness form NBR 1.5, NBR 2 and NBR 3 respectively. The result can be explained by the relation between bubble diameter and gas flow rate as the equation 2.12.

This purpose, Figure 12(b) presented the study of rigid diffuser on the variation of the interfacial area with the gas flow rate and a single orifice. The figures showed that the interfacial area continuously increased with gas velocity. Whereas, the similar gas velocity, the result show that D_{or} 0.3 at V_g 4.2×10^{-4} m/s show the highest interfacial area and slightly decrease with increased the D_{or} of rigid diffuser from 0.5 to 1.1 respectively. Comparing to the result of rigid and rubber membrane diffuser. The result show that the low gas velocity 8.4×10^{-5} and 1.7×10^{-4} m/s Interfacial valve of rigid and rubber membrane are almost similar. Then increasing gas velocity from 2.5×10^{-4} and 4.2×10^{-4} m/s, Interfacial valve of rubber membrane diffuser become lower than interfacial valve of rigid diffuser. The result can be explained the bubble size diameter which the increasing of bubble diameter relate to abate the interfacial valve.

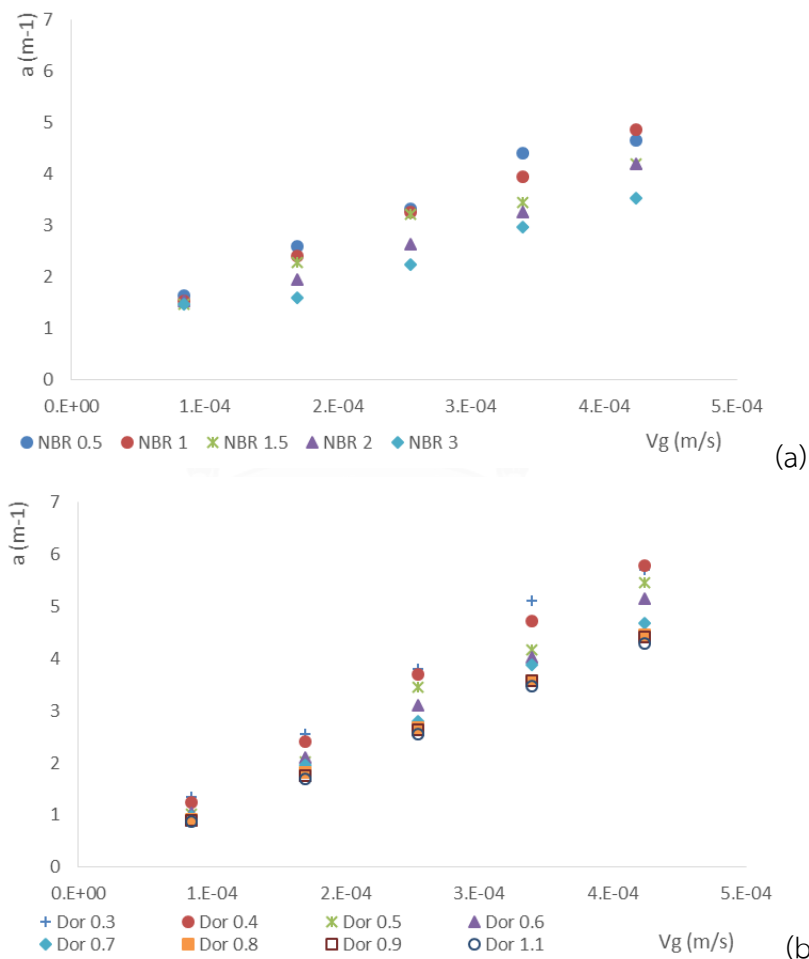


Figure 12 Interfacial area versus applied pressure for the rubber membrane diffusers (a) and rigid diffusers (b) with a single orifice

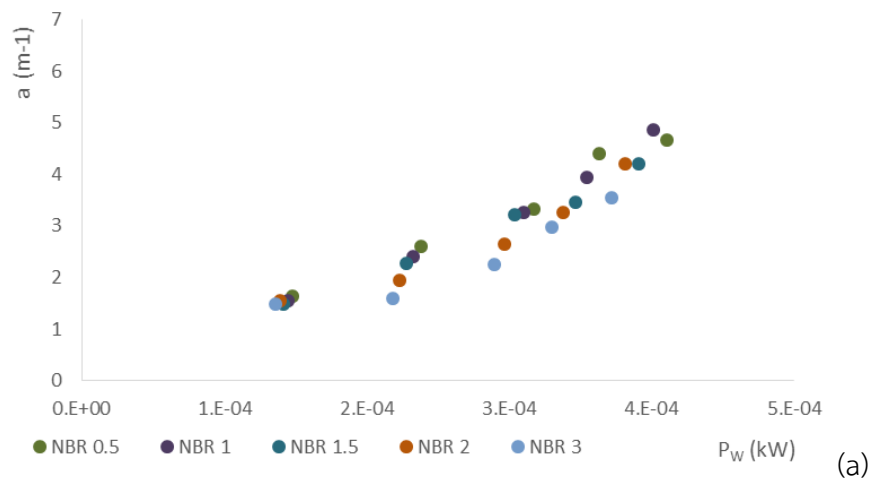
- **Power consumption**

The variations of the interfacial area with the power consumption for the rubber membranes and rigid diffuser with a single orifice shown in Figures A and B respectively.

According to these figures 13(a), the interfacial area of rubber membrane with a single orifices increases with the power consumption. Whereas, increasing of membrane thickness from 1.5 to 3 mm have a bad affects to decrease interfacial area respectively.

According to these figures 13(b), the interfacial area of rigid diffuser with a single orifices increases with the power consumption. Whereas, increasing of D_{or} from 0.5 to 1.1 mm have a disadvantage to decreasing interfacial area valve respectively.

Therefore, it can be concluded that for a given power consumption, the interfacial areas associated with rubber membrane thickness and D_{or} of rigid diffuser with a single orifices which have the similar effect. Moreover, the comparing of power consumption on rubber membrane and rigid diffuser. The result that rigid diffuser report the interfacial area value higher than rubber membrane diffuser and the highest valve show on D_{or} 0.3 mm.



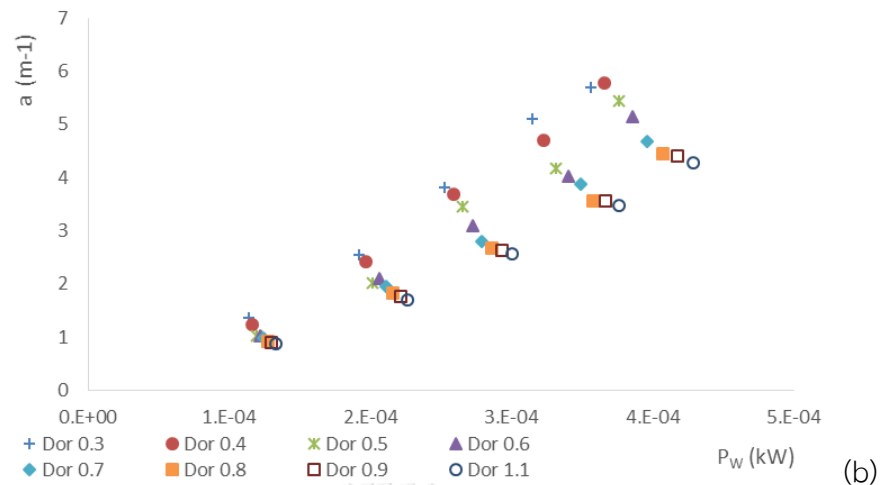


Figure 13 Power consumption versus applied pressure for the rubber membrane diffusers (a) and rigid diffusers (b) with a single orifice.

- **Volumetric mass transfer coefficient ($k_L a$)**

To study the volumetric mass transfer coefficient of rigid and rubber membrane diffuser, the variations in the gas flow rate which was measured oxygen transfer rate and then calculate the volumetric mass transfer coefficient by equation 2.15.

For this purpose, Figure 14(a) presented the study of rubber membrane on the variation of the volumetric mass transfer coefficient with the gas velocity with a single orifice. The figures showed that the interfacial area continuously increased with gas velocity. Whereas, the similar gas velocity, the result show that NBR 1 show the highest interfacial area. After that volumetric mass transfer coefficient slightly decrease with increased the membrane thickness form NBR 1.5, NBR 2 and NBR 3 respectively.

For this purpose, Figure 14(b) presented the study of rigid diffuser on the variation of the volumetric mass transfer coefficient with the gas velocity and a single orifice. The figures showed that the volumetric mass transfer coefficient continuously increased with gas velocity. Whereas, the similar gas velocity, the result show that D_{or} 0.3 at 4.2×10^{-4} m/s show the highest volumetric mass transfer coefficient and slightly decrease with increased the D_{or} of rigid diffuser form 0.5 to 1.1 respectively.

The result can be explained by the relation between volumetric mass transfer coefficient and interfacial area equation below. Comparing to the result of rigid and rubber membrane diffuser. The result show that the low gas flow rate 8.4×10^{-5} and 1.7×10^{-4} m/s. volumetric mass transfer coefficient of rigid and rubber membrane are almost similar. Then increasing gas velocity from 2.5×10^{-4} and 4.2×10^{-4} m/s, Interfacial valve of rubber membrane diffuser become lower than interfacial valve of rigid diffuser.

The result can be explained the bubble size diameter which the increasing of bubble diameter relate to abate the interfacial valve.

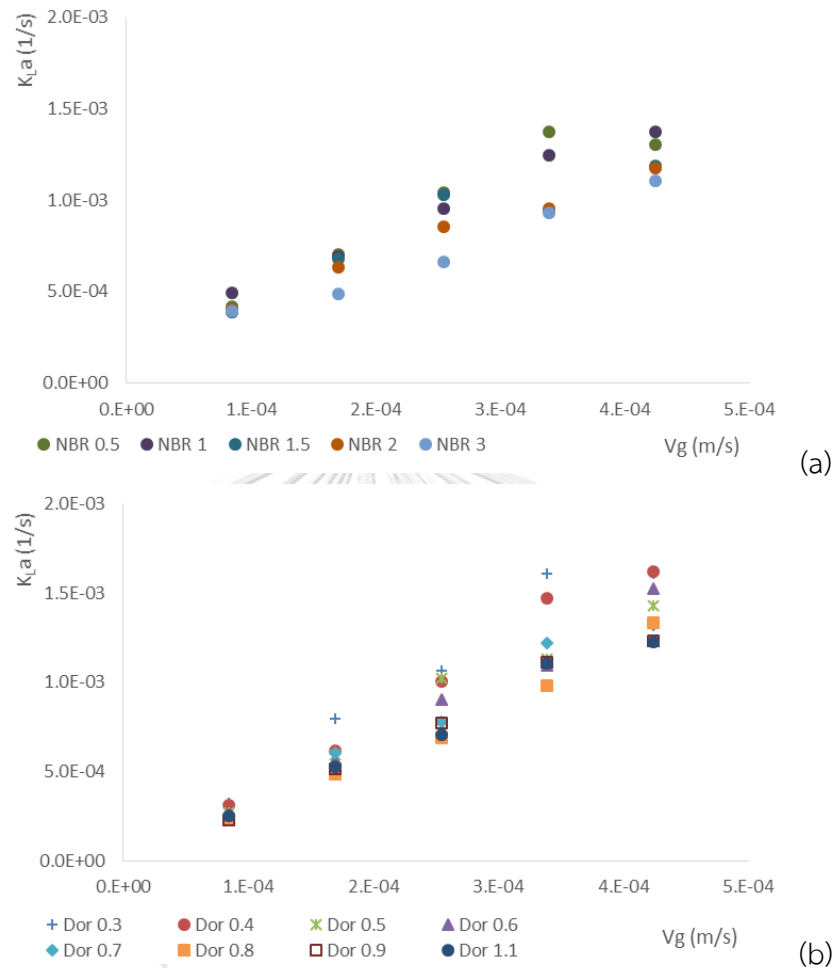


Figure 14 Volumetric mass transfer coefficient versus applied pressure for the rubber membrane diffusers (a) and rigid diffusers (b) with a single orifice.

- **Liquid-side mass transfer coefficient (k_L)**

To study the liquid-side mass transfer coefficient of rigid and rubber membrane diffuser, the variations in the gas flow rate. The liquid-side mass transfer coefficient was calculated by the volumetric mass transfer coefficient and interfacial area by equation 2.16. For this purpose, Figure 15(a) and Figure 15(b) presented the study of rubber membrane and rigid diffuser with a single orifice on the variation of the liquid-side mass transfer coefficient with the gas flow rate respectively. The figures showed that the liquid-side mass transfer coefficient continuously stable with gas flow rate from 2.5×10^{-4} - $3.5 \times 10^{-4} \text{ m}^{-1}$. Whereas, the similar gas flow rate, the result show that liquid-

side mass transfer coefficient constant in the different type of diffuser. The result can be explained the relation between volumetric mass transfer coefficient, interfacial area and liquid-side mass transfer coefficient by equation 2.16.

In this experiment, the relation of liquid-side mass transfer coefficient is not depended on volumetric mass transfer coefficient, interfacial area. Moreover, the increasing of volumetric mass transfer coefficient only relate to the increasing of interfacial area, which were show from previous experiment.

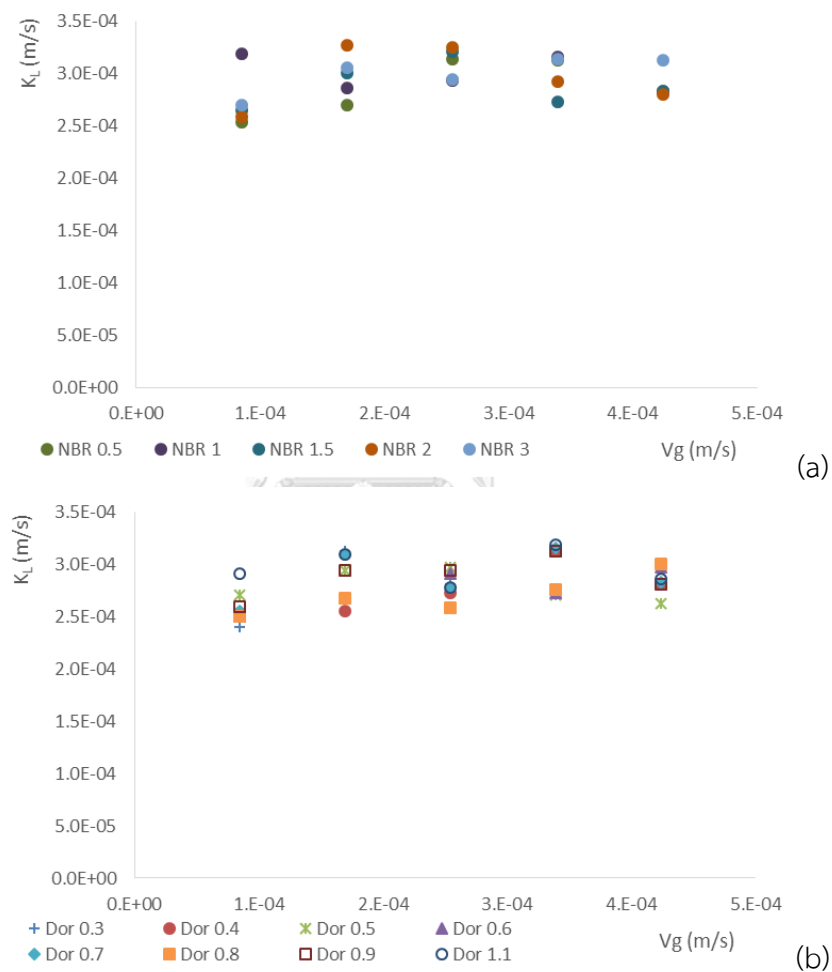


Figure 15 Liquid-side mass transfer coefficient versus applied pressure for the rubber membrane diffusers (a) and rigid diffusers (b) with a single orifice.

2.6 Conclusions

The objective of this work was to compare two type of diffuser (rubber membrane and rigid diffuser) commonly used in waste water treatment. For this purpose, the

membranes and rigid with a single orifice were characterized in terms of: physical properties, bubble generation and membrane performances. For the membrane with a single orifice, the results related to the physical properties and to the bubble generation have shown that:

- The hole diameter of rubber membrane in every thickness increase with gas flow rate.
- Pressure drops slightly increase with the thickness rubber membrane. For rigid diffuser pressure drop directly increase with decreasing of D_{or} .
- The result that rigid diffuser report the interfacial area value higher than rubber membrane diffuser and the highest value of interfacial with power consumption show on D_{or} 0.3 mm.
- Then increasing gas velocity from 2.5×10^{-4} and 4.2×10^{-4} m/s, Interfacial value of rubber membrane diffuser become lower than interfacial value of rigid diffuser. The result can be explained the bubble size diameter which the increasing of bubble diameter relate to abate the interfacial value.

In the next part of study should be conducted on effects of dimension in order to validate the role of bubble column configuration and operating condition obtained in this work as well as provide a better understanding on gas-liquid mass transfer mechanism and effect of membrane and rigid diffuser. Finally, the next part of study shall be use D_{or} close to 0.3 mm rigid diffuser which report in this part of experiment give the highest $k_L a$ and suitable operation condition.

CHAPTER 3

COMPARATIVE STUDY OF MASS TRANSFER AND BUBBLE HYDRODYNAMIC PARAMETERS IN BUBBLE COLUMN REACTOR: PHYSICAL CONFIGURATIONS AND OPERATING CONDITIONS

3.1 Introduction

Bubble column reactors belong to the general class of multiphase reactors which is basically a cylindrical vessel with a gas distributor (diffuser) at the bottom. The gas is sparged in form of bubbles into either liquid phase or liquid–solid suspension. In practice, bubble columns are widely used in industrial gas–liquid operations (absorption) and industrial chemical and biochemical processes due to their simple construction, low operating cost, and high-energy efficiency. From many advantages, this process is applied in aeration and purification process of VOCs, CO₂, and odor abatement (Deckwer, 1992). Gas-liquid mass transfer is one of the key factor governing the reactor performance, which relates to hydrodynamics and physical properties.

To improve the overall performance, numerous researches have studied the diffuser characteristics as well as influences of liquid phase for modifying and controlling the bubble hydrodynamic and mass transfer parameters. In industrial operation, various gas spargers (diffusers) are used as such as perforated plate, porous disk diffuser, membrane gas diffuser, which can be classified as rigid and flexible diffusers. Several studies regarding bubble diameters generated from different gas sparger types in bubble columns have been published by Bouaifi et al. (2001) and Hebrard et al. (1996).

The bubble hydrodynamic parameters (bubble diameter, bubble rising velocity and its formation frequency) can be significantly affected by different types of gas diffusers and contaminants (e.g., surfactants and organic substances) presence in liquid phases. Note that the interfacial area (a) can be experimentally determined using detached bubble diameters, bubble formation frequencies, and terminal bubble rising velocities as in Painmanakul et al. (2004). Concerning the study of mass transfer parameters, the volumetric mass transfer coefficient ($k_L a$), which is the product of the liquid-film mass transfer coefficient (k_L) and the interfacial area (a), is generally used for analyzing the global mass transfer mechanism and comparing different operating conditions in a bubble column. However, this $k_L a$ coefficient is global and insufficient to describe mass

transfer mechanisms relating with effects of gas diffusers and liquid phase contamination (Vázquez et al. (1997) and Akosman et al. (2004)). It is therefore necessary to separate the parameters, the k_L coefficient and the interfacial area, in order to provide a better understanding on gas-liquid mass transfer mechanism in bubble column.

Several studies on bubble column were regarded effects of various physical configurations (bubble column dimension and gas diffuser) and operating conditions (superficial gas velocity) on bubble hydrodynamic and mass transfer parameters (Hébrard et al. (1996) and Loubière et al. (2003)). Most of those results were in small bubble column, which should be validated in larger scale column with different gas diffusers. Higher superficial velocity of bubble should be also applied. Moreover, the role of orifice physical characteristic (size, thickness, and elasticity) should be well analyzed to propose a suitable bubble column design and operation for aeration and absorption processes. Therefore, the objective of this work was to study and validate influences of physical configurations and operating conditions on bubble column performance in terms of bubble hydrodynamic, and mass transfer parameters. Different bubble column dimension and gas diffusers (i.e., single and multiple orifices as well as rigid and flexible orifices) were applied. Air and tap water were respectively selected as absorbate and absorbent for operating under room temperature ($T = 25^\circ\text{C}$). The local experimental methods for measuring the bubble hydrodynamic parameters were applied. Moreover, the method for separately analyzing the liquid-film mass transfer coefficient (k_L) and the interfacial area (a) was used for enhance the absorption efficiency in a bubble column.

3.2 Objectives

- To study the effect of fixable and rigid diffuser on the bubble hydrodynamic and the mass transfer parameters in the different size of bubble column reactor
- To compare the effect of bubble column dimension no mass transfer and bubble hydrodynamic parameters in bubble column reactor

3.3 Literature Review

Bouaifi, (2001) have studied the comparison of the gas hold-up, bubble size, interfacial area and mass transfer coefficients in stirred gas-liquid reactors and bubble columns. The results indicated that there are no important difference between bubble

diameters provided by the two reactors. For the same total power consumption, the interfacial area created by the bubble columns is about 30% higher than that created by the stirred axial dual impeller systems. The volumetric transfer coefficient obtained with bubble columns are higher than those provided by the stirred gas–liquid reactor. This difference is explained by the higher values of interfacial area obtained in bubble columns.

Loubière, (2003) have investigated the bubble formation generated and gas flow rates from flexible orifices (membrane) in no viscid liquid. They found that an increasing gas flow rate intensifies the phenomenon of the bubble spread on the membrane surface. The variation in the bubble diameter at detachment as a function of gas flow rate is logarithmic and its result indicates that small bubbles generated by the membrane remain stable in the face of coalescence or breaking phenomena. The industrial membranes produce bubbles of comparable sizes. Nevertheless, significant differences in the bubble frequencies between membranes are observed, involving different gas hold-up. For the bubbles generated from a flexible orifice, the real forces governing the bubble growth are the buoyancy force, the surface tension force and near detachment the inertial force.

3.4 Materials and Methods

3.4.1. Experimental Setup

The experiment set up is schematically represented in Figure 16. The experiments were conducted in three bubble column configurations as summarized in Table 2. Bubble is generated by an air pump passing through different gas diffusers (5) with the flow rate regulated by a gas flow meter (2). Examples of gas diffusers installation are presented in Figure 16 and Figure 17.

Bubble hydrodynamic parameters were investigated by using the high speed camera with 120 images/sec (3) and image analysis software (4) (Basler Inc., USA). The Unisense oxygen micro sensor with very fast response time (≈ 50 ms) was used for measuring the change of dissolved oxygen concentration. All chemical solutions were injected at the top of the column. Note that sodium sulfite (Na_2SO_3) was used for decreasing amount of dissolved oxygen in water before $k_L a$ coefficient was analyzed.

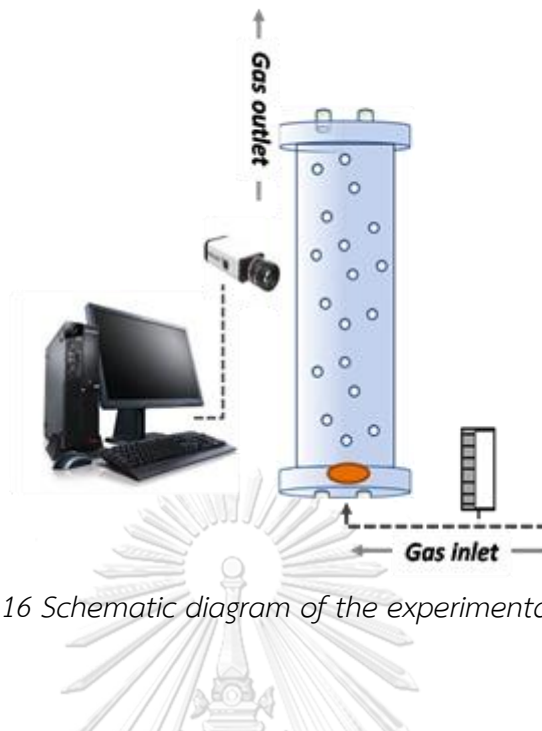


Figure 16 Schematic diagram of the experimental setup.

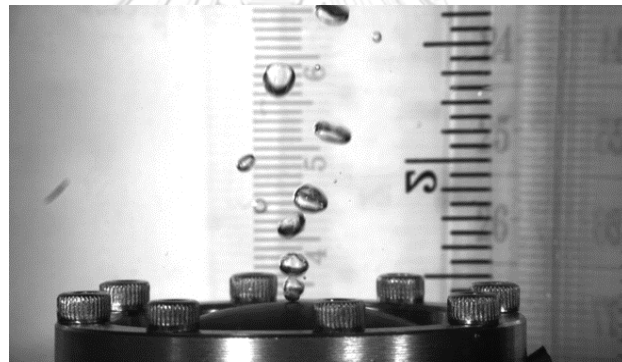


Figure 17 Installation of flexible orifice in bubble column - Fixable (F1).

3.4.2. Gas Diffusers Used in This Study

Air diffusers used in this work were 2 rigid diffusers (R1 and R2) and 5 flexible diffusers (Fo1, F1, F2, F3 and F4) as shown in Figure 18. Bubbles were generated by a diffuser that located at the membrane center. In case of small bubble column configuration, gas diffusers with single orifice (R1, F1 and Fo1) were applied. Therefore, it was necessary to close several holes without modifying the elastic properties of flexible diffuser.

The physical characteristics and the diffuser configuration in bubble column can be summarized in Table 2. Without liquid phase, the flexible orifice size measurements were based on the joint use of Sony DXC 930P 3CCD color camera

(Japan) and Nikon SMZ-U microscope (Japan). The image processing was performed by the Visilog 5.4 software (C++ program).



Figure 18 different types of gas diffusers used in this study.

Table 2 physical Characteristic of Diffuser and Operating Conditions.

Bubble column configuration			Gas diffuser types and characteristic			
	Diameter (cm)	Height (cm)		Type	Name	Thickness
Small	5	30		Rigid	R1	-
			Single orifice	Flexible	F1	2.06
				Flexible	Fo1	2.15
Medium	10	100		Rigid	R2	-
			Multiple orifice	Flexible	F2	1.65
				Rigid	R2	-
Large	15	100		Flexible	F3	2.9
				Flexible	F4	2.08

3.4.3. Determination of Bubble Hydrodynamic Parameters

In order to achieve statistically significant distribution, the average bubble diameter (D_b) in this study was deduced from the measurement of 150-200 bubbles. The average bubble

Formation frequency, f_B , (i.e., the number of bubbles formed at the membrane orifice per unit time) was determined as in Eq.(1). (Painmanakul et al., 2004)

$$f_B = \frac{Q_G}{V_B} \quad (3.1)$$

Where V_B is the average detached bubble volume and Q_g is the gas flow rate. Owing to the image processing system, the terminal rising velocity of bubble (U_B) can be estimated from the distance covered by a bubble (D) in two frames with known capture duration (T_{frame}) was determined as in Eq.(2).

$$U_B = \frac{D}{T_{frame}} \quad (3.2)$$

From Painmanakul et al. (2005), the interfacial area (a) is a function of f_B , U_B , and D_B . It can be expressed as in Eq. (3.3) where H_L and V_{Total} are height and overall volume of liquid phase in a column. S_B is a surface area of a bubble.

$$a_r = \frac{(Q_g + Q_{gr})}{V_{Br}} \times \frac{H_L}{U_{Br}} \times \frac{S_{Br}}{V_{Total}} = \frac{6}{D_{Br}} \cdot \frac{\epsilon_{gr}}{(1 - \epsilon_{gr} - \epsilon_{sr})} \quad (3.3)$$

3.4.4. Determination of Mass Transfer Coefficients

The experimental approach presented in Painmanakul et al. (2005) was used to determine the specific interfacial area (a) and the corresponding volumetric mass transfer coefficient ($k_L a$). Due to the absorption of oxygen in water, the gas-liquid mass transfer mechanism is governed by the liquid phase. The volumetric mass transfer coefficient ($k_L a$) then can be determined from Eq. (3.4)

$$\frac{dc}{dt} = k_L a (C_L^S - C) \quad (3.4)$$

C_L is the dissolved oxygen concentration, and C_L^S is the saturation a is the product of the liquid-side mass transfer coefficient (k_L oxygen concentration in liquid

phase. The coefficient (k_L) and the interfacial area (a). Therefore, k_L coefficient can be simply determined by Eq. (5);

$$k_L = \frac{k_L a}{a} \quad (3.5)$$

In this study, the relation between physical properties of diffusers and oxygen transfer efficiency are expected to be investigated, through the measurement of volumetric mass transfer coefficient and observation of bubble hydrodynamic parameters. Therefore, comparing the different type of diffusers and different size of bubble column. Then propose the suitable diffuser and bubble column dimension with concerning both term of oxygen transfer efficiency as show in Figure 19.

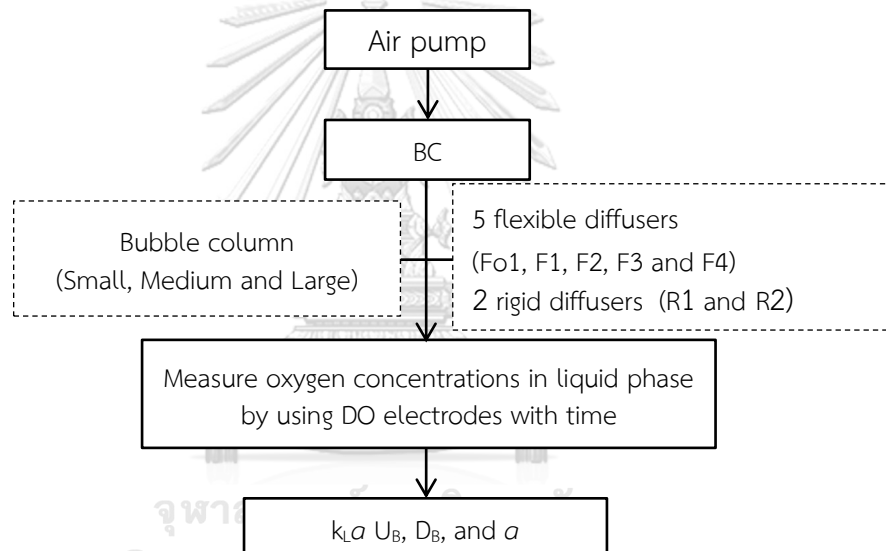


Figure 19 diagram of studying effect of bubble column dimension on mass transfer and Bubble hydrodynamic parameters in BC.

Table 3 Variable of studying effect of bubble column dimension on mass transfer and Bubble hydrodynamic parameters in BC.

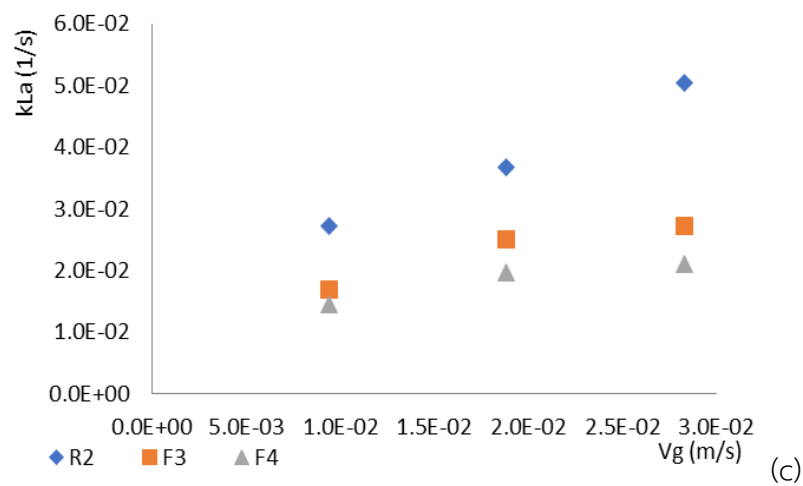
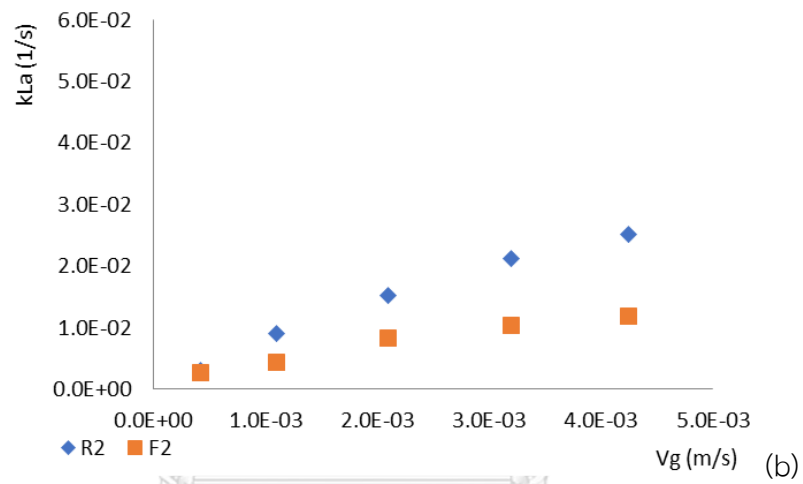
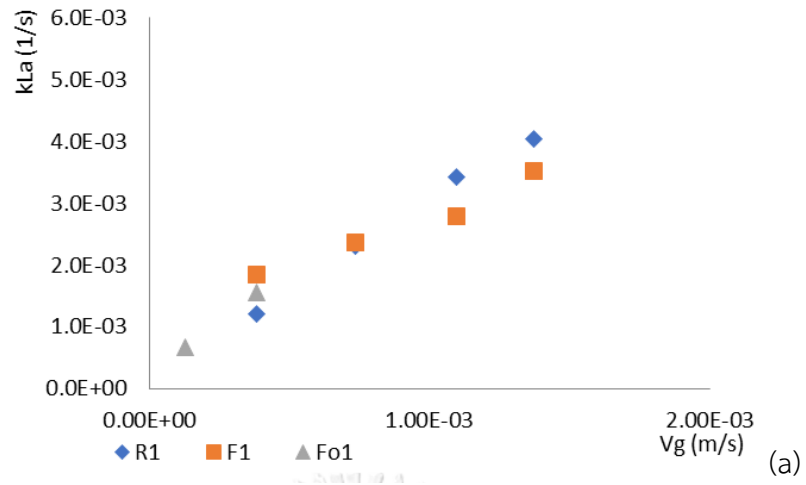
Fixed Variable	Parameter
Gas phase (absorbate)	Oxygen
Liquid phase (absorbent)	Tap water
Independent Variable	Parameter
Reactor	Bubble column (Small, Medium and Large)
Diffuser	5 flexible diffusers (Fo1, F1, F2, F3 and F4) 2 rigid diffusers (R1 and R2)
Gas flow rate	2.5, 5, 10, 15, and 20 L/min
Dependent Variable	Parameter
Mass transfer parameters	$k_L a$
Bubble hydrodynamic parameters	U_B , D_B , and a

3.5 Results and Discussion

3.5.1. Volumetric Mass Transfer Coefficient ($k_L a$)

Figure 19 presents the variation of $k_L a$ values with the superficial gas velocity (V_g) for different gas diffusers (rigid and flexible) and bubble columns types. Fig.20 (a)-(c) respectively present the $k_L a$ coefficients from the small, medium, and large column (i.e., column diameters of 5, 10, and 150 cm) with a summary in Figure 20(d).

As can be seen, the $k_L a$ coefficients were obviously affected by the V_g . The increase of bubble number in the column can enhance the total surface of bubble for gas-liquid mass transfer. The $k_L a$ values of $0.001 - 0.05 \text{ sec}^{-1}$ were obtained for the V_g of $0.000425 - 0.0283 \text{ m/sec}$ in all experiments. The coefficients obtained from larger column were higher than those of the smaller one. Influences of V_g and Q_g should be applied for describing the results.



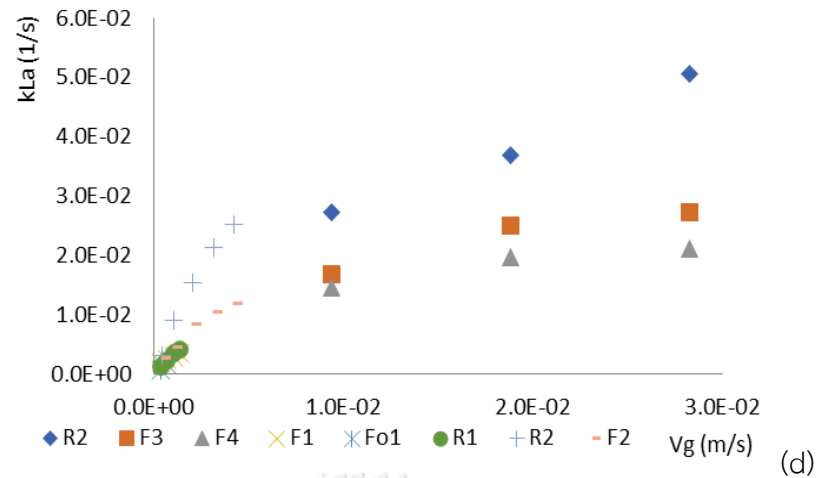


Figure 20 volumetric mass transfer coefficients (k_La) vs. superficial gas velocity (V_g) in (a) small bubble column, (b) medium bubble column, (c) large bubble column, and (d) summary.

Concerning effects of diffusers, the difference of k_La coefficients was more pronounced in the larger column as shown in Fig 20 (d). The diffusers with single orifice (R1, F1 and Fo1) provided similar k_La coefficients from small column. However, the k_La obtained in the medium column with rigid orifice with multi-orifice (R2) were higher than those of flexible one (F2). The same tendency can also be observed in large column as k_La (R2) > k_La (F3) > k_La (F4). These results presented the advantage of using rigid orifice in bubble column, especially for large diameter. Moreover, the experimental results in this work can be validated by using the same rigid diffuser (R2) in medium and large column. The k_La coefficients were increased continuously with the superficial gas velocity. Therefore, the simple prediction model can be proposed as expressed in equation 3.6.

$$k_La = 0.5643 \times V^{0.7332} \quad (3.6)$$

The k_La values calculated by Eq. (3.6) are compared with the experimental results in Figure 20a b and c for different gas diffusers (rigid and flexible) and bubble columns types (small, medium and large) respectively. The discrepancy range of 35% can be noticed. The differences of bubble column configurations and operating conditions should be responsible for these results. In addition, the k_La coefficients are generally too global and difficultly evaluated in practical application. Therefore, local measurement of bubble diameter and the interfacial area (a) was performed and

presented in next section to provide a better understanding on effects of gas diffusers and the gas–liquid mass transfer mechanisms.

3.5.2. Bubble Diameter (D_B)

Variations of bubble diameter (D_B) with the superficial gas velocity (V_g) in the small column are depicted in Figure 21(a). Rigid diffusers with single orifice (R1) tended to produce constant bubble sizes (> 4.5 mm) as the orifice was unchanged with increased gas flow rate ($D_{OR} = 0.5$ mm). On the contrary, bubble sizes from the flexible diffuser with single orifice (F1 and Fo1) were increased with the gas flow rate as the orifice sizes of the diffusers were enlarged at larger gas flow rate.

Figure 21 (b) depicts the growth of orifice size (0.25-0.55 mm) of flexible diffuser (F1) with increased V_g . It was worth noting that the bubble diameter was about 10 times of the orifice size. These results conformed to the data from flexible diffusers with small orifice size of 0.12-0.19 mm (Fo1) as well as the data from single orifice diffuser [4, 11]. The importance of orifice size and its characteristic can be concluded, especially for diffuser with single orifice. It should be noted that the flexible diffuser (Fo1) cannot be operated at higher V_g due to its manual fabrication and physical properties. The results therefore cannot be used for comparing with other diffusers (F1 and R1) regarding effects of superficial gas velocity.

For the results from R1 and F1, the difference in D_B was more pronounced at low superficial gas velocities ($V_B < 7.5 \times 10^{-4}$ m/sec). At low V_g , the difference in bubble diameter directly linked to the surface tension. The balance between the surface tension and the buoyancy force during the bubble growth and detachment was consequently different for dissimilar orifice diameter. However, a bubble diameter was no longer controlled by the force balance at higher V_g , but instead governed by the power dissipated in a liquid phase. This can cause the break-up of and coalescence of bubbles (Loubière et al. (2004) and Lessard et al. (1971))

Bubble sizes generated with different types of multi-orifice diffusers and column dimensions (medium and large column) is shown in Figure 22(a) and (b). Bubble sizes from the single orifice diffuser in the small column (2.5-6 mm) were larger than those from the multiple-orifice diffuser in the medium and the large columns (1.5-3.5 mm). Influence of the orifice characteristic (i.e., flexible or rigid) cannot be clearly seen as bubble sizes seemed to be constant at every condition. This can confirm effects of power dissipated in the liquid causing the bubble break-up and coalescence phenomena at high superficial gas velocity ($V_g > 7.5 \times 10^{-4}$ m/sec). Furthermore, the same ranges of bubble size (1.75-2.3 mm) were found from the rigid

diffuser (R2) in the medium and the large column, but smaller than bubbles generated from the R1 diffuser. The orifice size should be responsible for these results since the orifice diameter of R2 (0.25 mm) was smaller than that of R1 (0.5 mm).

In the medium column, bubble sizes from the flexible diffusers (F2, F3, and F4) were similar and close with the R2. The difference can be noticed in the large column with higher V_g that D_B from the F3 and F4 diffusers were obviously greater than that of R2 since the orifice sizes were enlarged with the gas velocity. According to the physical properties of diffusers in Table 2, the smallest bubbles were found from the F2 diffuser, which was the thinnest one (1.65 mm). Therefore, it can be stated that the physical property can affect the orifice size due to the elasticity or deflection at the centerline. The thin flexible diffuser provided small orifice size and smaller bubble size as a result

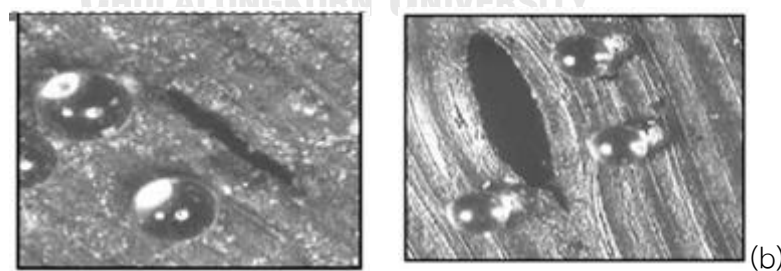
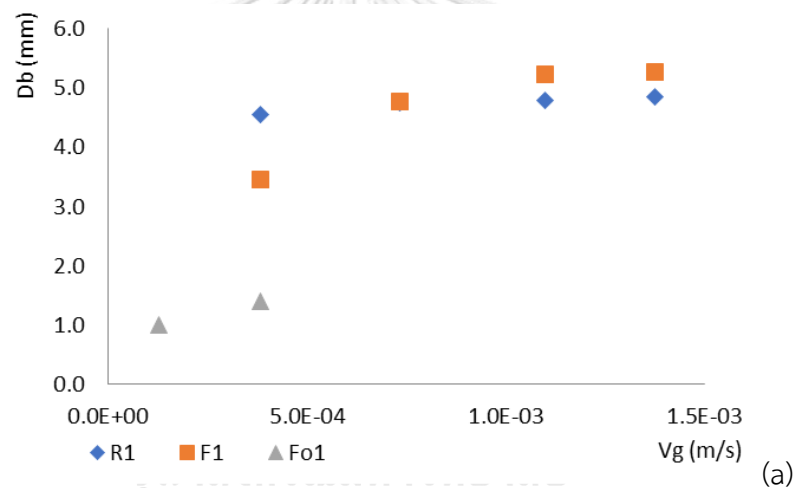


Figure 21 (a) Bubble diameter (D_B) vs. superficial gas velocity (V_g) for small bubble column, (b) example of orifice size obtained with flexible diffuser with single orifice (F1) at different superficial gas velocities.

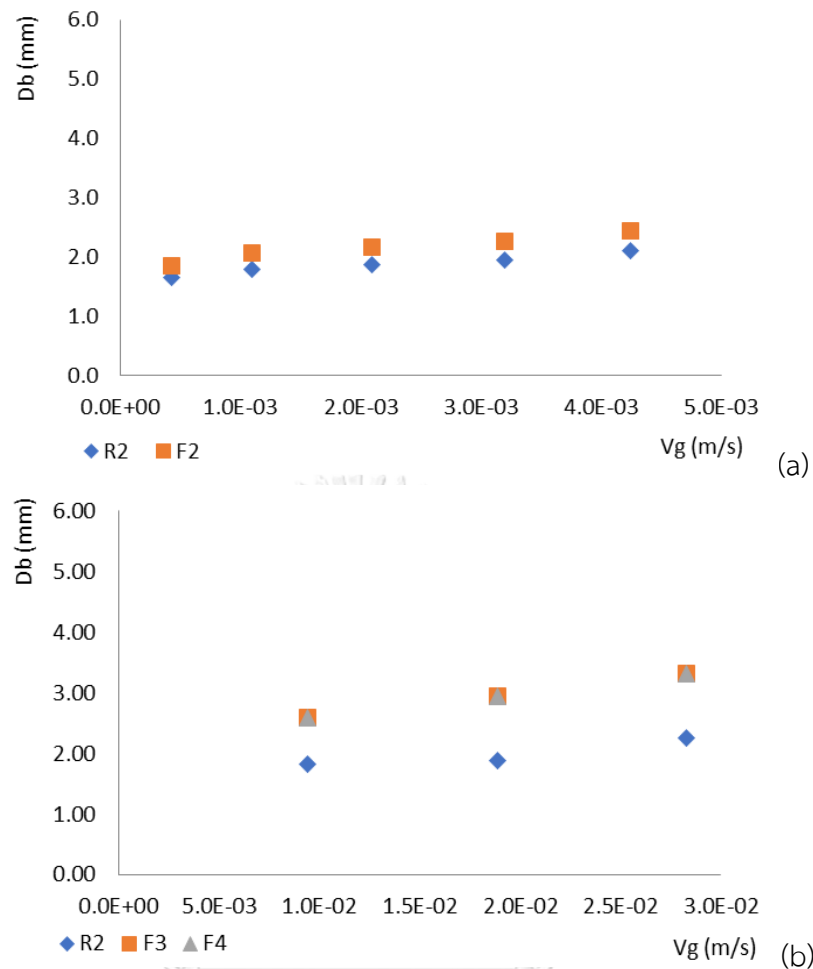


Figure 22 Bubble diameter (D_B) vs. superficial gas velocity (V_g) for (a) medium bubble column and (b) large bubble column.

In conclusion, the diffuser properties as in Table 2 can impact the generated bubble sizes. The rigid diffuser should be operated at high superficial gas velocity in a large bubble column as the produced bubble size was related with the orifice size. However, this kind of diffuser usually encounters the clogging problem, which should be well considered in the operation. In the case of flexible diffuser, the orifice size and the velocity V_g have to be controlled for maintaining the generation of small bubbles. In the next part, the interfacial area, which is one of key parameters in the gas-liquid mass transfer study, was determined from bubble sizes obtained experimentally.

3.5.3 Interfacial Area (a)

Figure 23 displays the relation between bubble velocities and bubble diameters in different bubble columns and operating conditions with the experimental

U_B values obtained by Grace & Wairegi. (1998). The bubble velocity (U_B) of 0.15 - 0.25 m/sec were obtained from the diameters of 1.6 - 6.2 mm. Small bubbles in the large column tended to have lower rising velocity than in the small column due to effects of power dissipated in the liquid resulting in the break-up of bubbles. Bubbles then obstructed movement of each other out of the column. Moreover, it can be stated that small bubbles (low U_B values) can enhance the retention time of bubble in column, thus increasing the bubble specific interfacial area (a).

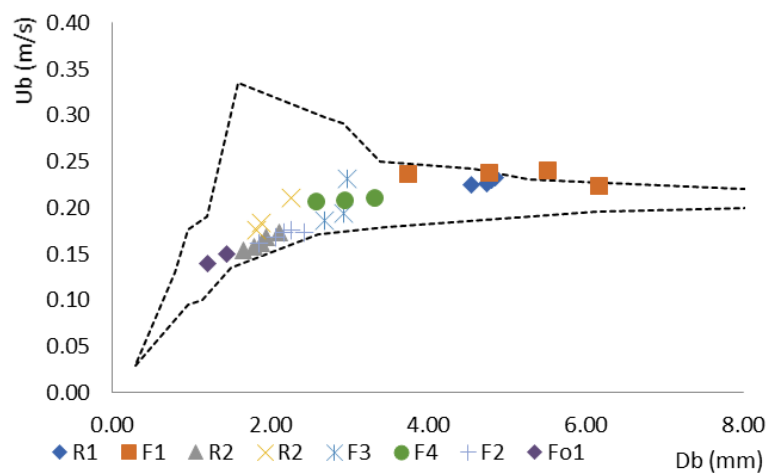
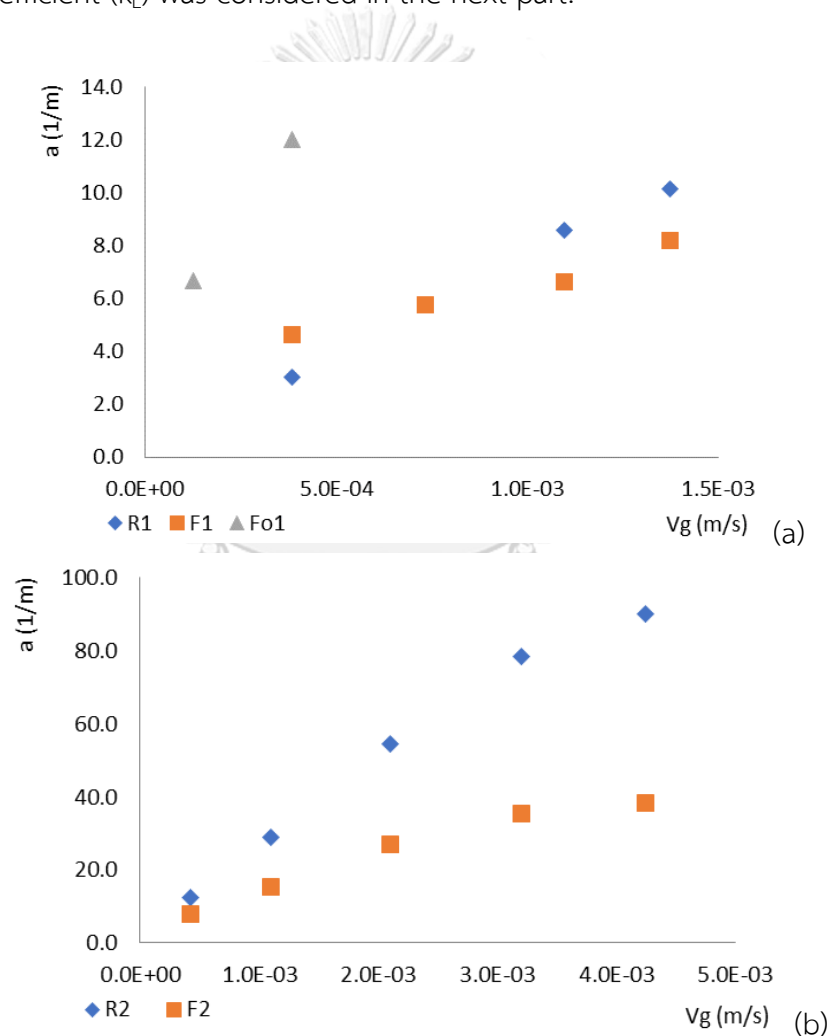


Figure 23 Bubble velocity (U_B) vs. bubble diameter (D_B).

By using the experimental results of the bubble sizes and their rising velocities, the bubble formation frequencies (f_B) at different gas superficial velocities can be calculated. The local interfacial area (a) can then be determined. Figure 24 presents the relation between the interfacial area (a) and the superficial gas velocity for different diffusers (F1, Fo1, F2, F3, F4, R1 and R2) and bubble column dimensions (small, medium and large) used in this work. For gas diffusers with single orifice, the interfacial areas (a) varied between 2.5 and 13 m^{-1} while superficial gas velocities were between 0.0002 and 0.0015 mL/sec as shown in Figure 24(a). Whatever the orifice type, the values of a were linearly increased with the superficial gas velocities. The values obtained from Fo1 were obviously greater than those of F1 and R1, which corresponded to the lowest D_B and U_B as aforementioned. However, the physical property of diffuser (Fo1) in terms of elasticity and shear stress should be well considered in practical operation, especially at higher superficial gas velocity. Regarding effects of diffuser and column types, interfacial area were rose along with V_g as shown Fig. 24 (b), (c) for the medium and large columns, respectively. Moreover, the increase of the cross-sectional area of column also played a role since the gas flow rate was

enhanced as a result. The a values obtained from the rigid diffuser (R2) were clearly greater than those of flexible diffusers (F2, F3 and F4). Small bubbles with low rising velocity from the rigid orifice (R2) were responsible for this result. Moreover, the results of the R2 diffuser were validated in the medium and the large columns as increased with V_g depicting in Figure 24(d). This result conformed to those obtained with the $k_L a$ coefficient as in Figure 22(d). Note that the difference in a can be clearly observed from the Fo1 diffuser in the small column whereas the related $k_L a$ coefficients were close to those obtained from different diffusers (F1 and R1) as shown in Fig. 21(a). For a better understanding of the gas-liquid transfer phenomena, the liquid-side mass transfer coefficient (k_L) was considered in the next part.



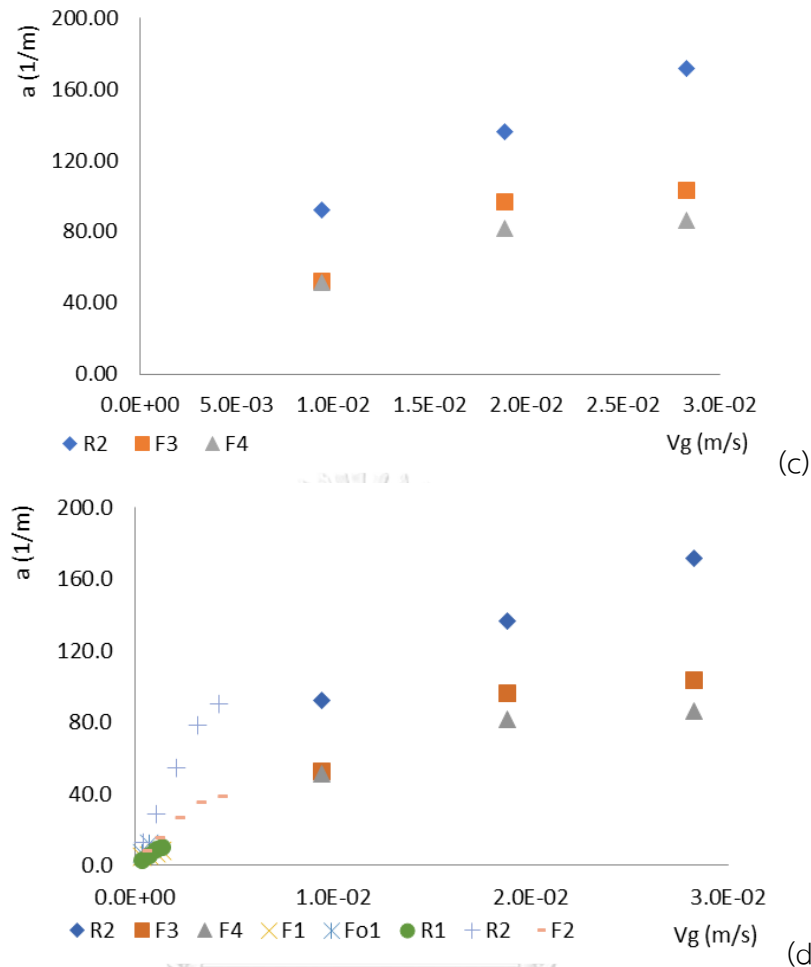


Figure 24 Interfacial area (a) vs. superficial gas velocity (V_g) for (b) small bubble column, (c) medium bubble column, and (d) large bubble column.

3.5.4 Liquid-side Mass Transfer Coefficient (k_L)

The k_L coefficient can be calculated from the experimental values of the volumetric mass transfer coefficient (Fig.21 and 22) and the interfacial were scatter since the calculation of k_L area (Fig.25) by Eq. (3.5). The values of k_L could possess errors from the measurements of both $k_L a$ and a . The average and maximum experimental errors for determining the k_L were estimated at 10% and 15%, respectively [10]. Figure 25 shows the variation of the liquid-side mass transfer coefficient (k_L) with the superficial gas velocity (V_g) for different gas diffusers and bubble column types.

According to Figure 25, the obtained k_L varied between 1×10^{-4} and 4×10^{-4} m/sec for V_g in the range of 0.0002-0.03 m/sec. At every operating condition, the k_L values tended to be constant for the gas flow rates greater than 0.0004 m/sec. On the

contrary, k_L was increased with V_g at lower velocities. Figure 26 displays the variation of k_L with the bubble diameter (D_B) for the different gas diffusers and bubble columns. This plot was applied for analyzing and comparing the results in this study with the three zones of k_L coefficients proposed by Painmanakul et al. (2005) and Sardeinget al. (2006).

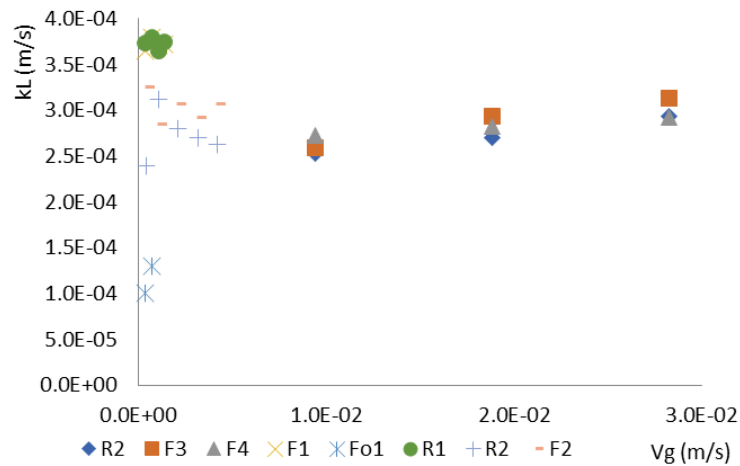


Figure 25 Liquid-side mass transfer coefficient (k_L) vs. superficial gas velocity (V_g) or different bubble column configurations.

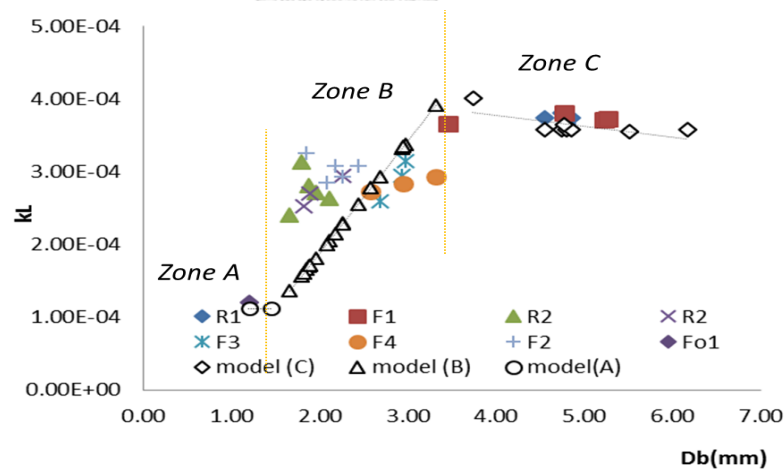


Figure 26 Liquid-side mass transfer coefficient (k_L) vs. bubble diameter (D_B).

According to Figure 26, the k_L larger than 3.5 mm and then slightly decreased up to the D_B of 1.5 mm before remaining constant until 1.5 mm. The dimension of bubble columns cannot affect the k_L coefficient. The coefficient k_L only depend on bubble sizes due to a modification of the gas-liquid interface nature (size and shape of generated bubbles) coupled with local hydrodynamic changes (terminal rising

bubble velocity and drag coefficient of bubbles). Three zone of the variation between k_L and D_B can be observed in Figure 26 as follows.

1) Zone A ($d_B < 1.5\text{mm}$): k_L are low for small bubbles (about 1×10^{-4} m/sec) [16] corresponded with the results obtained from the flexible diffuser (Fo1).

2) Zone B ($1.5 < d_B < 3.5\text{mm}$): k_L values were increased (1×10^{-4} to 4×10^{-4} m/sec) with the bubble diameter. The modification of the bubble shape (from sphere to ellipsoid) as well as the bubble interface should be responsible for these result [15]. The diffusers (R2, F2, F3, and F4) can provide the bubble sizes and the k_L coefficient in this zone.

3) Zone C ($d_B > 3.5\text{mm}$): k_L values were independent on bubble diameters conforming with the results of Higbie. R., (1953). The k_L were constant for larger bubble size behaving as fluid particles with a mobile surface. This zone can be related with the results obtained from the diffusers (F1 and R1).

Table 4 show summarizes the existing model for prediction of liquid-side mass transfer coefficient (k_L). Note that, the value of surface coverage ratio at equilibrium (se) in case of clean liquid phase, used in this work. The comparison between the experimental results and the predicted values from the existing models is presented.

Table 4 Prediction Model for Liquid-Side Mass Transfer Coefficient (k_L)

Prediction model for k_L coefficient	References
Zone A $k_L = \frac{D}{d_B} (2 + 0.6Re^{1/2}Sc^{1/3})$	Frossling equation Treybal [16]
Zone B $\frac{k_L - k_L^{ZoneA}}{k_L^{ZoneC} - k_L^{ZoneA}} = (1 - S_c) \times \left[\frac{d_B - d_B^1}{d_B^0 - d_B^1} \right]$	Sardieng et al. [15] d_B^1 is equal to 1.5 mm d_B^0 is equal to 3.5 mm
Zone C $k_L = 2 \sqrt{\frac{D}{\pi \cdot t_c}} = 2 \sqrt{\frac{D \cdot U}{\pi \cdot D_B}}$	Higbie [17]

This result shows that a good agreement between the experimental and the predicted k_L coefficients was obtained (average difference of $\pm 15\%$), especially for Zone A and Zone C. However, more experimental data are necessary for more accurate predicting and validating the Zone B correlation (average difference of $\pm 40\%$). These zone related with the diffusers (R2, F2, F3 and F4) operated at high superficial gas

velocities in medium and large columns. The bubble break-up and coalescence phenomena due to the power dissipated in the liquid phase should be responsible for these results. In the future, effects of the geometrical transition from the sphere to ellipsoid of bubbles on the k_L coefficient should be focused, especially for Zone B in order to propose more precision model for mass transfer parameters ($k_L a$ and k_L). Due to low k_L in Zone A, it can be stated that the generation of tiny bubbles ($D_B < 1\text{mm}$) was unnecessary to increase the mass transfer capacity. The increase of interfacial area from generated fine bubbles can be compromised by the great decrease of the k_L coefficient. These results conformed to the case of diffuser (Fo1) in the small bubble column. Even the increase of a can be clearly observed, the related $k_L a$ coefficients were close to those observed from the different diffusers (F1 and R1). Therefore, within the range of bubble sizes (1.5-2.3 mm) generated by the R2 diffuser, high interfacial area and moderate k_L coefficient can be obtained. These can provide the maximum $k_L a$ coefficient for gas-liquid mass transfer. In the case of a gas-liquid reactor equipped with gas diffuser, the total specific power consumption (P_g) for mixing condition could be related to the total gas pressure drop as in Eq. (7).

$$\frac{P_g}{V_{Total}} = Q \times \frac{\Delta P_{Total}}{V_{Total}} = Q \times \frac{\rho_L g H_L + \Delta P}{V_{Total}} \quad (3.7)$$

The total gas pressure drop (ΔP_{Total}) is a function of the liquid height ($\rho_L g H_L$) and the specific sparger pressure drop (ΔP), which is increased with the gas velocity through the orifice ($V_g = Q_g/A_{OR}$). From Painmanakul et al. (2005), the value of ΔP increases with the gas flow rate as well as the decrease of hole area or orifice size for small bubble generation. The drawback in term of energy consumption for small bubble size has to be taken into account as the important consequences for using the bubble column in real operating condition.

In conclusion, the influence of gas diffuser in bubble column can be concluded and validated within the different bubble column configurations and operating conditions. To obtain high interfacial area and $k_L a$ coefficient, small orifice size should be used for generating the small bubbles. From the obtained results, the advantage of rigid diffuser operated at high superficial gas velocity in the large bubble column can be found. However, the clogging problem of a diffuser must be taken into account. For flexible diffuser, the control of superficial gas velocity and orifice size should be well considered in order to maintain a small bubble generation in the reactor. Moreover, it was unnecessary to generate numerous fine bubbles at high superficial gas velocity for enhancing the $k_L a$ coefficient and absorption efficiency in the bubble

column. The increase of values can be withdrawn by the great decrease of the k_L coefficients as well as the increase of related power consumption.

3.6 Conclusions

The objective of this work was to study influences of bubble column dimensions, gas diffuser types, and superficial gas velocities (V_s) on bubble column performance in terms of bubble hydrodynamic and mass transfer parameters. For this purpose, the methods for determining the volumetric mass transfer coefficient ($k_L a$), bubble size (DB), interfacial area (a), and liquid-film mass transfer coefficient (k_L) were applied to enable the absorption efficiency in a bubble column. The following results were obtained:

- The $k_L a$ coefficients increased with the superficial gas velocity (V_g) and the bubble column size. The prediction model was proposed with the average difference between the experimental and predicted k_L of $\pm 35\%$:

$$k_L a = 0.5643 \times V^{0.7332} \quad (3.8)$$

- For single orifice gas diffuser, physical property of gas orifice can clearly influence the generated bubble size, especially at low superficial gas velocity. Less effect was found at higher V_g due to the power dissipated in the liquid resulting in the bubble break-up and coalescence phenomena;
- In the case of gas diffuser with multiple orifices, effects of orifice size, diffuser thickness, and superficial gas velocity were noticed on the modification of generated bubble size presence in bubble column;
- At highest interfacial area, the advantage of rigid diffuser can be obtained for high V_g operation in large bubble column due to the generation of small bubbles with low rising velocity;
- Three zones of k_L coefficients with different bubble sizes (1×10^{-4} m/sec in Zone A, 1×10^{-4} m/sec in Zone B, and 4×10^{-4} m/sec in Zone C) can be found. The result was validated with different bubble column configurations and operating conditions;
- To enhance the k_L coefficient and absorption efficiency in bubble column, it was unnecessary to generate numerous fine bubbles at high superficial gas

velocity for highest interfacial area as this a can be cancelled out by the great decrease of the k_L coefficients as well as the increase of power consumption.

In the future, further study should be conducted on effects of different liquid phase contamination in order to validate the role of bubble column configuration and operating condition obtained in this work as well as provide a better understanding on gas-liquid mass transfer mechanism. To propose more accurate model for predicting mass transfer parameters (k_L coefficients), more experimental data are required, especially for the gas diffuser or bubble size ranging within Zone B ($1.5 < d_B < 3.5$ mm). Finally, the industrial-scale bubble column (larger column dimension and higher superficial gas velocity) should be studied for extending the lab-scale results into the practical operating condition. a and k_L .



CHAPTER 4

STUDY OF ABSORPTION PROCESS IN BUBBLE COLUMN REACTOR (BC): MASS TRANSFER AND HYDRODYNAMIC

4.1 Introduction

Bubble column reactors belong to the general class of multiphase reactors which consist of three main categories namely, the trickle bed reactor (fixed or packed bed), fluidized bed reactor, and the bubble column reactor. A bubble column reactor is basically a cylindrical vessel with a gas distributor at the bottom. The gas is sparged in the form of bubbles into either a liquid phase or a liquid–solid suspension. These reactors are generally referred to as slurry bubble column reactors when a solid phase exists. Bubble columns are intensively utilized as multiphase contactors and reactors in chemical, petrochemical, biochemical and metallurgical industries. They are used especially in chemical processes involving reactions such as oxidation, chlorination, alkylation, polymerization and hydrogenation, in the manufacture of synthetic fuels by gas conversion processes and in biochemical processes such as fermentation and biological wastewater treatment. Some very well-known chemical applications are the famous Fischer–Tropsch process which is the indirect coal liquefaction process to produce transportation fuels, methanol synthesis, and manufacture of other synthetic fuels which are environmentally much more advantageous over petroleum-derived fuels.

Recent research with bubble columns frequently focuses on the following topics: gas holdup studies, bubble characteristics, flow regime investigations and computational fluid dynamics studies, local and average heat transfer measurements, and mass transfer studies. The effects of column dimensions, column internals design, operating conditions, i.e. pressure and temperature, the effect of superficial gas velocity, solid type and concentration are commonly investigated in these studies. Many experimental studies have been directed towards the quantification of the effects that operating conditions, slurry physical properties and column dimensions have on performance of bubble columns. Although a tremendous number of studies

exist in the literature, bubble columns are still not well understood due to the fact that most of these studies are often oriented on only one phase, i.e. either liquid or gas.

However, the effects of the liquid-bubble hydro-dynamics on mass transfer parameter by adding plastic media have not much studied in literature. To full fill this gaps, the purpose of this study improve the efficiency of bubble column reactor. Moreover, it was studied the effect of shape and amount of small size plastic media on oxygen mass transfer and hydrodynamic parameters (Q_g , ϵ_g , D_B , U_B and a) at a various gas flow rate in bubble column reactor. The finally explained the relation of air circulation rate on mass transfer parameter in bubble column reactor.

4.2 Objective

- To understand the effect of gas diffuser, operating condition on the bubble hydrodynamic and the mass transfer parameters for gas - liquid absorption process in Bubble column reactor.
- To study the effect of using plastic media in the different shape and concentration on the bubble hydrodynamic and the mass transfer parameters in Bubble column reactor.

4.3 Literature Review

Chen et al. (2014) studied to use DEEA/EEA mixed solvent as an absorbent and controlled pH value to explore the capture of CO₂ in the bubble column scrubber. This experiment study the effect of operation parameter, including the pH of the solution, gas flow rate, EEA/DEEA concentration on the removal efficiency, absorption rate, overall mass-transfer coefficient providing reference for operation and design. The result was show that the data obtained were in the range of 1.26×10^{-4} - 11.80×10^{-4} (mol/s.l), 0.0728-0.8395 (1/s), and 28 98.66% for absorption rate mass transfer rate, and removal efficiency, respectively In addition, the test of DEEA/EEA mixed solvent demonstrates that the mixed solvent can capture a large amount of CO₂ gas as compared with other solvents. Whereas, the absorption rate and overall mass transfer

coefficient obtained in this work are comparable with previous study and higher than obtained in packed bed.

Painmanakul et al., (2013) study the hydrophobic VOCs absorption in a bubble column in terms of bubble hydrodynamic and mass transfer parameters. The benzene was chosen as the hydrophobic VOCs in this study. The effects of different gas spargers (4 sizes of rigid orifices diameter) and liquid phases (tap water, aqueous solution with non-ionic surfactant and lubricant oily-emulsion) as absorbent, the relation between bubble hydrodynamic parameters (bubble size, bubble formation frequency, and bubble rising velocity) and the volumetric mass transfer coefficient ($k_L a$) were investigate. Moreover, the last part of experiment study the hydrophobic VOCs treatment efficiency in a bubble column. The result showed that the gas diffuser with 0.65 mm in orifice diameter (D_{OR} 0.65) is chosen as the suitable gas diffusers due to the smallest bubble sizes generated. This leads to the highest interfacial area (a) for mass transfer mechanism that occurs for VOCs absorption in a bubble column. The volumetric mass transfer coefficient ($k_L a$) increases with the gas flow rate regardless of the liquid phases and the $k_L a$ coefficients of lubricant oily-emulsion and non-ionic surfactants at different concentrations are smaller than those of tap water.

Painmanakul et al., (2005) studied the effect of liquid properties (surfactants) on bubble generation phenomenon, interfacial area and liquid-side mass transfer coefficient was investigated. The measurements of surface tension (static and dynamic methods), critical micelle concentration (CMC) and the surface coverage ratio were explained the effects of surfactants on the mass transfer efficiency and also used tap water and aqueous solutions with surfactants (cationic and anionic) were absorbent. The result showed that the k_L values for both surfactants are significantly smaller than those of the water and the volumetric mass transfer coefficient increases with the gas flow rates. Whatever the liquid phases and the $k_L a$ values for both surfactants are significantly smaller than the result from water. The correlation was proposed from this study, Equation used the surface coverage ratio, has allowed a quite good agreement between the experimental and predicted k_L (average difference about 10%)

$$k_L = k_L^1 s_e + k_L^0 (1 - s_e) \quad (4.1)$$

4.4 Materials and Methods

4.4.1 Experimental Setup

This research focus on study the effect of using plastic media on mass transfer ($k_L a$ and k_L) and the bubble hydrodynamic parameters (Q_g , ϵ_g , D_{Br} , D_{Bd} , U_{Br} , U_{Bd} and a). The experiment were set up in a cylindrical acrylic column with 0.15 m inside diameter and 1 m in height. BC was setup an acrylic plate for liquid recirculation. Moreover, mass transfer determination, liquid phase was removed dissolved oxygen by using sodium sulphite (Na_2SO_3) after that the aeration was conducted by air compressor which supplied air pass through the sparger at the bottom of column. The schematic diagram was showed in Figure 27. Air flow rate various from 2.5 to 15 l/min. The bubble hydrodynamic mechanisms are investigated by the high speed camera (100 images/sec) and image analysis program is used to determine the bubble hydrodynamic parameters. The bubbles are generated by rigid diffuser which located at the bottom of column. Plastic media were added into the bubble column at 2% 5% 10% and 15% v/v in the different shapes (figure 28). For plastic media characteristics were showed in table 5.

Table 5 Plastic media characteristics

Media Shape	Bed porosity, ϵ	Surface area, A (mm ²)	Volume, V (mm ³)	Bed porosity, ϵ (g/mm ³)
Ring (a)	0.68	156.69	49.48	0.000950
Circle (b)	0.38	43.05	26.56	0.000941
Rod (c)	0.39	40.07	29.35	0.001022
Square (d)	0.30	38.43	17.69	0.000961

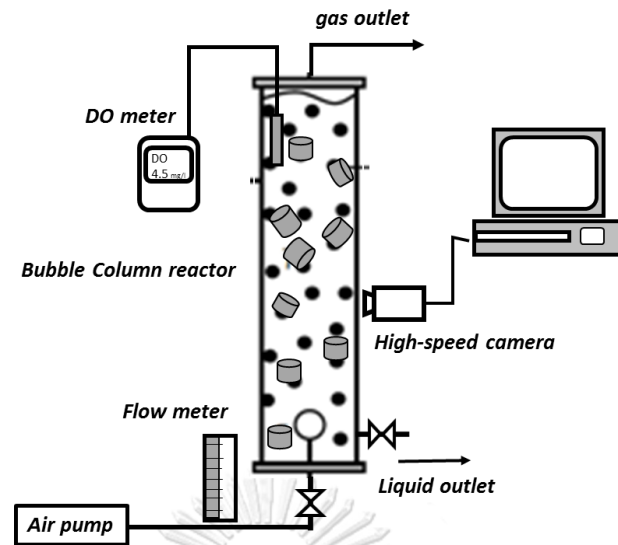


Figure 27 the experiment set up.

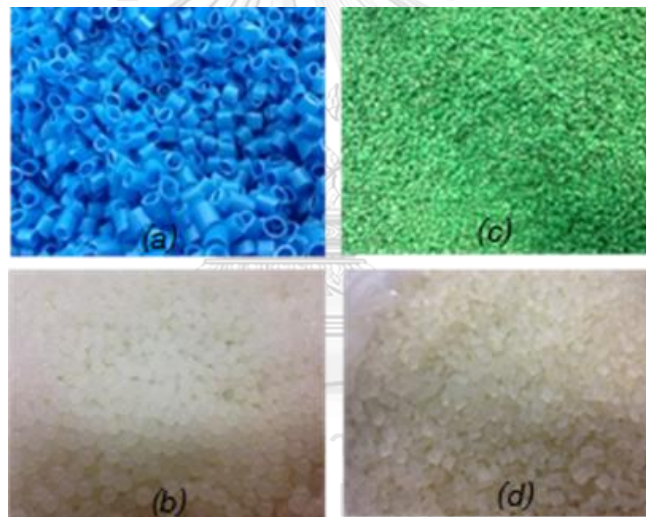


Figure 28 Shape of plastic media (a)Ring, (b)Circle, (c)Rod and (d)Square.

4.4.2. Method for determining the mass transfer and bubble hydrodynamic parameter

The volumetric mass transfer coefficient ($k_L a$)

- Volumetric mass transfer coefficient ($k_L a$)

Volumetric mass transfer coefficient ($k_L a$) was determined the efficiency of mass transfer in the system. The mathematic is used to determine $k_L a$ value be written as following equation: (Painmanakul et al., 2005).

$$\frac{dC}{dt} = k_L a (C^* - C_t) \quad (4.1)$$

Then integration Eq 4.2,
$$\ln(C^* - C_t) = -k_L a t + \ln C^* \quad (4.2)$$

Where C^* and C_t are the saturated concentration of dissolved oxygen in liquid and the concentration of dissolved oxygen measured at time t , respectively. The $k_L a$ values can be estimated graphically from the slopes of linear equation of $\ln(C^* - C_t)$ versus time.

- **Bubble diameter (D_B)**

The measurement of bubble diameter at any flow rate (Q_g) can be determined by image analysis technique. The observed bubbles have mainly ellipsoidal shapes characterized by the major axis, E , which represents the largest distance between two points on a bubble, and the minor axis, e , which represents the smallest length of the bubble. Both axis were measured using ImageJ software and the bubble as the ellipsoid was calculated as follows (Painmanakul et al., 2005);

$$D_B = \sqrt[3]{E^2 e} \quad (4.3)$$

- **Local interfacial area (a)** (Painmanakul et al., 2004)

The gas/liquid interfacial area can be estimated from gas holdup, solid holdup and bubble diameter with the following equation:

$$a = \frac{6}{d_B} \cdot \frac{\epsilon_g}{1 - \epsilon_g - \epsilon_s} \quad (4.4)$$

- **Bubble rising velocity (U_B)**

Bubble rising velocity (U_B) was calculated by taking picture in reactor to analyze its distance (D) at any time frame (T_{frame}). Thus, the U_B was calculated by equation: (Painmanakul et al., 2005)

$$U_B = \frac{D}{t_{frame}} \quad (4.5)$$

- **Gas hold up (ϵ_g)**

The global gas hold-up corresponds to the gas fraction present in the bed. It is calculated from the solid volume, liquid volume and gas volume by the following equation: (Maldonado, 2008)

$$\epsilon = \frac{V_{Gas}}{V_{Total}} = \frac{V_G}{V_G + V_L + V_s} \quad (4.6)$$

This study, the relation of plastic media shapes, plastic media concentration and gas flow rate on oxygen transfer efficiency are measured, through the measurement of volumetric mass transfer coefficient and observation of bubble hydrodynamic parameters. Therefore, comparing the different type of diffusers and bubble column. Then propose the suitable diffuser and bubble column dimension with concerning both term of oxygen transfer efficiency.

- **Study of oxygen mass transfer and bubble hydrodynamic parameters in BC.**

The objective of this part is to study the oxygen mass transfer and bubble hydrodynamic characteristics in BC with a variety of gas flow rates. The outline of this study was presented in Figure 29 and the summary variables concerning to this study can be presented in Table 6.

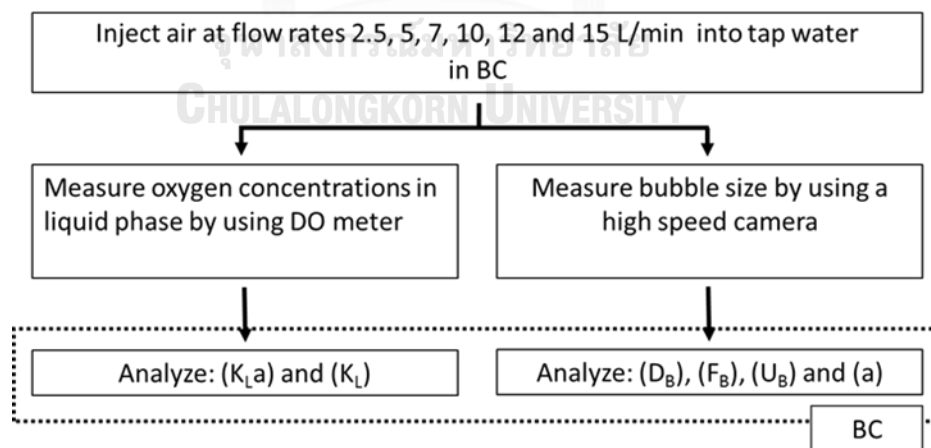


Figure 29 Diagram of study oxygen mass transfer and bubble hydrodynamic parameters in BC.

Table 6 Variable for oxygen mass transfer and bubble hydrodynamic parameters in BC.

Fixed VariablesParameter	Parameter
Reactor	Diameter 15 cm of bubble column
Gas phase (absorbate)	Oxygen
Liquid phase (absorbent)	Tap water
Independent Variables	Parameter
Gas flow rate	2.5, 5, 7, 10, 12 and 15 L/min
Dependent Variables	Parameter
Mass transfer parameters	$k_L a$ (Riser and down-comer zone)
Bubble hydrodynamic parameters	U_B , D_B , and a (Riser and down-comer zone)

- Study the effect of plastic media on overall mass transfer coefficient and bubble hydrodynamic parameter in BC.

The aim of this study is to evaluate the effect of plastic media on hydrodynamic and oxygen mass transfer characteristics in BC with a variety of gas flow rates. The outline of this study was presented in Figure 30 and the summary variables concerning to this study can be presented in Table 7.

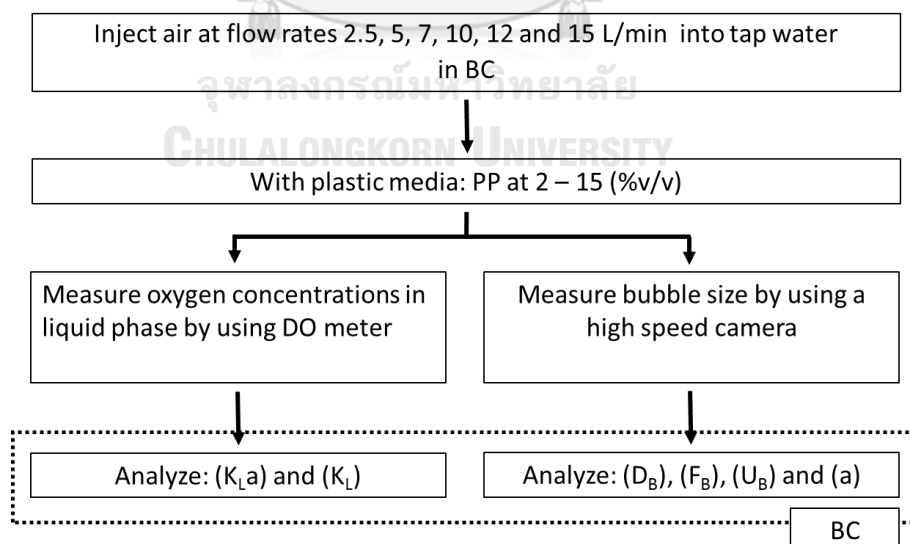


Figure 30 Diagram of study the effect of plastic media in BC.

Table 7 Variable for study the effect of plastic media in BC.

Fixed Variables	Parameter
Reactor	Diameter 15 cm of bubble column
Liquid phase (absorbent)	Tap water
Independent Variables	Parameter
Gas flow rate	2.5, 5, 10 and 15 L/min
Media Shape	Ring, Square, Rod and circle
Media concentration	2, 5, 10, 15 (%v/v)
Dependent Variables	Parameter
Mass transfer parameters	$k_L a$ (Riser and down-comer zone)
Bubble hydrodynamic parameters	U_B , D_B , and a (Riser / down-comer zone)

4.5 Results and Discussion

4.5.1 Effect of plastic media on overall mass transfer coefficient in BC.

The aim of this study was to determine overall mass transfer coefficient ($k_L a$) at a variety of gas flow rate in the BC. For analyzed the $k_L a$ values, oxygen concentrations in the liquid phase were measured with time using dissolved oxygen electrode, and calculated as previously described in equation 4.5.

- Effect of without plastic media on overall mass transfer coefficient

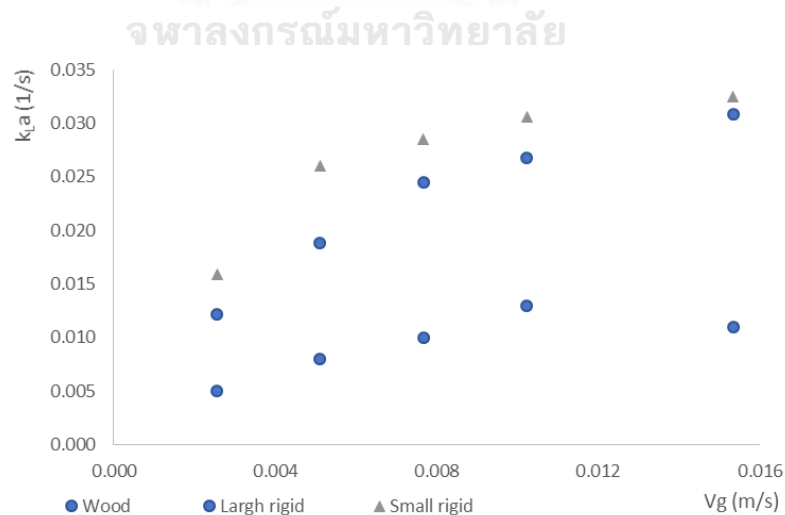
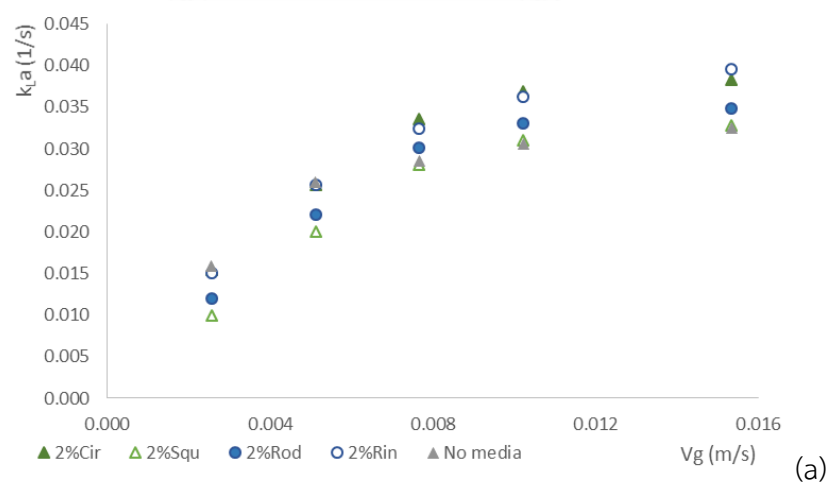


Figure 31 presents the variation of overall mass transfer coefficient with gas flow rates obtained with three types of diffuser without plastic media.

As shown in Figure 31, it can be seen that the values of $k_L a$ obtained with BC varied between 0.0530 and .4130 s^{-1} for gas velocity changing between 2.6×10^{-2} - 1.5×10^{-2} m/s. The $k_L a$ values increased with the gas velocity. It also observed that the slow increase of $k_L a$ values at a high flow rate. This result was due to the bubble coalescence phenomena at high gas flow rate. For type of diffuser, small rigid produce the lowest $k_L a$ and wood diffuser give the highest $k_L a$ respectively, the bubble size relate to the hole size of diffuser. Thus affected the specific interfacial area and the $k_L a$ coefficient. This was similar to the observation that was reported by others (Gourich *et al.*, 2006 and Pjontek *et al.*, 2014).

- **Effect of plastic media on overall mass transfer coefficient.**

The aim of this study was to determine the impact of plastic media with different density on overall mass transfer coefficient ($k_L a$) at a variety of gas flow rate in the BC. For analyzed the $k_L a$ values, oxygen concentrations in the liquid phase were measured with time using dissolved oxygen electrode, and calculated as previously described in equation 4.2. Different types and amounts of plastic media were added into the BC. In order to study the overall mass transfer coefficients. Figure 32 - Figure 34 present the variation of overall mass transfer coefficient with gas flow rates and three different shapes of plastic media were obtained in the BC.



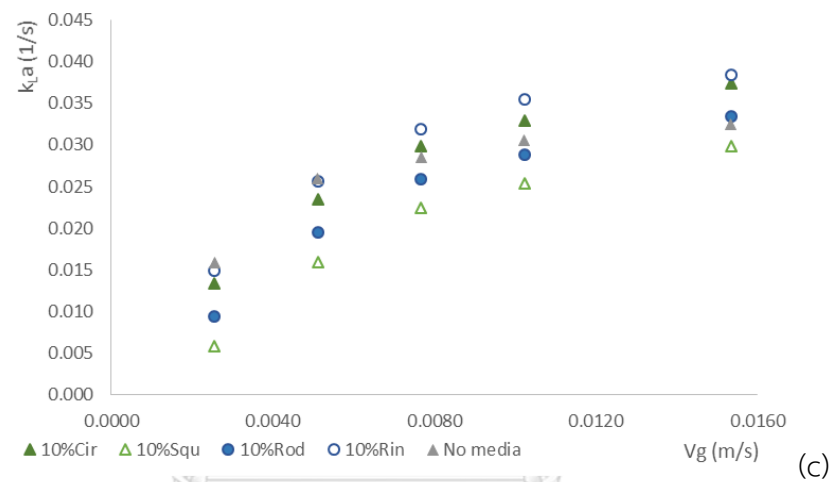
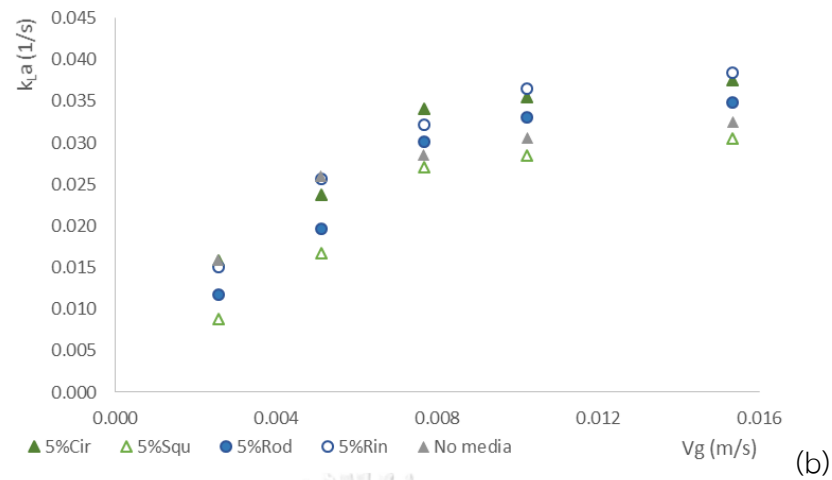
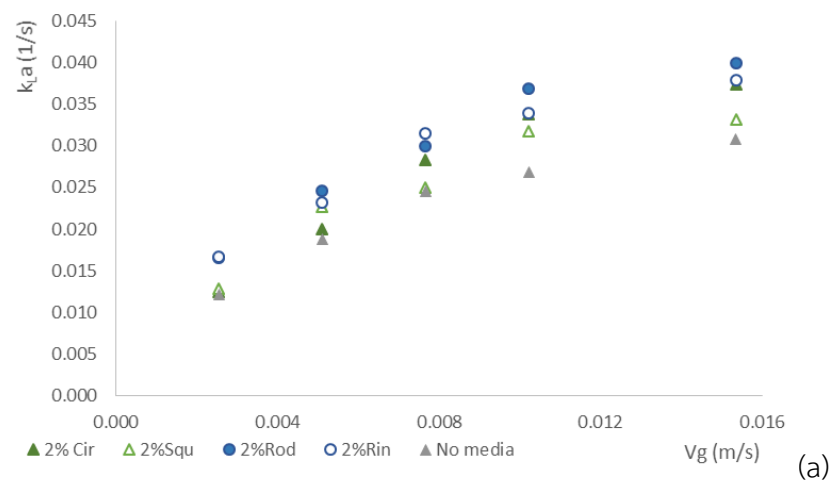


Figure 32 overall mass transfer coefficient versus gas flow rate in BC, shape of plastic media and plastic media concentration 2% 5% and 10% v/v with small rigid diffuser respectively.



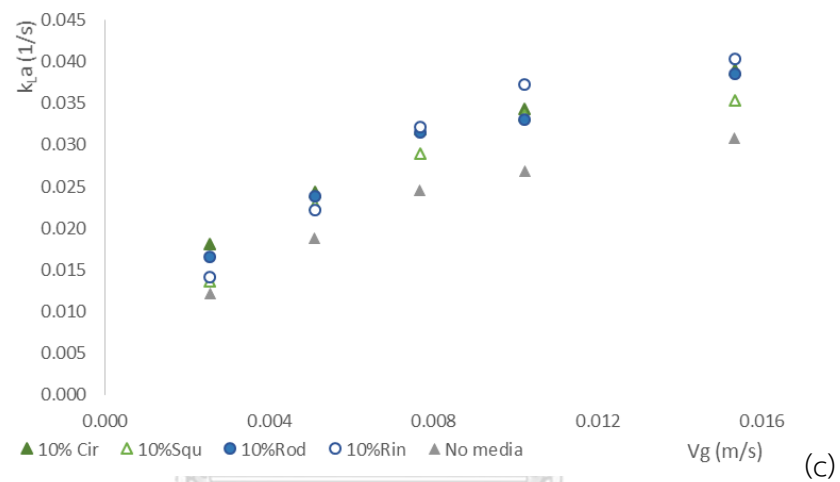
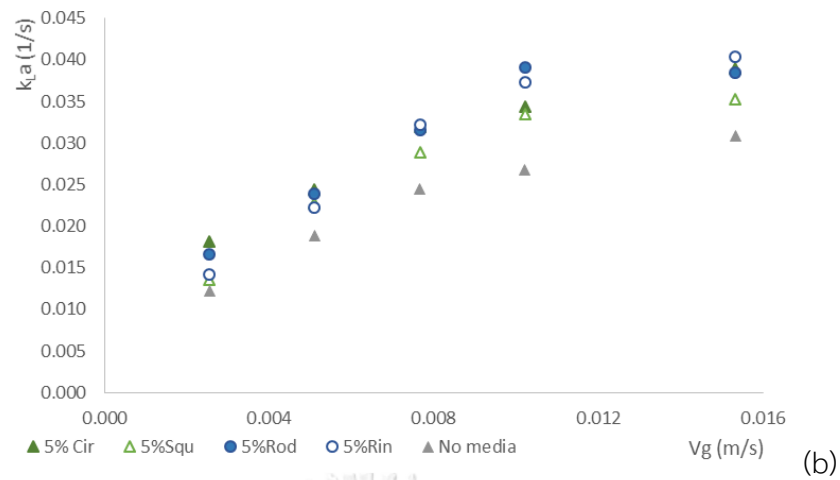
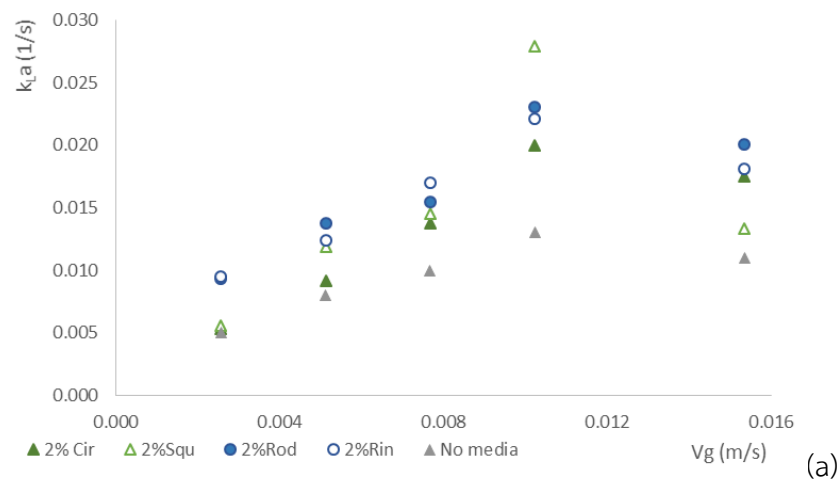


Figure 33 overall mass transfer coefficient versus gas flow rate in BC, shape of plastic media and plastic media concentration 2% 5% and 10% v/v with large rigid diffuser respectively.



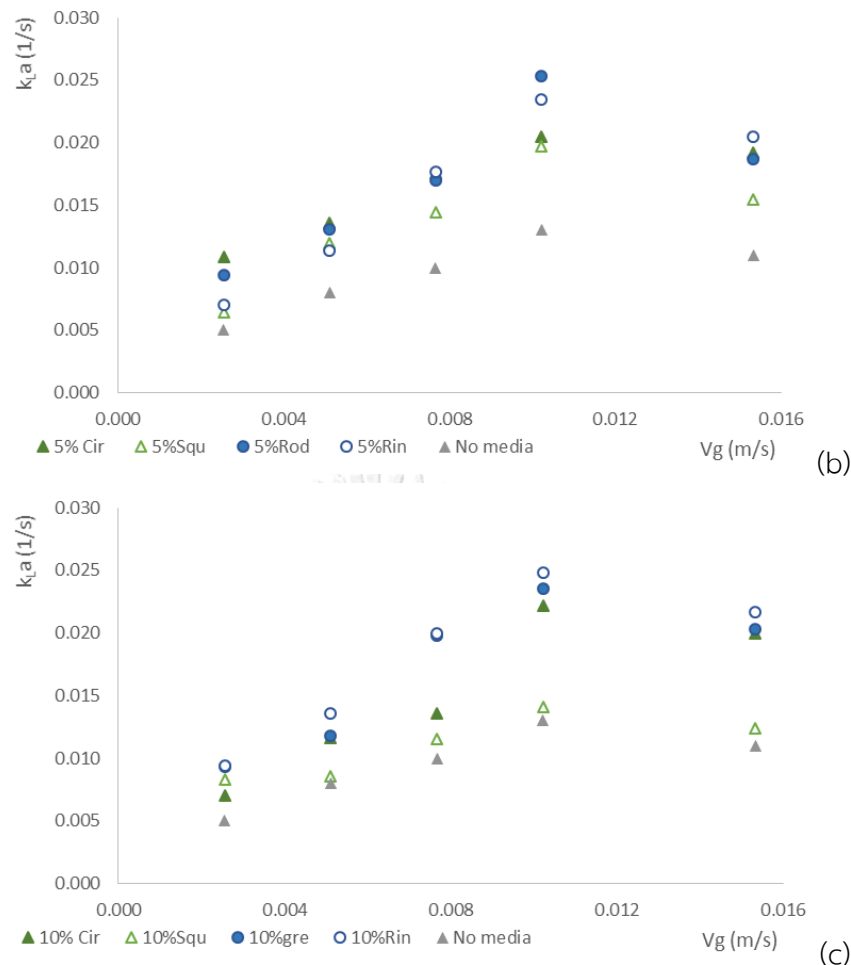


Figure 34 overall mass transfer coefficient versus gas flow rate in BC, shape of plastic media and plastic media concentration 2% 5% and 10% v/v with wood diffuser respectively.

According to Figure 33 – Figure 34 the result were shown that the k_{La} values varied between 0.0500 to 0.4030 s^{-1} when gas velocity (V_g) augmented between 2.6×10^{-3} – 1.5×10^{-2} m/s. The k_{La} values increased with the gas flow rate. The addition of media can modify the k_{La} coefficient; therefore, the positive effect can be found in the case of 2–10% for each shape of plastic. Ring shape showed the highest k_{La} when compare to another shape, it can be explained that the advantage of ring shape block the movement of bubble which increase the retention time of bubble in BC. The high k_{La} value round 0.4 - 0.45 s^{-1} were reported with using Small rigid and Large rigid diffuser. Which are higher than wood diffuser, it can be explain that the hole diameter of wood diffuser is bigger than Small rigid and Large rigid diffuser. Which relate to produce the big bubble, which is disadvantage to interfacial value was show in equation (4.4)

Moreover, increasing gas flow rate correspond to the $k_L a$ coefficient, the positive effect can be found in the case of $2.6 \times 10^{-3} - 1.0 \times 10^{-2}$ m/s. whereas in case of gas 1.5×10^{-2} m/s showed the negative affect to $k_L a$ value become slightly decrease with gas velocity higher 1.0×10^{-2} m/s. Due to large amount of gas tend to increase the bubble diameter by accumulation of bubble in the system. it can be considered that the large amount of gas flow rate and plastic media loadings in the BC (10% of media loadings) can cause the adversely effect on the $k_L a$ values due to high concentration, which settled down at the bottom of the reactor, blocking or modifying the bubble generation from the diffuser.

By considering the highest $k_L a$ values were reported with the 10% of ring shape addition and small rigid diffuser respectively. As the $k_L a$ coefficient related with the liquid-side mass transfer coefficient (k_L) and the specific interfacial area (a); the bubble size (D_B) and the terminal rising bubble velocity (U_B) are the important factors governing the previous mass transfer parameters. Therefore, it is interesting to continue analyzing on the bubble size and U_B value obtained with different types of media and operating conditions in the next section in order to provide a better understanding on mass transfer mechanism occurred within the reactor.

4.5.2 Effect of plastic media on bubble hydrodynamic parameter in BC.

Propose of this part was study the effect of plastic media on bubble hydrodynamic parameter in the BC. Bubble diameter (D_B) and terminal rising bubble velocity (U_B) in the BC were analyzed for different shape and concentrations of small plastic media particles.

- **Effect of plastic media on the bubble size in BC.**

In this section, the variation of the bubble diameter (D_B) with different plastic media addition (shape and amount) and operating conditions (gas flow rates) were studied in the BC. The values of bubble diameter can be measured by using the Image Techniques by using the high speed camera (350 images/second). Moreover, the average bubble diameter (D_B), presented in this study, was deduced from the measurement of 150-200 bubbles. The Sauter mean bubble diameter (d_{32}) from equation 3.4 was used as the bubble diameter (D_B) in this part of experiment.

Effect of without plastic media on the bubble size in BC.

Figure 35 presents the variation of bubble diameter with gas velocity obtained in the BC.

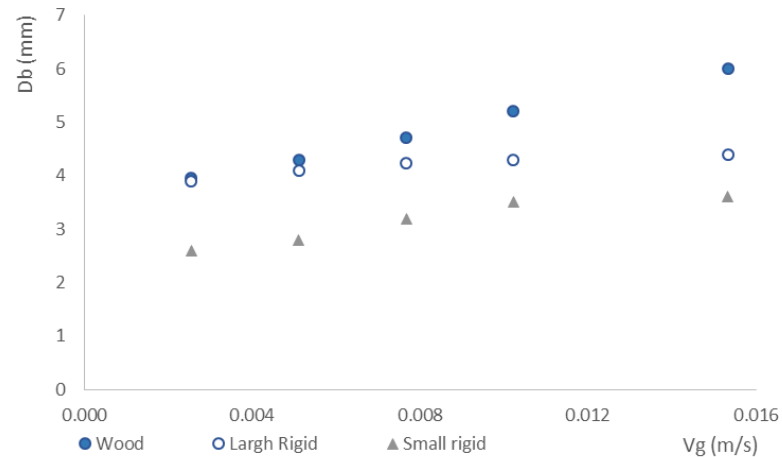


Figure 35 presents the variation of bubble diameter with gas flow rates obtained with three types of diffuser without plastic media.

According to Figure 35, the bubble diameter obtained in BC were in range from 2.60 to 6.0 mm when gas flow rates changing between 2.6×10^{-3} – 1.5×10^{-2} m/s. The bubble sizes were slightly increased with the gas flow rate due to the coalescence phenomena of many small bubbles suspended in the reactor. The photographs of bubbles in BC at different gas flow rate were shown in the Figure 36.

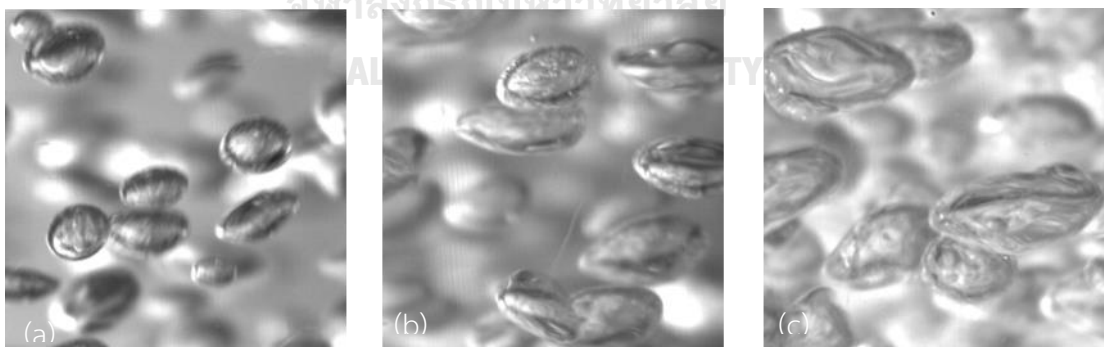


Figure 36 bubble formation photographs in BC at gas velocity : (a) 2.6×10^{-3} m/s, (b) 1.0×10^{-2} m/s, and (c) 1.5×10^{-2} m/s of small rigid diffuser.

Effect of with three different shape of plastic media on the bubble size in BC.

Figure 37- Figure 39 presents the variation of bubble diameter with gas velocity obtained in the BC for different amount of plastic media.

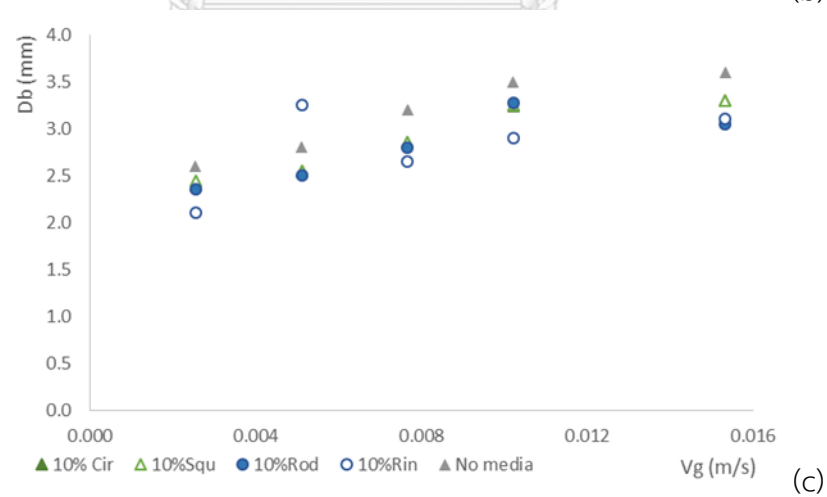
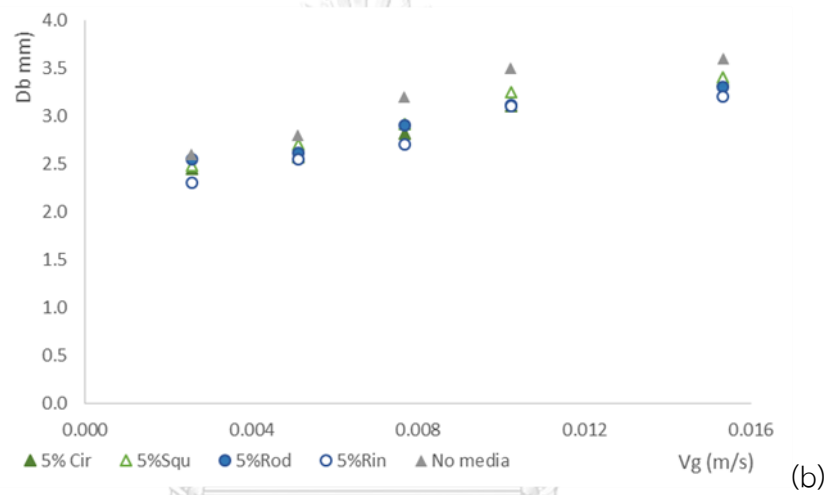
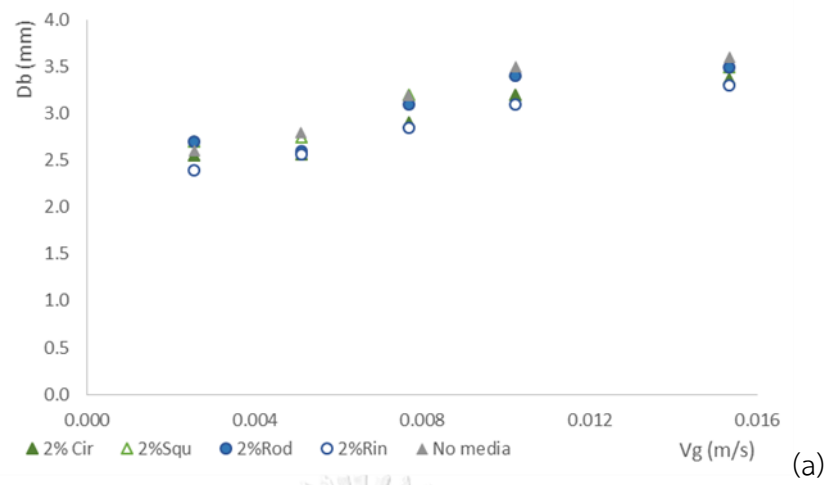


Figure 37 bubble diameter versus gas velocity in BC, shape of plastic media and plastic media concentration 2% 5% and 10% v/v with small rigid diffuser respectively.

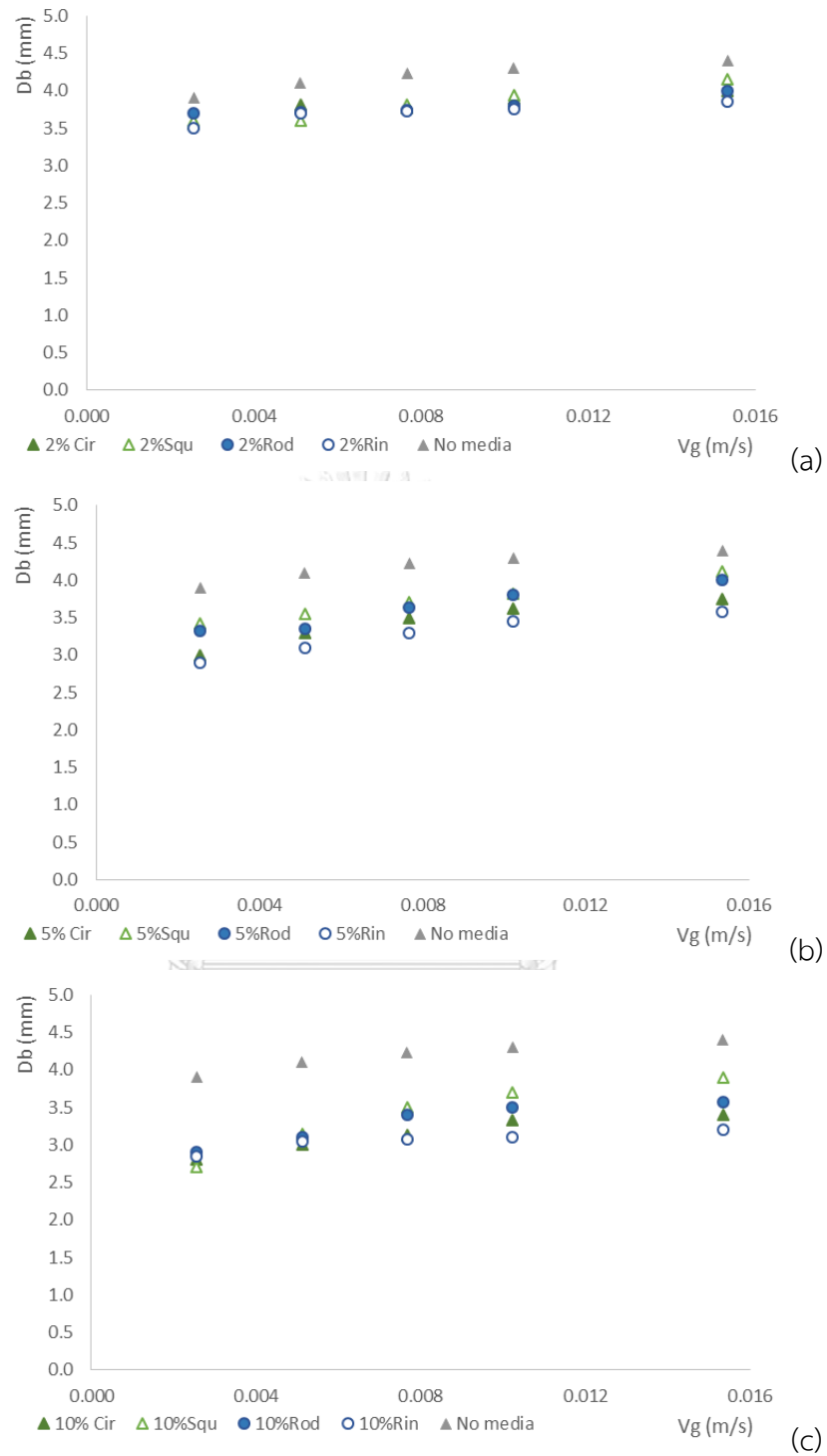


Figure 38 bubble diameter versus gas velocity in BC, shape of plastic media and plastic media concentration 2% 5% and 10% v/v with large rigid diffuser respectively.

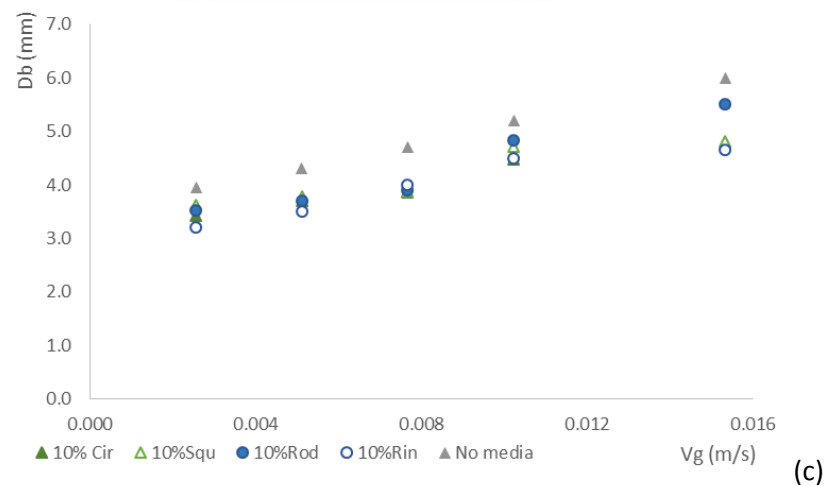
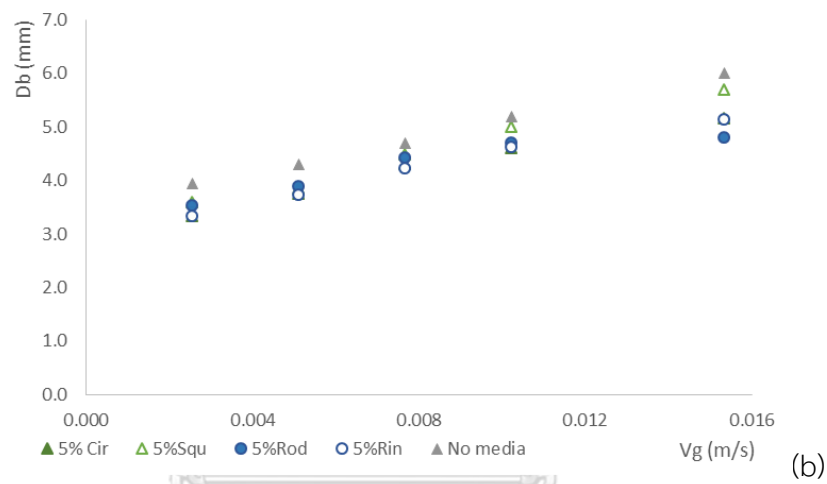
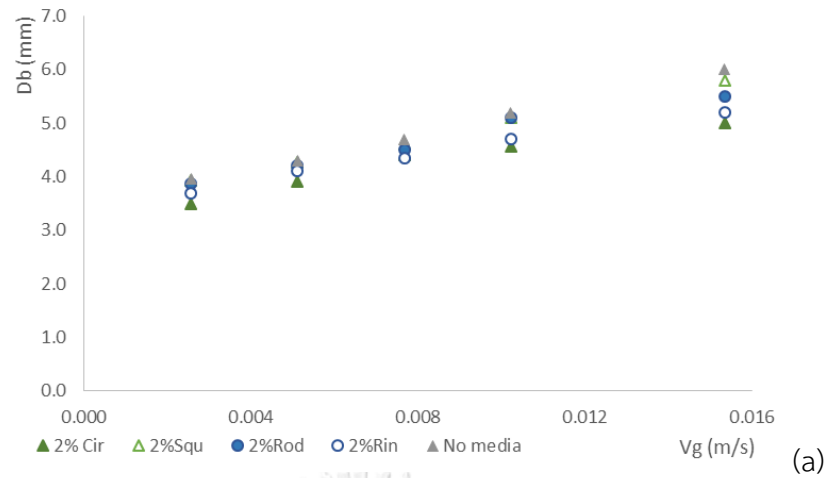


Figure 39 bubble diameter versus gas velocity in BC, shape of plastic media and plastic media concentration 2% 5% and 10% v/v with wood diffuser respectively.

According to Figure 37 - Figure 39 for plastic media loading in the BC, it can be shown that the bubble diameters were obtained at a range of 2.00 - 6.10 mm for gas

velocity changing between 2.0×10^{-3} - 1.5×10^{-2} m/s. The result showed that the bubble sizes slightly decrease with increasing media concentration from 2-15% loadings). Due to number of plastic media abstract and brake down the bubble size, which correspond to the decreasing of the bubble with media concentration from 2-10% loading as show in Figure 40 and Figure 41 respectively.

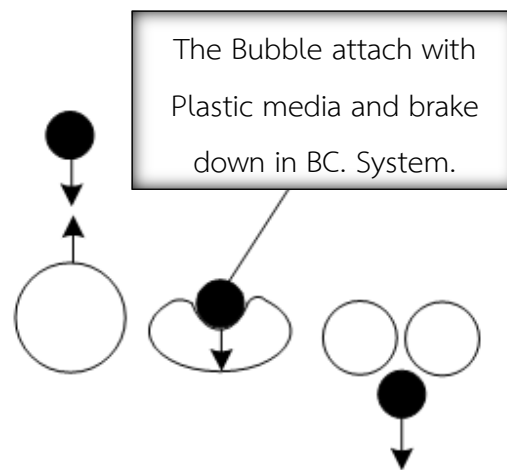


Figure 40 the Bubble attach with Plastic media and brake down in the system.

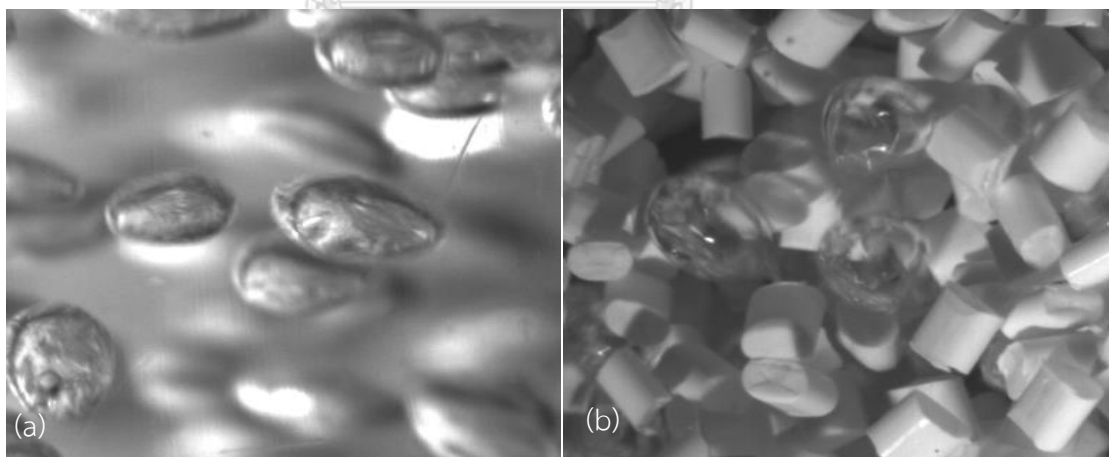


Figure 41 bubble in BC without plastic media and bubble in BC with plastic media.

As shown in Figure 38 – Figure 39, it can be shown that the bubble diameter increase with gas velocity between 2.0×10^{-3} - 1.5×10^{-2} m/s. The bubble diameter directly increased with the gas flow rate, which three different types of diffuse also have the similar trend of result. Due to amount of gas velocity increase from 2.0×10^{-3}

- 1.5×10^{-2} m/s, relate to increase amount of bubble in the system. Which can be attached and accumulated become bigger bubble diameter as show in Figure 42. The figure show the bubble attachment and bubble abstraction with plastic media in BC. And the small rigid diffuser reported the smallest bubble diameter with ring shape plastic media and become bigger by large rigid and wood diffuser respectively.

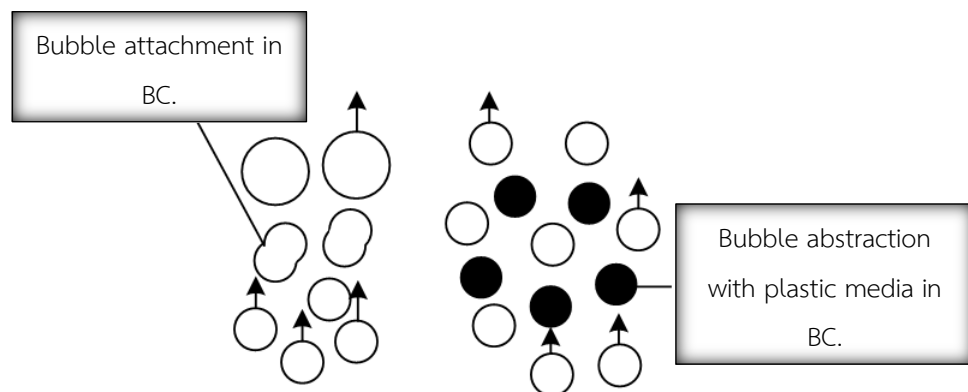


Figure 42 the bubble attachment and bubble abstraction with plastic media in BC.

By considering the results from previous part, the $k_L a$ values significantly increased with increasing the amount of PP media in the BC. Whereas, the addition of the plastic media at high concentration not significantly effect on the bubble sizes. Therefore, the increase in $k_L a$ value must due to the change in other parameter. The terminal rising bubble velocity (U_B) is an important parameter that deducted to the specific interfacial area (a), and also to the $k_L a$ values. The decreased in U_B value was due to the increased in specific interfacial area and $k_L a$ values. Therefore, the next section, effect of the three plastic media on U_B values in the BC will be studied.

- **Effect of plastic media on terminal rising bubble velocity (U_B) in BC.**

In this section, the variation of the terminal rising bubble velocity (U_B) with different shape (ring rod, circle and square) and amount of plastic media particles (2, 5, 10, 15 (%v/v)) were studied at different gas flow rate (2.5, 5, 10 and 15 L/min) in the BC. As same as the measuring of bubble diameter, the U_B values can be obtained by using the Image Techniques by using the high speed camera (350 frames/second). The U_B values were calculated from equation 4.5.

Effect of without plastic media on terminal rising bubble velocity (U_B) in BC.

Figure 43 presents the variation of terminal rising bubble velocity with gas flow rates obtained in the BC.

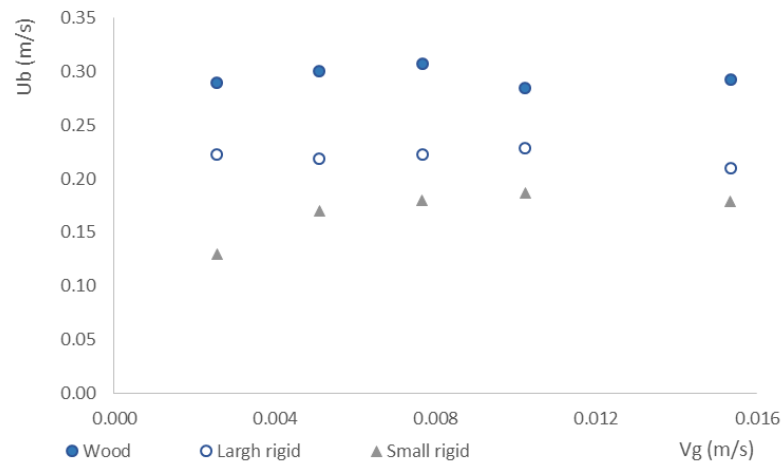


Figure 43 the variation of terminal rising bubble velocity with gas velocity obtained with three types of diffuser without plastic media.

Concerning to Figure 43, the U_B values obtained in BC. for no plastic media addition varied between 0.130 to 0.307 m/min for gas flow rates varying between 2.0×10^{-3} - 1.5×10^{-2} m/s. From the Figure, it can be noted that the U_B values linearly increased with the gas flow rate from 2.0×10^{-3} - 1.5×10^{-2} m/s. Moreover comparing to type of diffuse report that small rigid diffuser shoe the lowest terminal rising bubble velocity in the system 0.13 – 0.179 from 2.0×10^{-3} - 1.5×10^{-2} m/s. and wood diffuser show the highest terminal rising bubble velocity. Doe to terminal rising bubble velocity relate to the bubble diameter which were produced from diffusers. The result can be confirmed by previous experiment.

Effect of with plastic media on terminal rising bubble velocity (U_B) in BC.

Figure 44 - Figure 46 present the variation of terminal rising bubble velocity with gas flow rates obtained in the BC for different amount and shape of plastic media.

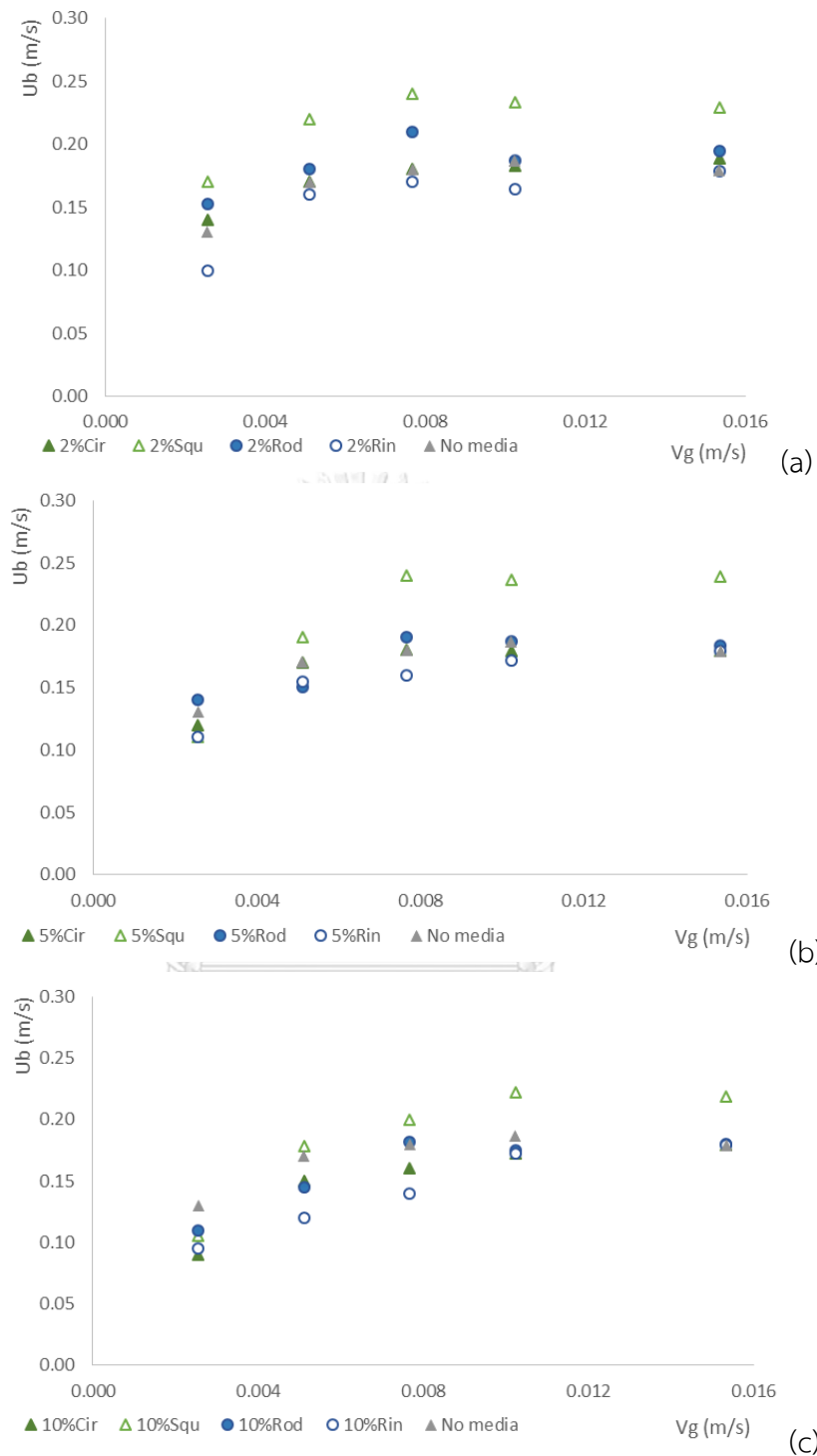


Figure 44 terminal rising bubble velocity versus gas velocity in BC., shape of plastic media and plastic media concentration 2% 5% and 10% v/v with small rigid diffuser respectively.

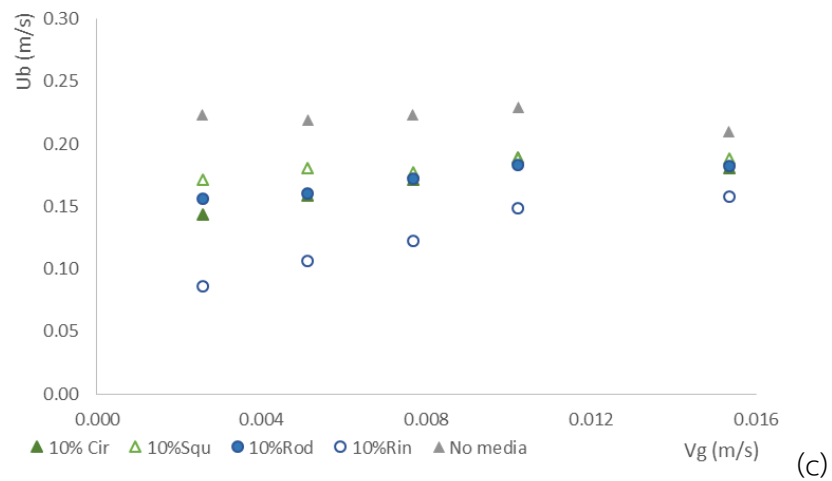
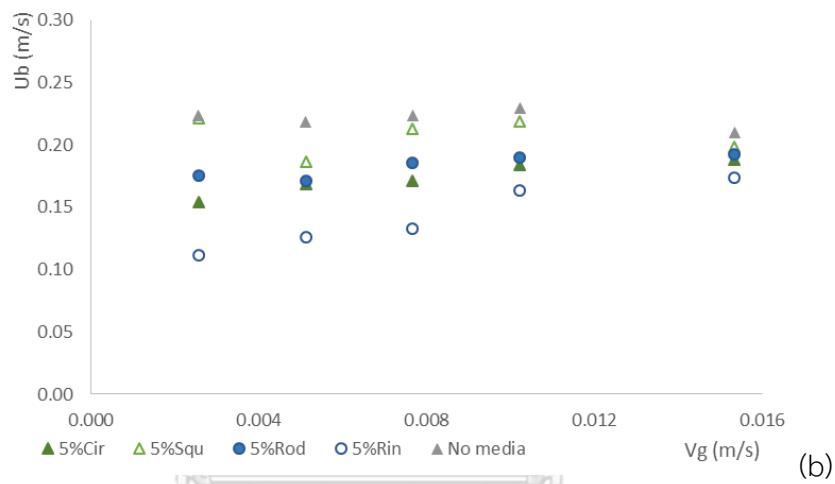
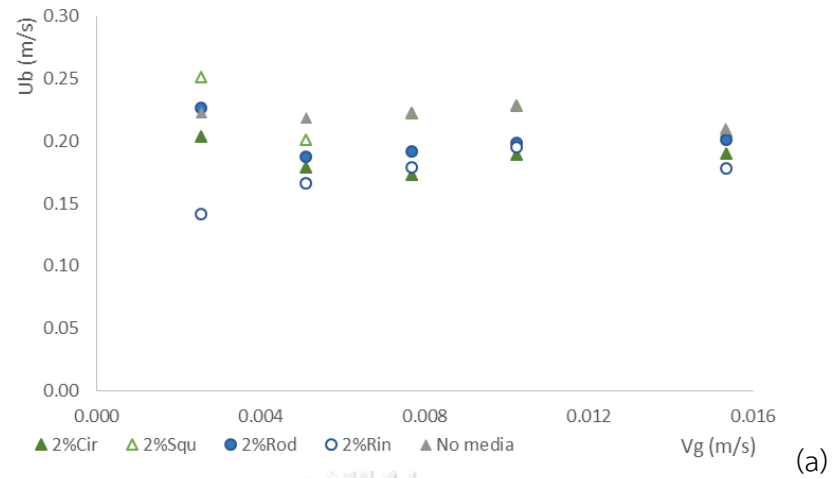


Figure 45 terminal rising bubble velocity versus gas velocity in BC., shape of plastic media and plastic media concentration 2% 5% and 10% v/v with large rigid diffuser respectively.

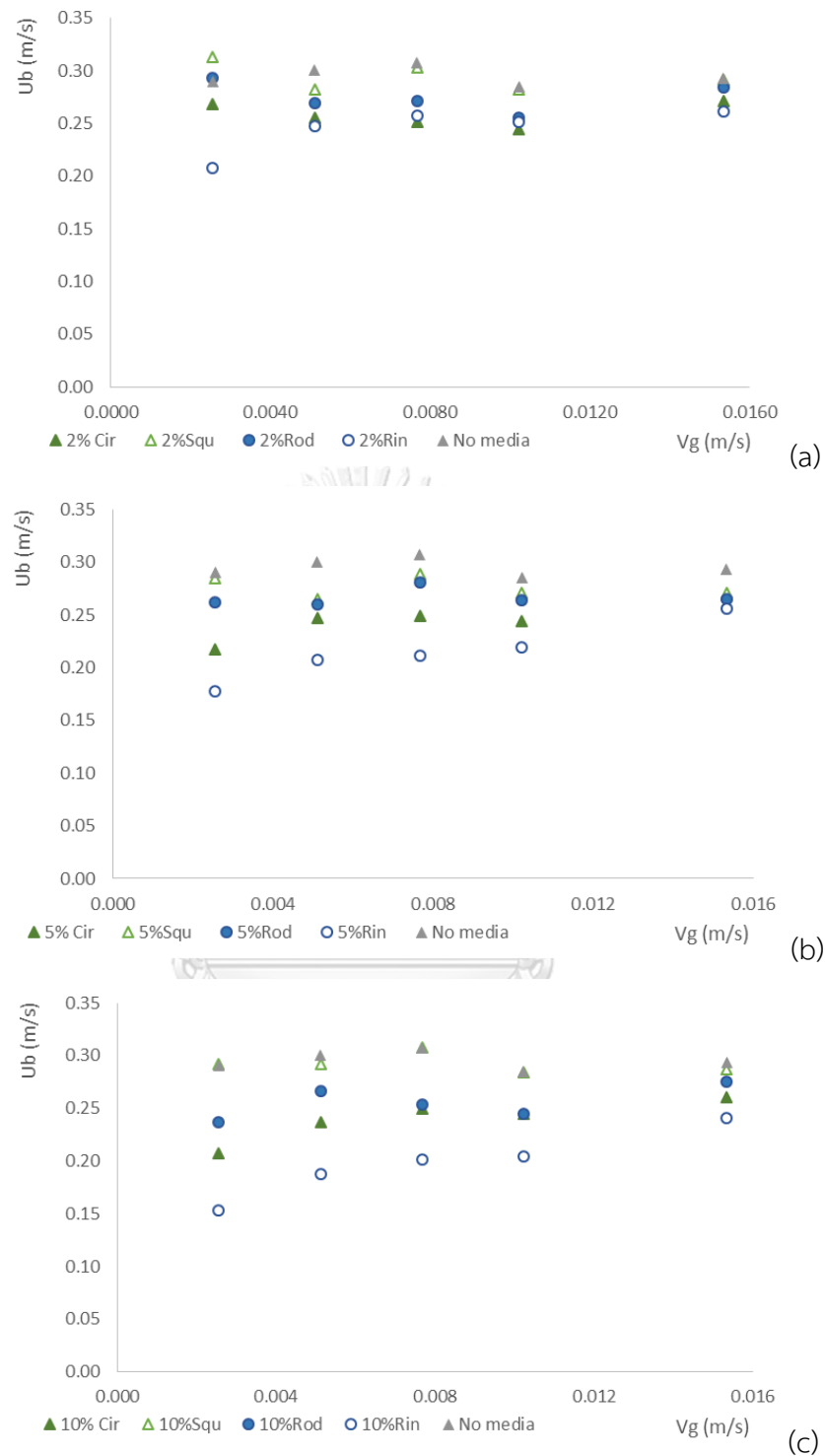


Figure 46 terminal rising bubble velocity versus gas flow rate in BC., shape of plastic media and plastic media concentration 2% 5% and 10% v/v with wood diffuser respectively.

Form the results in Figure 44 - Figure 46, the U_B values obtained with the BC for 2-15% of plastic media loading varied between 0.950 and 0.307 m/s for gas velocity changing between 2.0×10^{-3} - 1.5×10^{-2} m/s. It may be seen from the Figure that U_B values slightly increase with increasing gas flow rate. This result correspond with previous that the increase of terminal rising bubble velocity, relate to the rising of bubble diameter, which three types of diffuser show the similar effect.

Furthermore, the increased of plastic media loading decreasing the U_B values especially at high gas flow rate. Which the ring shape report the lowest terminal rising bubble velocity, when compare to another shape of plastic in every concentration and gas flow rate. Therefore, it can conclusion that the addition media provided the decreased in U_B values, which related to the increased in the specific interfacial area and also the $k_L a$ values.

In conclusion, the addition of media in the BC were significantly reduced the values of terminal rising bubble velocity (U_B), which deducted to an increase in values of specific inter facial area (a). Therefore, the next section, the effect of plastic media on the specific interfacial area obtained in the BC. was investigated.

- **Effect of plastic media on the specific interfacial area (a) in BC**

In this section, the interfacial area, which calculated from the bubble size, bubble formation frequency and their rising velocity as previously described in equation 3.5, were presented.

Effect of without plastic media on the specific interfacial area (a) in BC

Figure 47 presents the variation of specific interfacial area with gas velocity obtained in the BC.

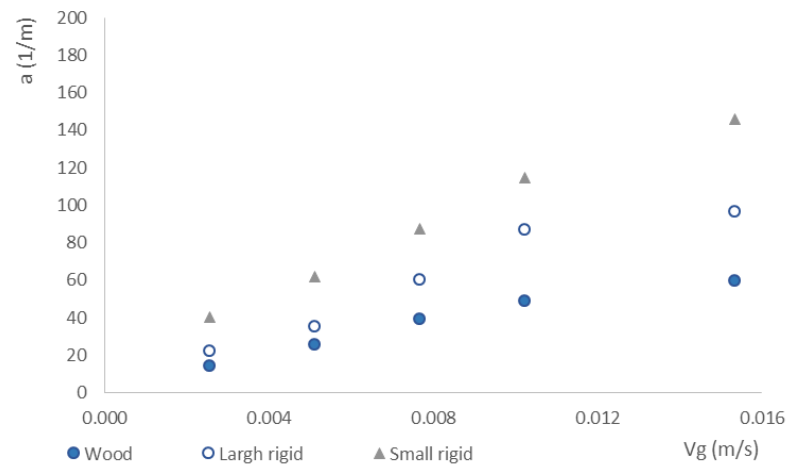


Figure 47 the variation of interfacial area with gas flow rates obtained with three types of diffuser without plastic media.

From Figure 47, the specific interfacial area increase with the velocity. These values varied between 21.90 and 79.09 m^{-1} for gas velocity varying between 2.0×10^{-3} - 1.5×10^{-2} m/s. The specific interfacial area obtained with high gas velocity was greater than low gas velocity. Which small rigid diffuser report the highest. Which relate to the previous work that small rigid diffuse provided the smallest bubble size in BC. Moreover, it can be note that the slow increase of the specific interfacial area in high gas velocity (2.0×10^{-3} - 1.5×10^{-2} m/s). It was observed at high gas velocity due to the bubble coalescence phenomena in the reactor.

Effect of with plastic media on the specific interfacial area (a) in BC

Figure 48- Figure 50 present the variation of specific interfacial area with gas velocity obtained in the BC. for different amount of plastic media.

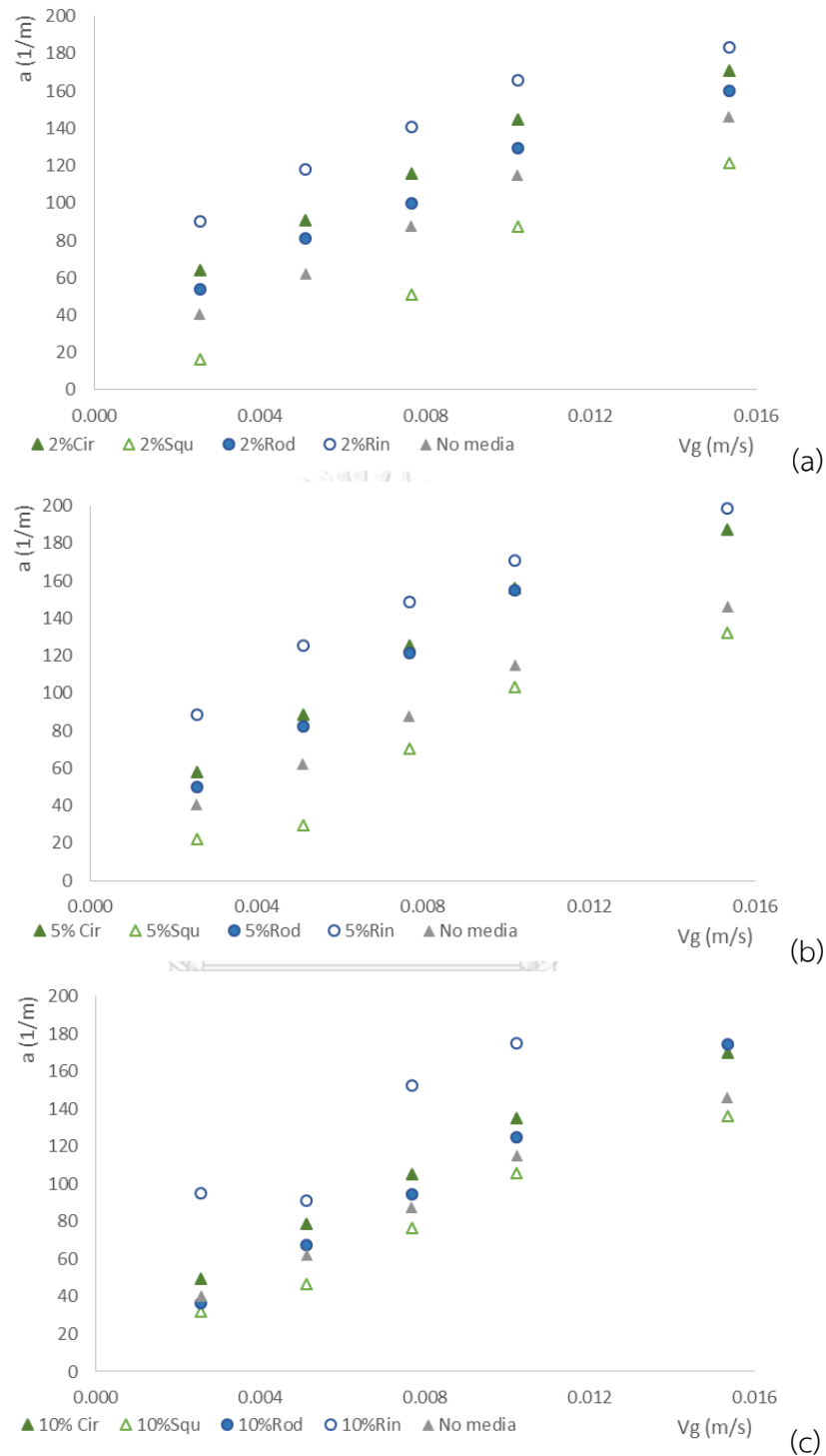


Figure 48 Specific interfacial area versus gas velocity in BC, shape of plastic media and plastic media concentration 2% 5% and 10% v/v with small rigid diffuser respectively.

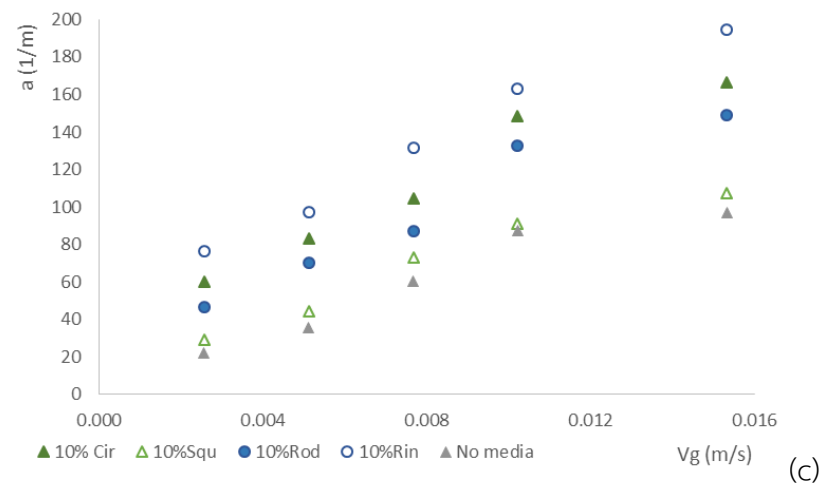
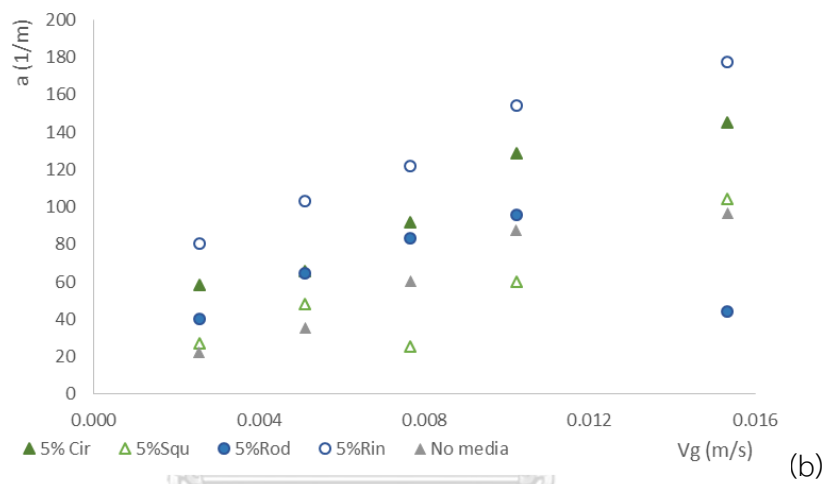
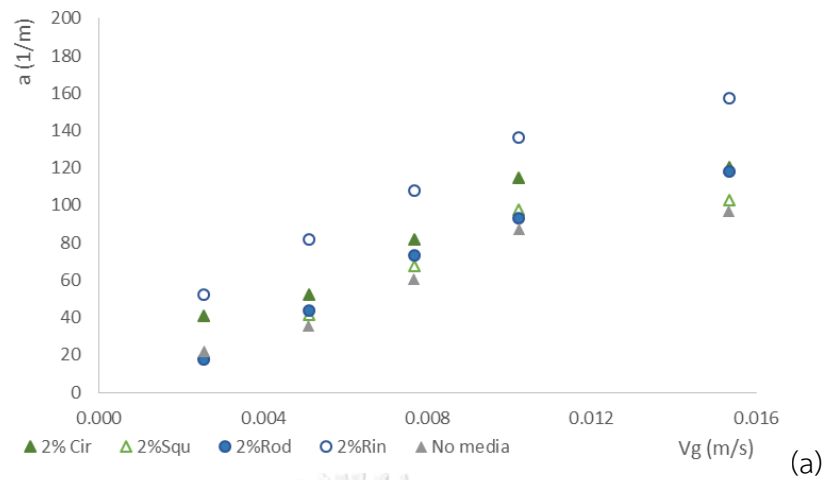


Figure 49 Specific interfacial area versus gas velocity in BC, shape of plastic media and plastic media concentration 2% 5% and 10% v/v with large rigid diffuser respectively.

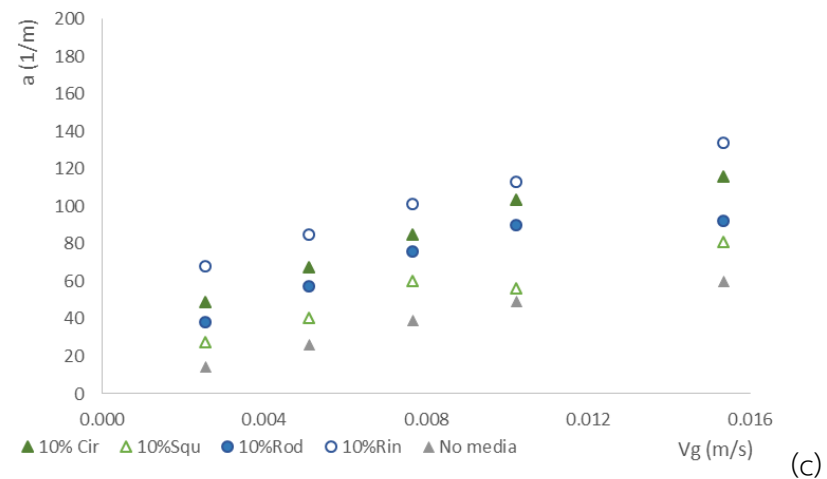
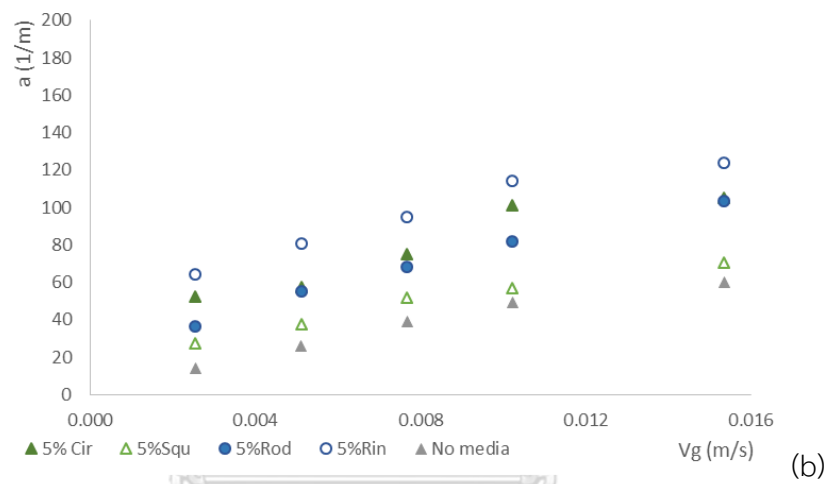
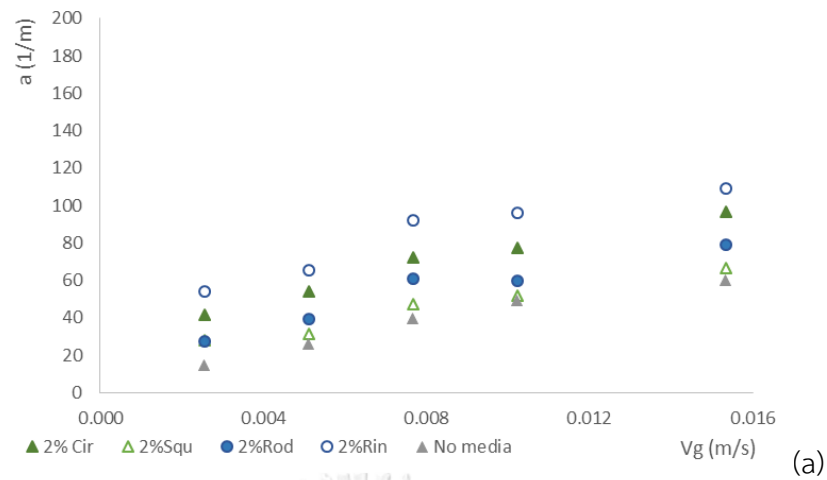


Figure 50 Specific interfacial area versus gas velocity in BC, shape of plastic media and plastic media concentration 2% 5% and 10% v/v with wood diffuser respectively.

From the Figure 48- Figure 50, the specific interfacial area obtained in the BC increased with the gas velocity from 2.0×10^{-3} - 1.5×10^{-2} m/s and 2-15% of plastic media

loading. The specific interfacial area values varied between 27.33 to 198.00 m^{-1} when gas velocity ranged between 2.0×10^{-3} - 1.5×10^{-2} m/s. As discussed previously, the plastic media can be well suspended within the reactor and reduced the bubble diameter and terminal rising velocity U_B in the BC reactor, which small rigid show the highest interfacial area and wood diffuse report the lowest interfacial area respectively. Therefore; the enhancement of specific interfacial area can be thus obtained.

From the part 4.1 and 4.2, it can be conclusion that the addition of plastic media can provide the increase in mass transfer rate in the BC. However, the adversely affect due to the high concentration of plastic particles located, and modifying the bubble size from the diffuser was observed. An internal loop airlift reactor (ILALR) was an interested reactor to increase the $k_L a$ values due to the increase in liquid-gas contact time. Moreover, the liquid and gas recirculation in the reactor may be able to increase the suspension of plastic media and also reduce their accumulation at the bottom of the reactor. Therefore, the effect of plastic media on oxygen mass transfer and bubble hydrodynamic parameters in an ILALR will be analyzed in the next part.

4.6 Conclusions

For the oxygen absorption part, the effect of small plastic media particles on overall mass transfer coefficient ($k_L a$), bubble diameter (D_B), terminal rising bubble velocity and specific interfacial area (a) in BC. The operating conditions were as follows: liquid phase is tap water and gas flow rate of 2.5, 5, 7, 10, 12 and 15 L/min. The three different shape of plastic media (ring, rod, square and circle) with different concentration (2, 5, 10, 15 (%v/v)) were used. In this part, the following results have been obtained;

- For no plastic media, the overall mass transfer coefficient ($k_L a$) lower than using plastic media
- The trend line of bubble diameter in BC, the bubble diameter increase with gas velocity whereas, the bubble diameter were become lower by using plastic media. Moreover, ring shape report the lowest bubble size when compare to another shape
- The similar effect of plastic media loading on the U_B value in BC. The following results were observed. At high amount of plastic loading relate to produce the small size bubbles in BC reactor which decrease the U_B value in the system.

- The similar effect of plastic media loading on the specific interfacial area in BC. The following results were observed. At high amount of plastic loading relate to produce the small size bubbles in BC reactor which increase the interfacial area value in the system.

In conclusion for the oxygen absorption part to provide the higher oxygen mass transfer rate than BC. In next experiment. ILALR was study by using the best condition of BC. Therefore, the best condition for oxygen absorption in this part such as 15% of ring shape of plastic media will be applied in ILALR part.



CHAPTER 5

STUDY OF ABSORPTION PROCESS IN INTERNAL LOOP AIRLIFT REACTOR (ILALR): MASS TRANSFER AND HYDRODYNAMIC

5.1 Introduction

Airlift reactors are a type of bubble columns, they widely used in the absorption processes. There are two types of airlift reactors: internal-loop and external-loop airlift reactors. Internal loop reactors consist of concentric tubes or split vessels, in which a part of the gas is entrained into the down comer, whereas external loop reactors are two tubes connected at the top and the bottom. Two major hydrodynamic properties of the airlift reactors are the gas holdup and liquid circulation velocity. The gas holdup can be an indicator for the mean residence time of the gas phase and the gas-liquid mass transfer coefficient. Besides, it also affects the liquid circulation velocity. Moreover, the liquid circulation velocity also affects the mixing behavior in airlift reactors. (Couvert et al, 1999)

In many research work on an internal-loop airlift reactor with-out a gas-liquid separator, there are different regimes of bubble swarm in the down-comer according to the bubble circulation in the riser and down-comer. We (2008) [2] explained flow regimes, the bubble flow based on the liquid velocity in the down-comer. Which described into three regimes, low superficial gas velocities, the flow is in the bubble-free regime (I). This regime no bubbles exist in the down-comer zone. When increase in the superficial gas velocity, the gas flow enters the transition regime (II) where some bubbles are entrained flow into the down-comer. But the bubbles does not completely circulate in the system. When increase more superficial gas velocity, the flow enters the complete bubble circulation regime (III) where the liquid circulation velocity becomes larger than gas bubbles velocity in the down-comer. In this case, the bubbles move back to the riser zone from below the draft tube.

However, the effects of the liquid-bubble hydro-dynamics on mass transfer parameter by adding plastic media have not much studied in literature. To full fill this gaps, the purpose of this study improve the efficiency of ILALR. Moreover, it was studied the effect of shape and amount of small size plastic media on oxygen mass transfer and hydrodynamic parameters (Q_g , ϵ_g , D_{Br} , D_{Bd} , U_{Br} and U_{Bd}) at a various gas flow rate in ILALR. The finally explained the relation of air circulation rate on mass transfer parameter in ILALR.

5.2 Objectives

- To study the effect of batch system and operating condition on the bubble hydrodynamic and mass transfer parameter in Internal loop air lift reactor
- To study the effect of using plastic media on the bubble hydrodynamic and mass transfer parameter which relate the increasing of gas flow rate, liquid velocity and air circulation rate (Q_{gr}) in internal air lift reactor

5.3 Literature Review

Chisti et al. (1990) studied the influence of motionless mixers on the $k_L a$ value in an external-loop type airlift bioreactor. This study used aqueous salt solution and pseudoplastic solution of carboxymethyl cellulose as liquid phase. The presence of SMV-12 static mixers increased $k_L a$ by 30-500%, depending on the fluid thickness. The increased $k_L a$ involved the increased gas hold-up and gas-liquid interfacial area, which depend on bubble breakup accomplished by the static mixing elements.

Hossein N. et al. (2005) investigated gas hold-up and mass transfer rates of three volatile organic chemicals (VOCs) in an external loop airlift bioreactor (ELAB), with and without packing. They used a stainless steel mesh packing with 99.0% porosity as a packed bed in the riser section of ELAB. The results show that the packing enhanced the overall volumetric mass transfer coefficient ($k_L a$) by an average of 65.1% and 33.4% for toluene and benzene, respectively, in comparison with unpacked bed. Moreover, the packing increased gas hold-up and decreased bubble size in the reactor, which increase the mass transfer rates. Desorption of VOCs was slower than absorption, which was explained by the change in gas bubble sizes in the presence of VOCs.

Moraveji et al. (2011) Investigated the turbulence on the rate of induced liquid circulation, gas hold-up, mixing time and overall gas-liquid volumetric oxygen mass transfer coefficient in packed bed internal loop airlift reactor (Figure 51). The reactor used a glass column with 1.3 m height and rectangular Plexiglas baffle 0.129 m width, 1.0 m height and 0.005 m thickness and studied the effect various types of surfactants (containing Brij58, TritonX-405, Tween40, HCTBr) with various concentrations of 1-5 ppm were examined on the operational characteristics of the reactor. The result show that surfactants existence increases gas holdup and mixing time although it decreased the liquid circulation velocity and the rate of oxygen mass transfer. HCTBr which is a

cationic surfactant was the most effective surfactant. Packing installation increased mass transfer by increasing flow turbulence. Whereas, gas hold-up increased and liquid velocity decreased when gas bubbles movement increased. In the packed bed system, homogenous flow regime was highly observed while in the unpacked bed system the transition flow regime overcame at the high superficial gas velocities.

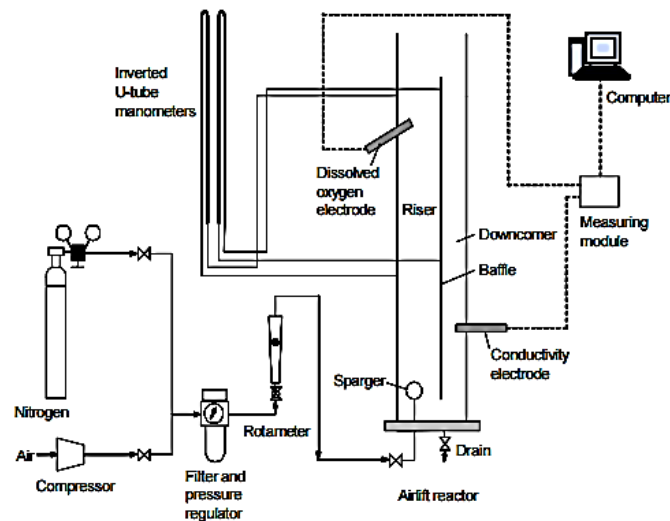


Figure 51 schematic diagram of the split-cylinder airlift reactor.

5.4 Materials and Methods

5.4.1 Experimental Setup

This research focus on study the effect of using plastic media on mass transfer ($k_L a$ and k_L) and the bubble hydrodynamic parameters (Q_g , ϵ_g , D_{Br} , D_{Bd} , U_{Br} , U_{Bd} and a). The experiment were set up in a cylindrical acrylic column with 0.15 m inside diameter and 1 m in height. ILALR was setup an acrylic plate for liquid recirculation. Moreover, mass transfer determination, liquid phase was removed dissolved oxygen by using sodium sulphite (Na_2SO_3) after that the aeration was conducted by air compressor which supplied air pass through the sparger at the bottom of column. The schematic diagram was showed in Figure 52. Air flow rate various from 2.5 to 15 l/min. The bubble hydrodynamic mechanisms are investigated by the high speed camera (100 images/sec) and image analysis program is used to determine the bubble hydrodynamic parameters. The bubbles are generated by rigid diffuser which located at the bottom of column. Plastic media were added into the bubble column at 2% 5% 10% and 15% v/v in the different shapes (fig.53). For plastic media characteristics were showed in table 8.

Table 8 Plastic media characteristics

Media shape	Bed porosity, ϵ	Surface area, A (mm ²)	Volume, V (mm ³)	Bed porosity, ϵ (g/mm ³)
Ring (a)	0.68	156.69	49.48	0.000950
Circle (b)	0.38	43.05	26.56	0.000941
Rod (c)	0.39	40.07	29.35	0.001022
Square (d)	0.30	38.43	17.69	0.000961

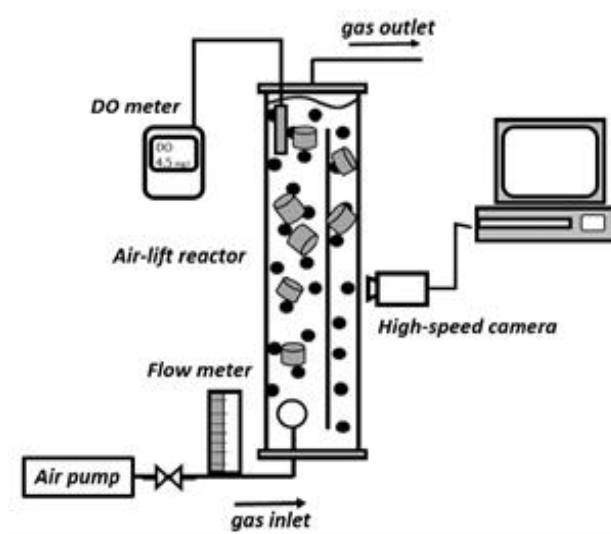


Figure 52 the experiment set up.

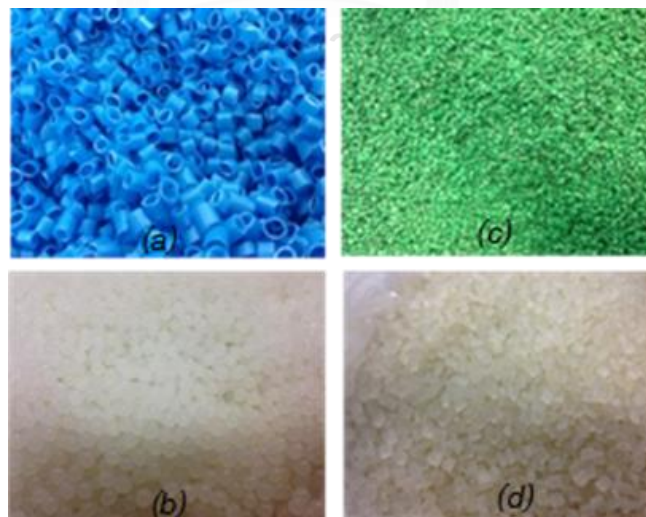


Figure 53 shape of plastic media (a)Ring, (b)Circle, (c)Rod and (d)Square.

5.4.2. Method for determining the mass transfer and bubble hydrodynamic parameter

- The volumetric mass transfer coefficient ($k_L a$)

The volumetric mass transfer coefficient ($k_L a$) was determined the efficiency of mass transfer in the system. The mathematic is used to determine $k_L a$ value be written as following equation: (Painmanakul et al, 2005)

$$\frac{dC}{dt} = k_L a (C^* - C_t) \quad (5.1)$$

Then integration Eq 5.2,
$$\ln(C^* - C_t) = -k_L a t + \ln C^* \quad (5.2)$$

Where C^* and C_t are the saturated concentration of dissolved oxygen in liquid and the concentration of dissolved oxygen measured at time t , respectively. The $k_L a$ values can be estimated graphically from the slopes of linear equation of $\ln(C^* - C_t)$ versus time.

- Bubble rising velocity (U_B)

Bubble velocity (U_B) was calculated by taking picture in reactor to analyze its distance (D) at any time frame (T_{frame}). Thus, the U_B was calculated from equation: (Painmanakul et al, 2005)

$$U_B = \frac{D}{t_{frame}} \quad (5.3)$$

- Gas hold up (ϵ_g)

Gas hold up (ϵ_g) is the volume fraction of the gas phase, it was measured by recording the changes in the liquid height in the ILALR by using a high camera together with a fine scale fixed on the top of the column. The global gas hold-up corresponds to the gas fraction present in the bed. It is calculated from the solid volume, liquid volume and gas volume by the following equation: (Maldonado, 2008)

$$\epsilon = \frac{V_{Gas}}{V_{Total}} = \frac{V_G}{V_G + V_L + V_s} \quad (5.4)$$

- **Interfacial area (a)**

Interfacial area (a) is a function of f_B , U_B , and d_B . It can be expressed as in Eq. (5.5) where H_L and V_{Total} are height and overall volume of liquid phase in a column. S_B is a surface area of a bubble.

$$a_r = \frac{(Q_g + Q_{gr})}{V_{Br}} \times \frac{H_L}{U_{Br}} \times \frac{S_{Br}}{V_{Total}} = \frac{6}{D_{Br}} \cdot \frac{\epsilon_{gr}}{(1 - \epsilon_{gr} - \epsilon_{sr})} \quad (5.5)$$

This study, the relation of plastic media shapes, plastic media concentration and gas flow rate on oxygen transfer efficiency are measured, through the measurement of volumetric mass transfer coefficient and observation of bubble hydrodynamic parameters. Therefore, comparing the different type of diffusers and internal loop airlift reactor. Then propose the suitable diffuser and bubble column dimension with concerning both term of oxygen transfer efficiency

- **Study of oxygen mass transfer and bubble hydrodynamic parameters in ILALR.**

The objective of this part is to study the oxygen mass transfer and bubble hydrodynamic characteristics in ILALR with a variety of gas flow rates. The outline of this study was presented in Figure 54 and the summary variables concerning to this study can be presented in Table 9.

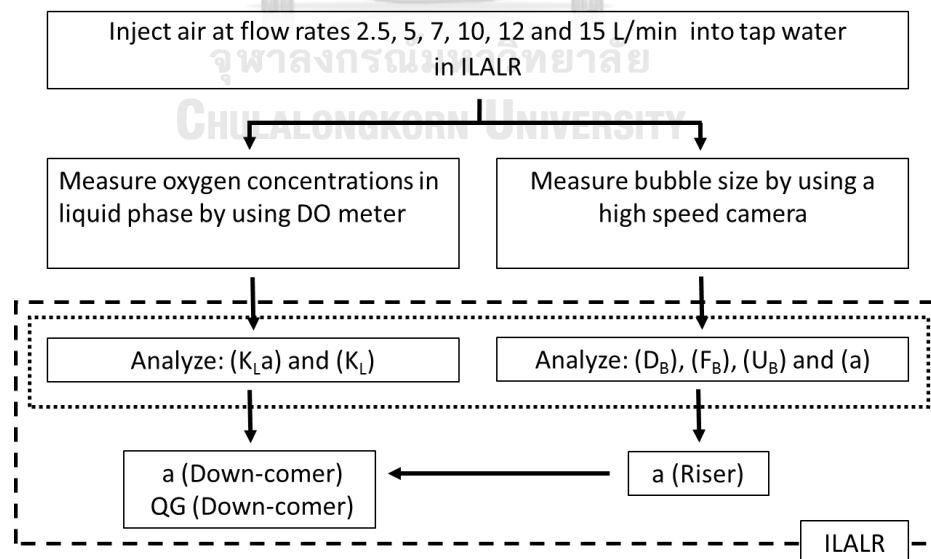


Figure 54 Diagram of study oxygen mass transfer and bubble hydrodynamic parameters in ILALR.

Table 9 Variable for oxygen mass transfer and bubble hydrodynamic parameters ILALR.

Fixed VariablesParameter	Parameter
Reactor	Internal loop airlift reactor
Gas phase (absorbate)	Oxygen
Liquid phase (absorbent)	Tap water
Independent Variables	Parameter
Gas flow rate	2.5, 5, 7, 10, 12 and 15 L/min
Dependent Variables	Parameter
Mass transfer parameters	$k_L a$ (Riser and down-comer zone)
Bubble hydrodynamic parameters	U_B , D_B , and a (Riser and down-comer zone)

- Study the effect of plastic media on overall mass transfer coefficient and bubble hydrodynamic parameter in ILALR.

The aim of this study is to evaluate the effect of plastic media on hydrodynamic and oxygen mass transfer characteristics in ILALR with a variety of gas flow rates. The outline of this study was presented in Figure 55 and the summary variables concerning to this study can be presented in Table 10.

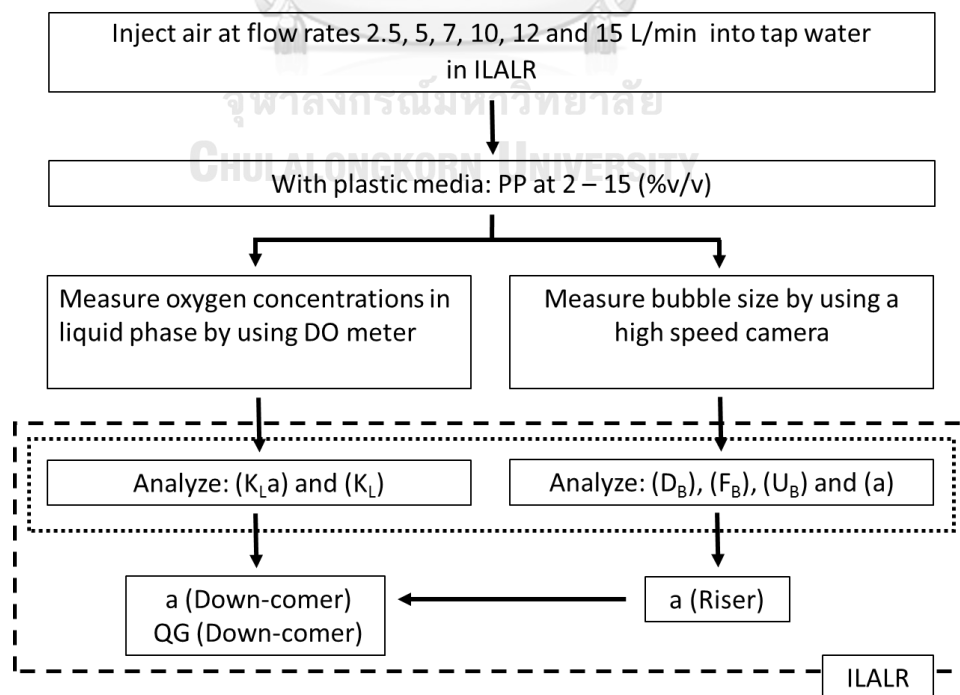


Figure 55 diagram of study the effect of plastic media in ILALR.

Table 10 Variable for study the effect of plastic media in ILALR.

Fixed Variables	Parameter
Reactor	Diameter 15 cm with Internal loop airlift reactor
Liquid phase (absorbent)	Tap water
Independent Variables	Parameter
Gas flow rate	2.5, 5, 10 and 15 L/min
Media type	Ring, Square, Rod and circle
Media concentration	2, 5, 10, 15 (%v/v)
Dependent Variables	Parameter
Mass transfer parameters	$k_L a$ (Riser and down-comer zone)
Bubble hydrodynamic parameters	U_B , D_B , and a (Riser / down-comer zone)

5.5 Results and Discussion

5.5.1 Study the oxygen mass transfer and bubble hydrodynamic parameters in ILALR.

- Overall mass transfer coefficient ($k_L a$) in ILALR.

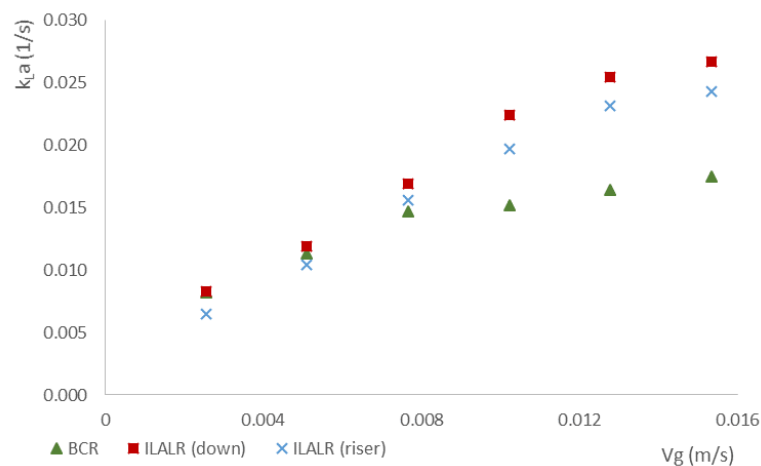


Figure 56 overall mass transfer coefficient versus gas velocity in ILALR for different amount of ABS: (a) Riser zone, (b) Down-comer zone.

According to the data as figure 56. Showed the relation of mass transfer in ILALR and BC. The results showed that ILALR in riser and down-comer zone had the $k_L a$ value higher than BC. The $k_L a$ value related to gas velocity from 2.0×10^{-3} - 1.5×10^{-2} m/s which

$k_L a$ value slightly increase from gas velocity 2.0×10^{-3} - 1.2×10^{-2} m/s. After that $k_L a$ value stabled from gas velocity 1.2×10^{-2} - 1.5×10^{-2} m/s. The reason that ILALR has the advantage of liquid and gas phase circulate within system. These were increasing the retention time of the bubble in the system which was more than the retention time in BC. The next section, the study was proved the efficiency of ILALR by adding plastic media.

- **Bubble size in ILALR.**

Figure 57 presents the variation of bubble diameter with gas flow rates obtained in ILALR.

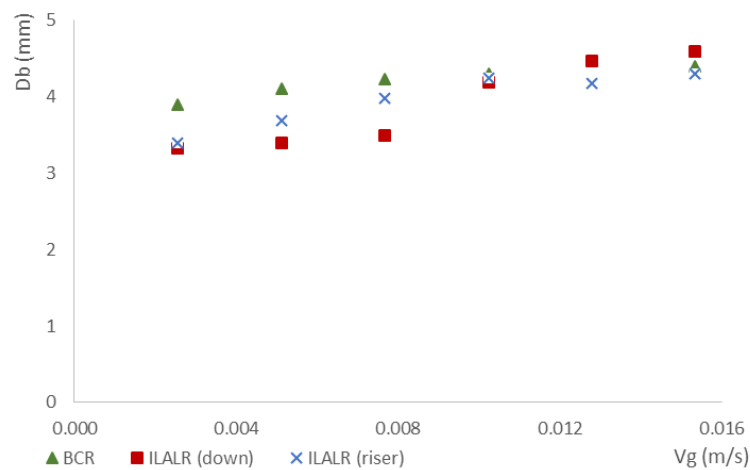


Figure 57 Bubble diameter versus gas velocity in BC and ILALR.

According to Figure 57, the gas velocity augmented between 2.0×10^{-3} - 1.5×10^{-2} m/s. For ILALR, at the same range of the gas velocity, it can be found that the range of bubble sizes are 3.38 - 4.17 mm for the riser zone, and 3.35 - 4.46 mm for the down-comer zone. Moreover, the bubble sizes from both reactors were closed and linearly increased with the gas velocity. The photographs of bubbles in ILALR at different gas velocity were shown in the Figure 58. The similar diffuser used in this work should control the average bubble size. This result proved that the difference of $k_L a$ values obtained with ILALR not depended on the change in bubble size. Therefore, the next section, the terminal rising bubble velocities were analyzed in both side of the ILALR for different gas flow rates.

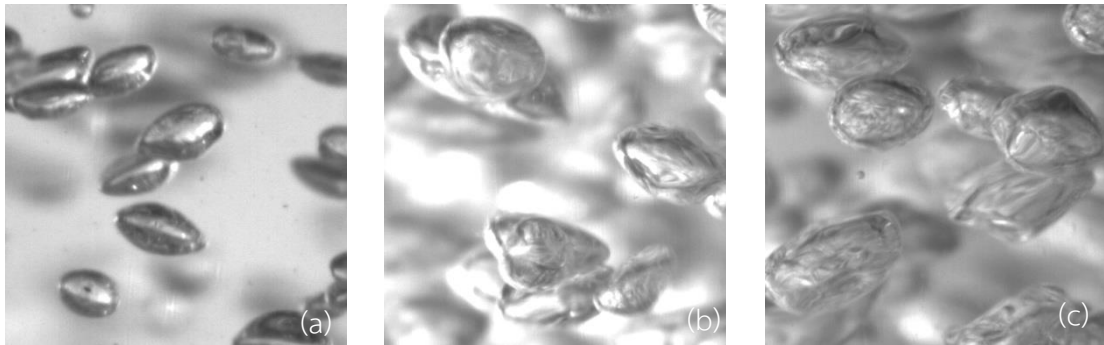


Figure 58 Bubble formation photographs in ILALR at gas flow rate: (a) 2.0×10^{-3} m/s, (b) 5×10^{-3} m/s, and (c) 1.5×10^{-2} m/s.

- Terminal rising bubble velocity (U_B) in ILALR.

Figure 59 presents the variation of terminal rising bubble velocity with gas velocity obtained in the BC and ILALR.

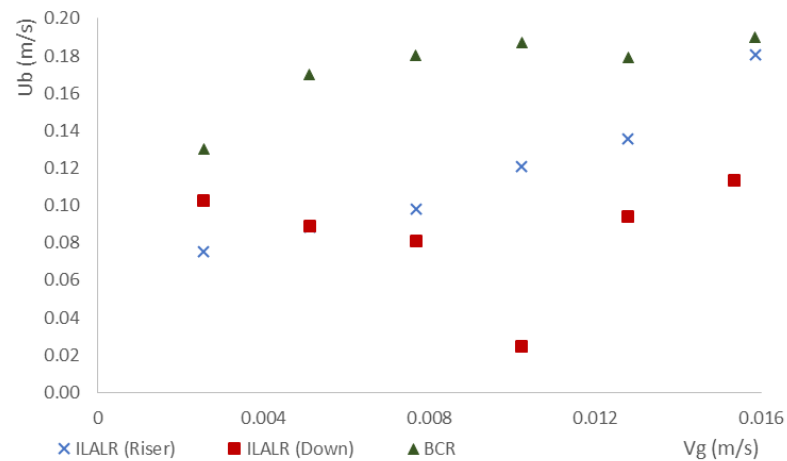


Figure 59 Terminal rising bubble velocity versus gas velocity in ILALR.

According to Figure 59, for the riser zone, it was shown that the U_B values varied between 0.075 to 0.135 m/s for riser zone, whereas, for the down-comer zone, the U_B values varied between 0.024 to 0.103 m/min, when gas flow rates changing between 2.6×10^{-3} to 1.5×10^{-2} m/s. The U_B values obtained with the riser zone increased with the gas flow rate. Moreover, the U_B values obtain in the riser zone of ILALR were closed to those obtain in BC. For the down-comer zone of the reactor, the values of the U_B decreased with the gas velocity. It can be noted that the liquid recirculated from the riser zone reduced the rising of bubble in the down-comer zone. The rising bubbles in down-comer zone of ILALR at different gas velocity were shown in the Figure 59. Note

that, the low values of the U_B in the down-comer zone caused an increase in the bubble-liquid contact time in the reactor.

- **Specific interfacial area (a) in ILALR.**

The specific interfacial area in the ILALR can divide into two parts: Riser zone and down-comer zone. For the riser zone, the specific interfacial area was calculated by equation 5.5, which was the same as case of BC. However, the cross-sectional area (A) of reactor was changed to the cross-sectional area of the riser zone. And for the down-comer zone, the specific interfacial area was calculated by the overall mass transfer coefficient divide by the liquid film mass transfer coefficient.

Figure 60 presents the specific interfacial area with gas flow rates obtained in the BC. and ILALR.

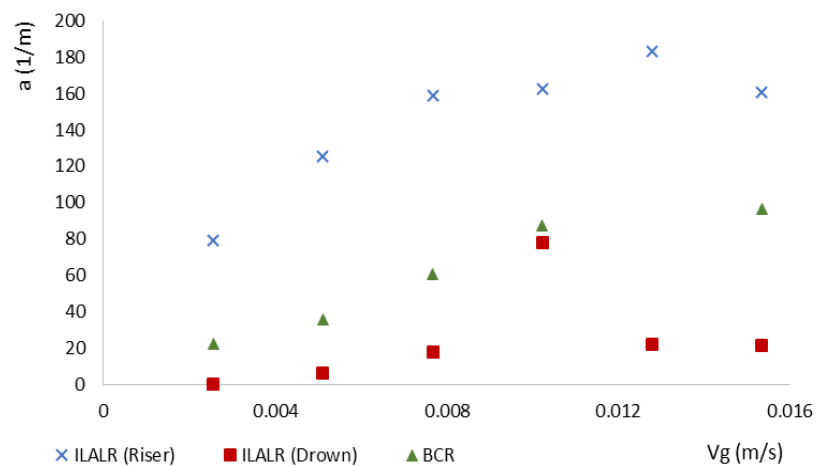


Figure 60 Specific interfacial area versus gas flow rate in BC. and ILALR.

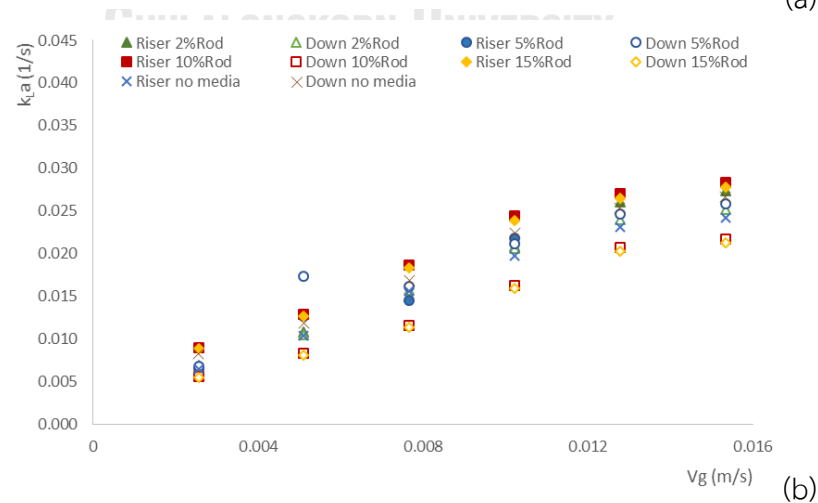
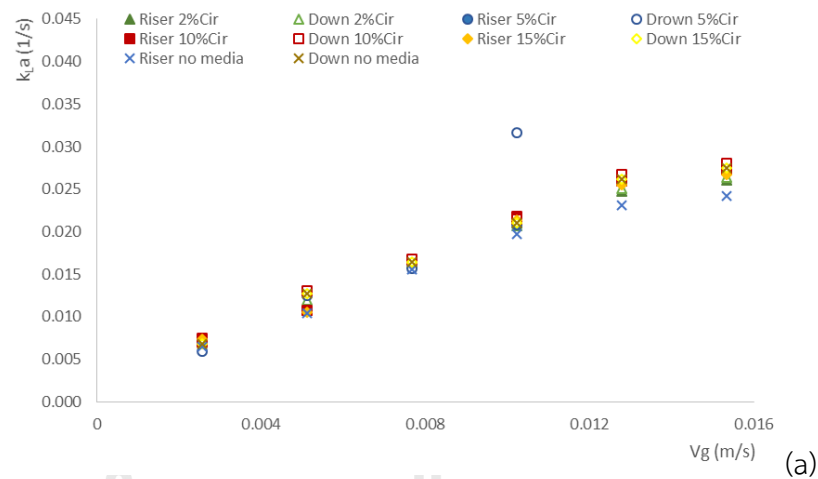
As shown in Figure 60, it can be shown that the values of specific interfacial area obtained with ILALR in riser and down comer zone. For ILALR, at gas velocity changing between 2.6×10^{-3} to 1.5×10^{-2} m/s, the specific interfacial area varied between $60.23 - 135.33 \text{ m}^{-1}$, and $45.01 - 592.16 \text{ m}^{-1}$ obtained in the riser zone and the down-comer zone, respectively. The specific interfacial area increased with the gas velocity. It should be observed that the slow increase of the specific interfacial area at a high flow rate. This result was due to the bubble coalescence phenomena at high gas flow rate, and thus affected the specific interfacial area.

5.5.2. Effect of plastic media on oxygen mass transfer and bubble hydrodynamic parameters in ILALR.

The objective of this part was to study the impact of different types and amounts of plastic media on oxygen mass transfer and bubble hydrodynamic parameters in ILALR. The overall mass transfer coefficient, bubble diameter, and terminal rising bubble velocity were observed at different gas flow rates. The methods for analyzed the values of these three parameters were the same as in the BC.

- Effect of plastic media on the overall mass transfer coefficient ($k_L a$) in ILALR

Figure 61 presents the variation of bubble diameter with gas velocity obtained in the ILALR for different shape and amount of plastic media.



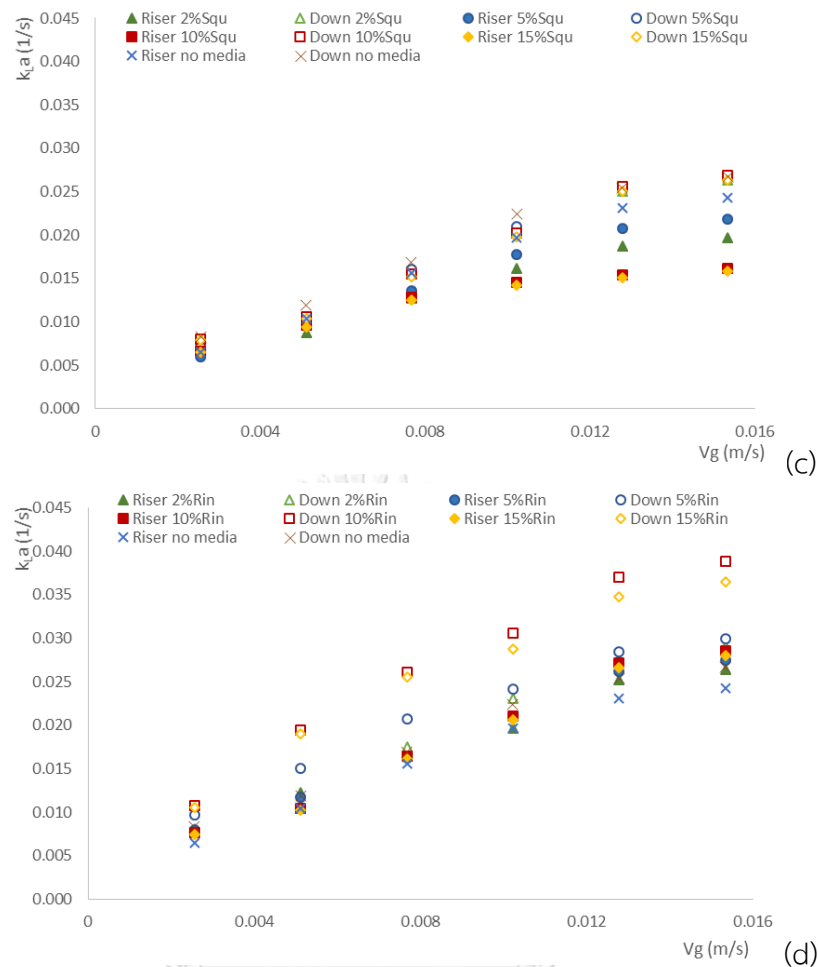


Figure 61 Overall mass transfer coefficient versus gas velocity for different amount and shape of plastic media: (a) circle, (b) Rod, (c) Square and (d) Ring respectively.

According to Figure 61, the k_{La} values obtained with ILALR rose with the gas flow rates. When the gas velocity varied between 2.6×10^{-3} to 1.5×10^{-2} m/s, the values of k_{La} coefficient were in range of $0.006 - 0.027 \text{ s}^{-1}$ and $0.95-0.037 \text{ min}^{-1}$ for the riser zone and the down-comer zone of the ILALR, respectively. The k_{La} coefficient obtained from both zones of the reactor were closed. The highest k_{La} value was obtained with 15% of plastic media loading with ring shape as show in figure 61 (d).

The reason that amount of plastic media increase which increase the effect of attraction between bubble and plastic media and obstruct the bubble movement in ILALR, this phenomena could be explained by physical properties of ring shape that structure of ring shape has the highest specific surface area and hold bubble inside the structure (fig. 62) and the effect of liquid and air circulation increase with increasing air flow rate and media concertation in down comer zone.

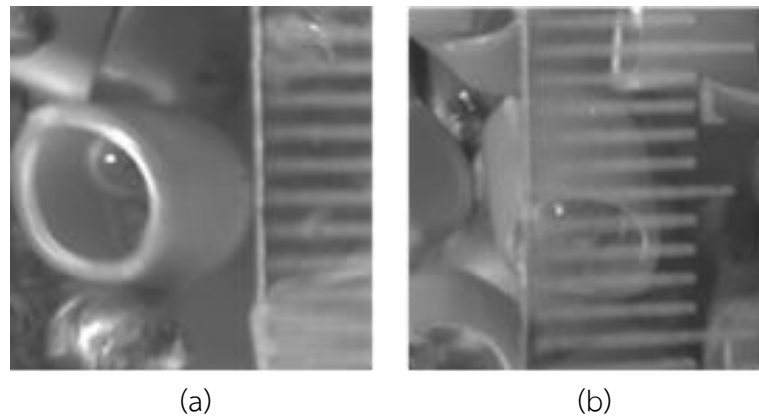
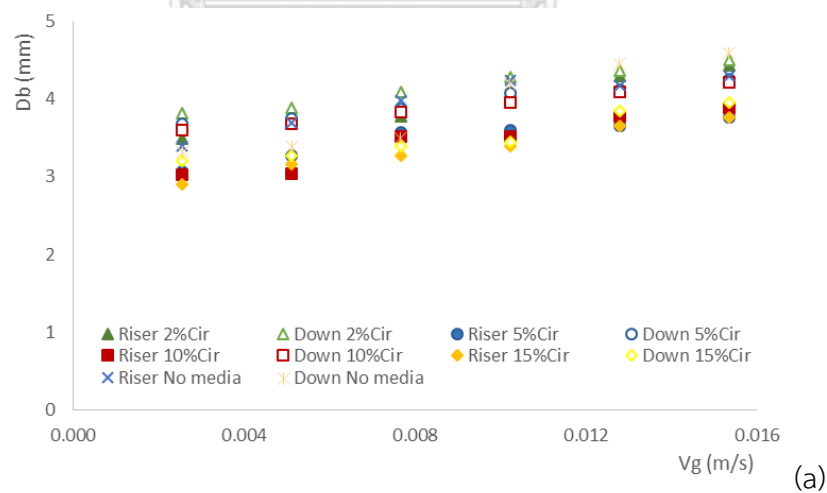


Figure 62 Bubble formation photographs in ILALR (Riser zone) at gas velocity 1.5×10^{-2} m/s and 15% plastic media loading of ring shape: (a) Riser Zone and (b) Down comer Zone.

- Effect of plastic media on bubble size parameter in ILALR.

In this part of experiment studied shape of media were classified into 4 types, square, rod, circle, and ring shape and study the various concentration of plastic media such as 2%, 5%, 10% and 15% (v/v). Figure 63 presents the variation of bubble diameter with gas flow rates obtained in the ILALR for different shape and amount of plastic media.



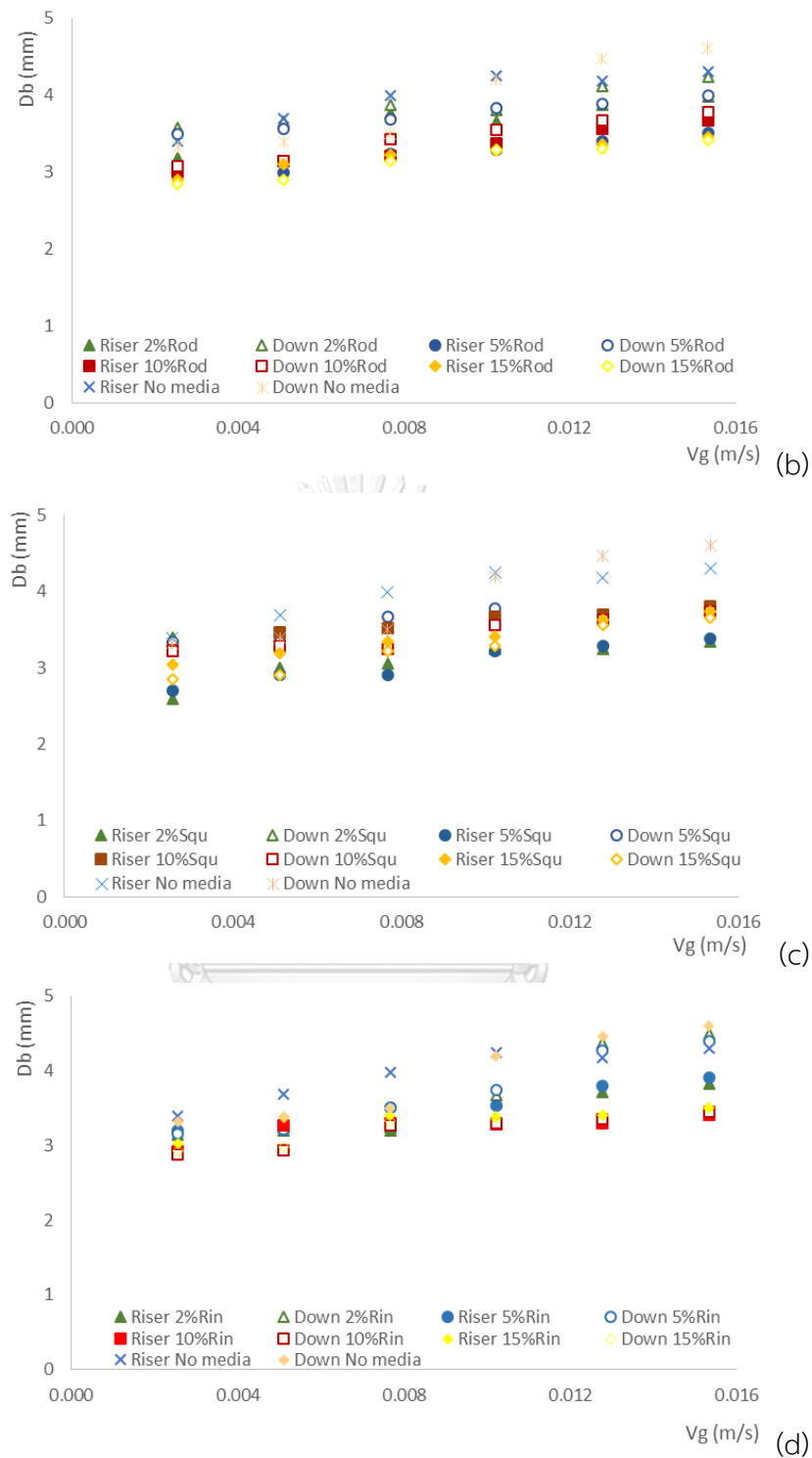


Figure 63 Bubble sizes versus gas velocity for different amount and shape of plastic media: (a) circle, (b) Rod, (c) Square and (d) Ring respectively.

According to the Figure 63, the bubble sizes obtained in the riser zone and the down-comer zone increased with the gas flow rate. The bubble diameters obtained at

gas velocity ranged between 2.6×10^{-3} to 1.5×10^{-2} m/s varied between 2.58 - 4.28 mm and 2.90 - 4.46 mm for the riser zone and the down-comer zone, respectively. The same trend line of the bubble sizes increase with gas velocity for both zone of the reactor. In conclusion, the addition of ring shape were reported the lowest bubble diameter for 15% plastic media loading which compared to another shape of plastic media as show in Figure 64.

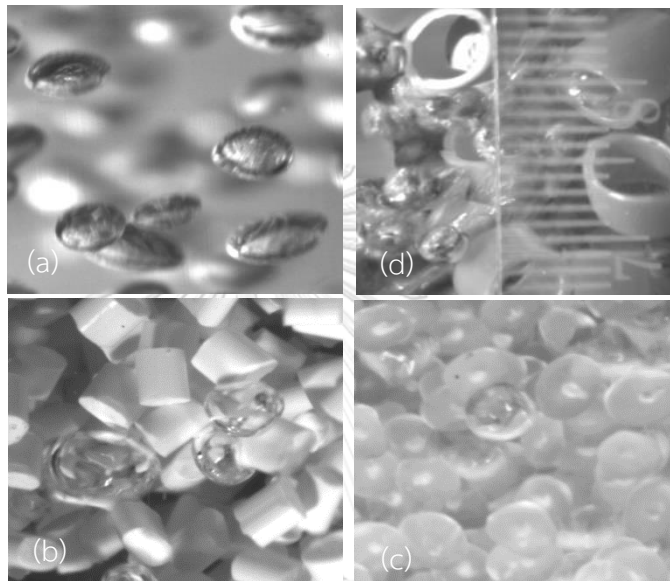
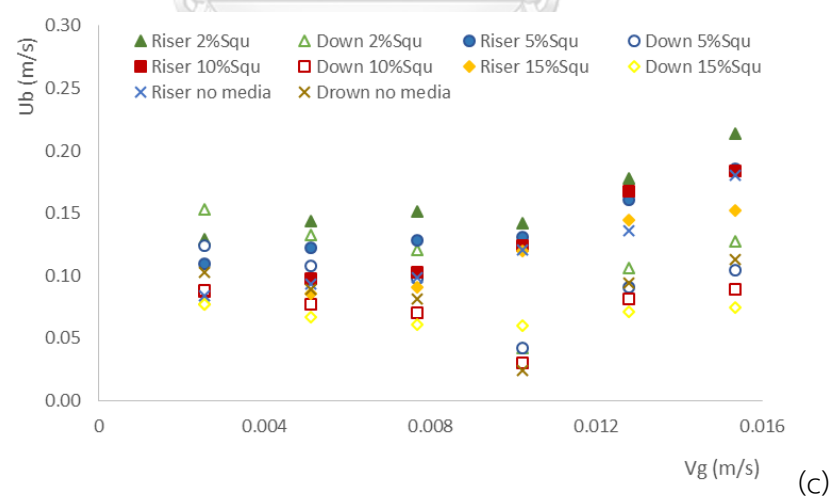
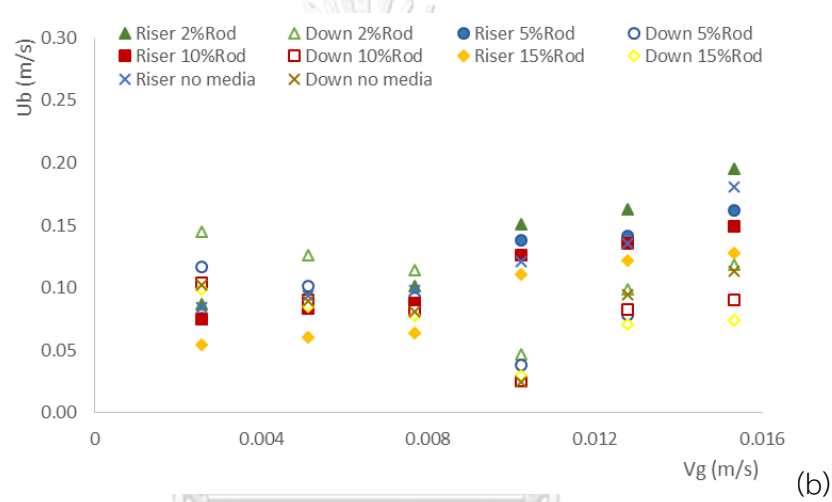


Figure 64 bubble formation photographs in ILALR (Riser zone) at gas velocity 1.5×10^{-2} m/s for: (a) No plastic media and 15% loading of Rod (b), Circle (c) and (d) Ring shape respectively.

- Effect of plastic media on terminal rising bubble velocity in ILALR

Figure 65 presents the variation of terminal rising bubble velocity with gas velocity obtained in the ILALR for different shape and amount of plastic media.



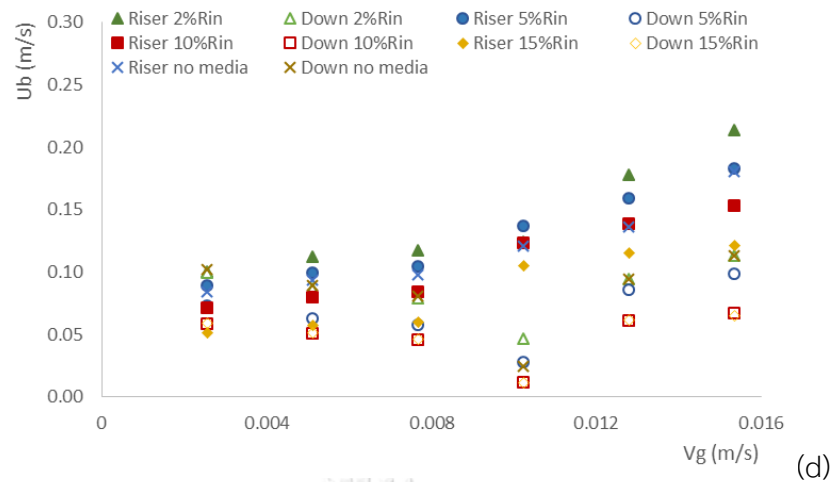


Figure 65 Terminal rising bubble versus gas velocity for different amount and shape of plastic media: (a) circle, (b) Rod, (c) Square and (R) Ring respectively.

Concerning to Figure 65, the variation of U_B obtained experimentally varied between 0.075 – 1.86 m/s for the riser zone and 0.45 – 0.01 m/s while gas flow rates can change between 2.6×10^{-3} to 1.5×10^{-2} m/s. The values of the U_B increased with gas flow rate in the riser zone, whereas, decreased with gas flow rate in the down-comer zone. It can be stated that the addition of plastic media provided the lower of U_B values in the riser zone, due to adding plastic media provide the small bubble size obtained in the ILALR. Which is corresponded the result from previous work. Whereas, the lower of U_B values in the down-comer zone, correspond to the obstruction gas and liquid circulation in the system.

- **Bubble hydrodynamic parameters determination**

In this part of experiment determined the bubble hydrodynamic parameters such as bubble velocity (U_B), gas hold up (ϵ_g) and interfacial area (a). These were used to describe air circulation rate (Q_{gr}) and mechanism in ILALR.

Table 11 the relation between Q_g , ϵ_g , D_{Br} , D_{Bd} , U_{Br} and U_{Bd} in ILALR at 10% concentration.

Q_g (m^3/s)	ϵ_g (-)	D_{Br} (mm)	U_{Br} (m/s)	D_{Bd} (mm)	U_{Bd} (m/s)
2.5	0.0229	2.9212	0.0643	2.8719	0.0584
5.0	0.0344	3.2674	0.0757	2.9305	0.0508
7.5	0.0410	3.2988	0.0841	3.2674	0.0462
10.0	0.0530	3.2881	0.1238	3.2988	0.0117
12.5	0.0620	3.3023	0.1390	3.3493	0.0610
15.0	0.0665	3.4014	0.1529	3.4497	0.0671

Table 11. Showed the result from the calculation, for example; air flow rate (Q_g), gas hold up (ϵ_g), bubble diameter in riser zone (D_{Br}), bubble diameter in down-comer (D_{Bd}), bubble velocity in riser (U_{Br}) and bubble velocity in down-comer (U_{Bd}) in ILALR at 10% concentration. The result explained the relation of ϵ_g , D_{Br} , D_{Bd} , U_{Br} and U_{Bd} with Q_g in ILALR that the bubble hydrodynamics slightly increase with in air flow rate 2.5 to 15 l/min. Moreover, the result from this experiment used to calculate the air circulation rate (Q_{gr}) in the next section.

- **Air circulation rate (Q_{gr}) determination**

Air circulation rate (Q_{gr}) is the gas bubbles velocity in the down-comer. In this case, the bubbles move back to the riser zone from below the splitter plate. It can be determined by the equation of interfacial area in riser and down-comer zone. The interfacial area (a) is a function of the bubble formation frequency, the terminal bubble rising velocity and the generated bubble diameter. In this study, local interfacial area for riser (a_r) and down comer zone (a_d) can be calculated from equation (5.6) and (5.7) respectively;

$$a_r = \frac{(Q_g + Q_{gr})}{V_{Br}} \times \frac{H_L}{U_{Br}} \times \frac{S_{Br}}{V_{Total}} = \frac{6}{D_{Br}} \cdot \frac{\epsilon_{gr}}{(1 - \epsilon_{gr} - \epsilon_{sr})} \quad (5.6)$$

$$a_d = \frac{(Q_{gr})}{V_{Bd}} \times \frac{H_L}{U_{Bd}} \times \frac{S_{Bd}}{V_{Total}} = \frac{6}{D_{Bd}} \cdot \frac{\epsilon_{gd}}{(1 - \epsilon_{gd} - \epsilon_{sd})} \quad (5.7)$$

To find air circulation rate (Q_{gr}), the gas holdups in the riser (ϵ_{gr}) and down-comer (ϵ_{gd}) were written down in equation (5.8), A_r and A_d are the cross-sectional area of the riser and down-comer, respectively. (Deng, 2010)

$$\epsilon_g = \frac{\epsilon_{gr}A_r + \epsilon_{gd}A_d}{A_r + A_d} \quad (5.8)$$

According to Figure 66, the relation of air circulation rate (Q_{gr}) and gas velocity in ILALR. The increasing of Q_{gr} relates to the increasing of gas velocity and increasing of media concentration when it was compared to the different plastic media concentration at the similar gas velocity. The result proves that adding plastic media has an advantage to the bubble circulation.

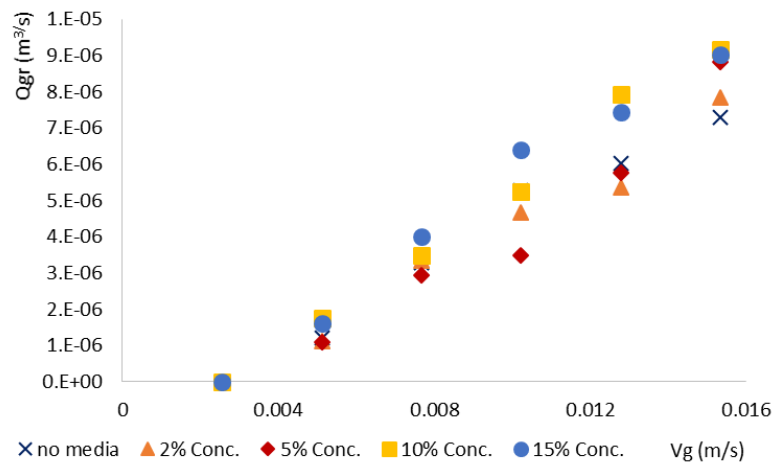
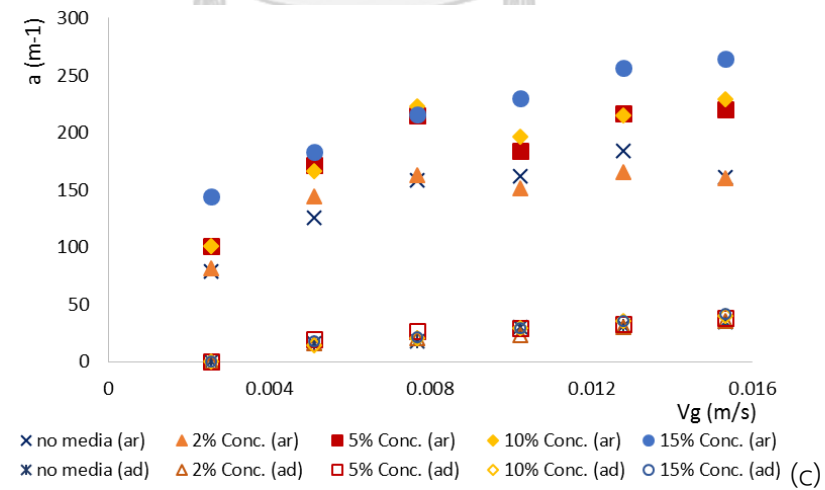
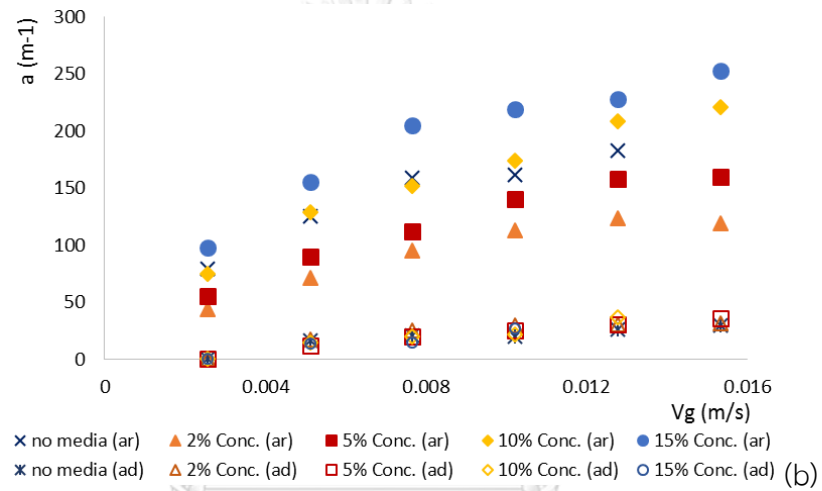
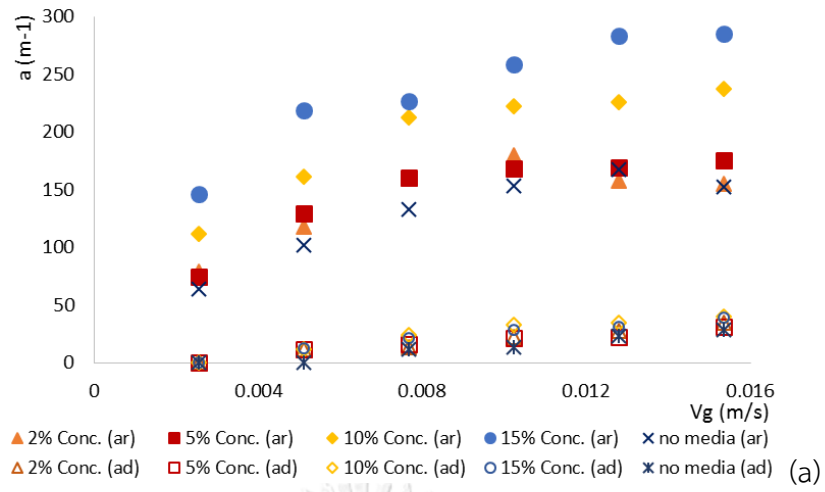


Figure 66 relation of Q_{gr} and air flow rate in ILALR.

- Effect of plastic media on the specific interfacial area (a) in ILALR

Figure 67 presents the variation of specific interfacial area with gas velocity obtained in the ILALR for different shape and amount of plastic media.



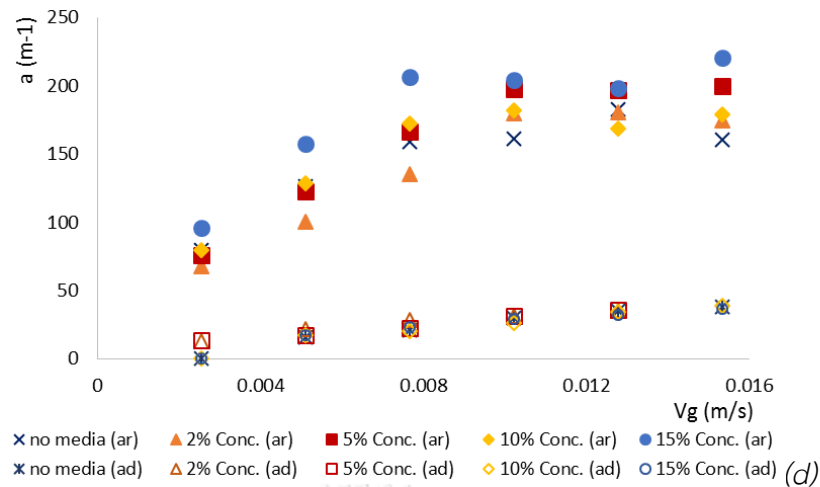


Figure 67 specific interfacial area versus gas velocity for different amount and shape of plastic media: (a) Ring, (b) Circle, (c) Rod and (d) Ring respectively.

Considering the Figure 67, it was shown that the specific interfacial area varied between 19.77 to 80.14 m^{-1} for riser zone, and 36.86 to 78.57 m^{-1} for down-comer zone, when gas velocity ranged between 2.6×10^{-3} to 1.5×10^{-2} m/s. The specific interfacial area in both zones were closed and continuously increased with the gas velocity. The highest values obtained for both zone of the reactor were observed for 10% of ring shape particles at 1.5×10^{-2} m/s

The relation of interfacial area and air flow rate in ILALR In this part of experiment studied the relation of interfacial area and air flow rate in ILALR. The result showed in Figure 67, interfacial area in riser (a_r) and interfacial area in down-comer zone (a_d) increase with air flow rate. The a_d directly relate to gas flow rate circulation (Q_{gr}), which happen in regime II and III. The highest a_d were showed at 10% media concentration which corresponded with the highest $k_L a$ valve in previous experiment.

- The Comparison of experimental and predicted of k_L

In this part of the experiment was rechecked air circulation rate (Q_{gr}) determination method by using k_L from experiment and k_L from Higbie equation. The liquid-side mass transfer coefficient (k_L) was determined by the volumetric mass transfer coefficient, $k_L a$ and the interfacial area, a . The local liquid-side mass transfer coefficient is simply determined by equation below. (Deng, 2010)

$$k_L = \frac{k_L a_r + k_L a_d}{a_r + a_d} \quad (5.9)$$

Moreover, the prediction of the liquid-side mass transfer coefficient (k_L) in this study, the predicted k_L coefficient is calculated from Higbie equation below. (Painmanakul et al, 2009)

Higbie equation:
$$k_L = \sqrt{\frac{D_B U_G}{\pi d_B}} \quad (5.10)$$

In this study, the predicted k_L coefficient is calculated as the product of the calculated values from Higbie equation. Figure 68 shows that a relatively good agreement between the experimental and the predicted k_L coefficient is obtained (average difference about $\pm 20\%$). However, the differences happen at the values of k_L due to the human error and the technical for measuring are probably responsible for the difference value

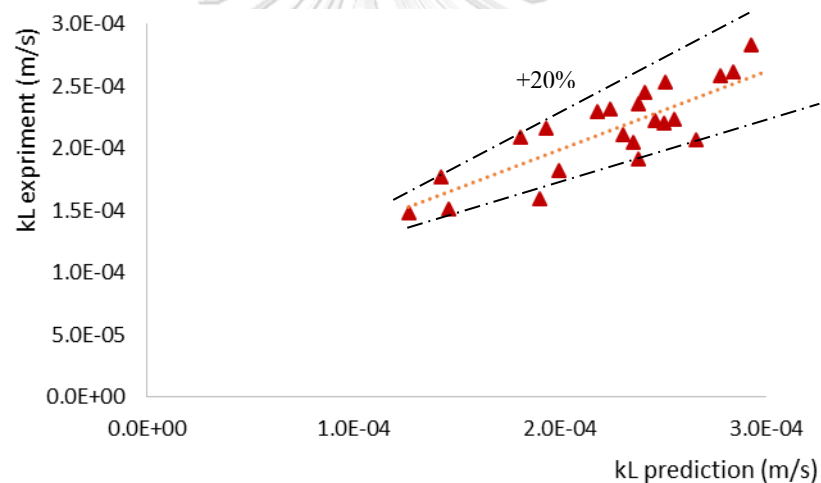


Figure 68 Comparison of experimental and predicted of k_L by using the different gas flow rates.

5.5.3 Comparison the effect of best plastic media condition on mass transfer and bubble hydrodynamic parameters in BC and ILALR.

By analyzed the best condition for oxygen absorption in this work, the impacts of 10% plastic media loading (best type and concentration of plastic media) obtained with the ILALR on the $k_L a$, D_B , a , and k_L parameters were show in Figure 5.20-5.22.

- Overall mass transfer coefficient ($k_L a$) in BC and ILALR

Figure 69 present the variation of overall mass transfer coefficient with gas velocity obtained in the BC and ILALR for no media and 10% of ring shape.

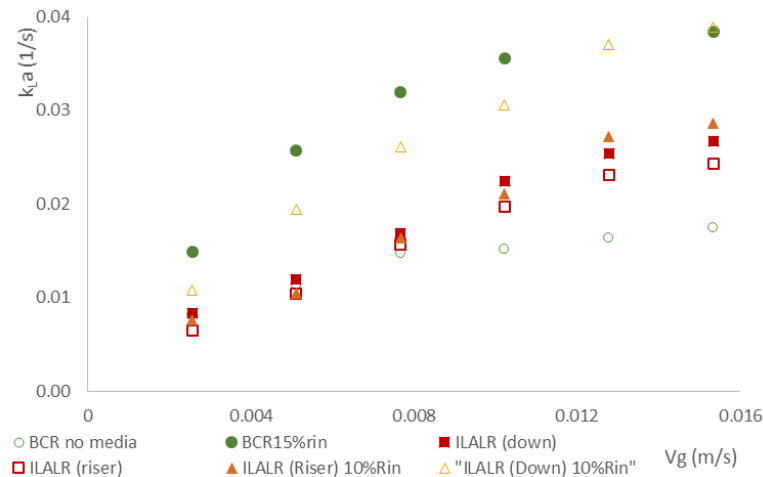


Figure 69 overall mass transfer coefficient versus gas velocity in BC and ILALR.

According to the Figure 69, the $k_L a$ values obtained with ILALR were higher than those obtained with BC. Moreover 1.5×10^{-2} m/s, the addition of 10% ring shape adding provided an increase in the $k_L a$ values for 33% and 54% obtained with BC and ILALR, respectively. It can be noted that the higher increase in $k_L a$ values obtained with ILALR was due to the higher amount of suspended PP particles within the tap water. Therefore, the bubble and liquid recirculation in ILALR should be responsible for this result.

- Bubble diameter (D_B) in BC and ILALR

Figure 70 presents the variation of bubble diameter (D_B) with gas velocity obtained in the BC and ILALR for no media and 10% of ring shape.

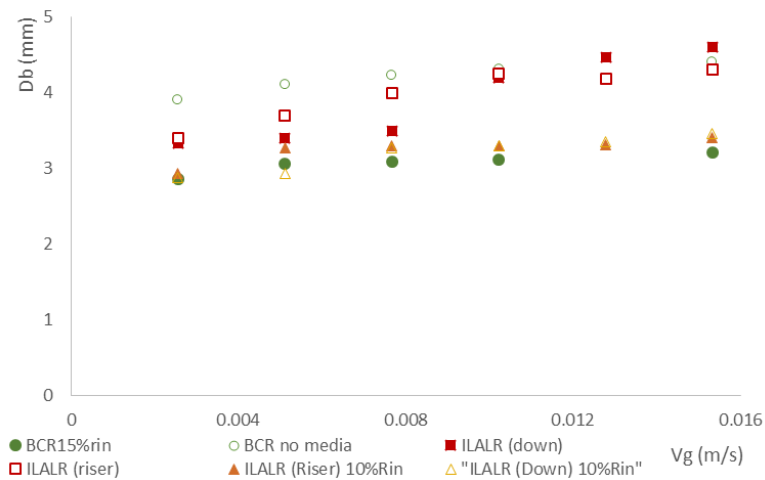


Figure 70 Bubble diameter versus gas velocity in BC and ILALR.

By considering to the Figure 70, the bubble diameters obtained with BC and ILALR (Riser and down-comer zone) were close. From the Figure, it can be stated that:

- For all gas velocity, the bubble size obtained with BC and ILALR for no media and 10% plastic media addition were close. The similar gas diffuser used in this work should be responsible for this result.
- The bubble size obtained for all cases depend only on the gas velocity. The increased in gas flow rate provided an increase in bubble diameter. In this regard, the bubble coalescence phenomena should be responsible for this result.
- The addition of 10% plastic media, and the different shape of reactors not modified the bubble size in BC. and ILALR
- By considering the bubble diameter in the ILALR, for both no media and 10% of plastic media addition, the bubble diameters obtained with riser zone were close to those of down-comer zone.

From these results, it can be again concluded that the change in specific interfacial area by adding plastic media was not related to the change in bubble size.

- **Specific interfacial area (a) in BC and ILALR**

Figure 71 presents the variation of specific interfacial area (a) with gas flow rates obtained in the BC and ILALR for no media and 10% of ring shape.

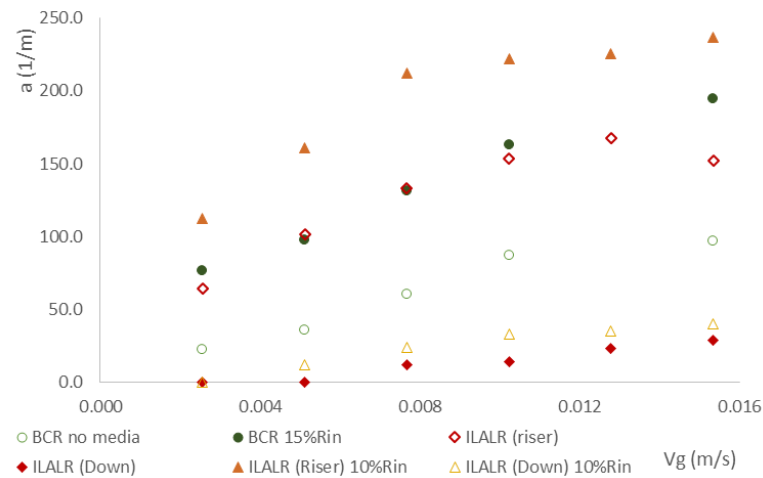


Figure 71 specific interfacial area versus gas velocity in BC. and ILALR.

From the Figure 71, the specific interfacial areas obtained with ILALR (Riser and down-comer zone) were higher than those of BC. Moreover, at 1.5×10^{-2} m/s and the 10% of plastic media loading caused an increase in the specific interfacial area values for 38%, 36%, and 36% obtained with the BC, the riser zone, and the down-comer zone of ILALR, respectively. It can be observed that the increase in the specific interfacial area obtained with the BC and ILALR respectively.

5.6 Conclusions

The increasing of $k_L a$ value relate with shape and suitable concentration of plastic media due to the physical properties of ring shape such as, structure and specific surface which obstruct the bubble movement and increasing mass transfer rate in the system. The result from figure 65 confirmed the reason that high concentration of plastic media decrease bubble rising velocity in riser and down comer zone because high concentration increase the frequency of collision between media and also bubble and media. Moreover, air circulation rate (Q_{gr}) determination method suitable for explain the bubble hydrodynamic in the ILALR which k_L value from the experiment showed good agreement with the predicted k_L coefficient is obtained the average difference about $\pm 20\%$. In the future, the new knowledge for air circulation rate (Q_{gr}) determination method will be applied for the operating design in ILALR.

CHAPTER 6

STUDY THE EFFECT OF CONTINUOUS SYSTEM ON BUBBLE HYDRODYNAMIC AND VOCs MASS TRANSFER PARAMETER IN ILALR

6.1 Introduction

A continuous-flow internal loop airlift reactor, absorption processes, is an ongoing separation in which a mixture is continuously (without interruption) fed into the process and separated fractions are removed continuously as output streams. ILALR are widely used in the chemical and biochemical industries (Kralik et al., 1990) because of the advantages they offer such as the lack in moving parts, high-gas-liquid contact area, good mass/heat transfer rates, and large liquid hold-up. For processes. The main parameters determining the performance of ILALR are the superficial gas velocity, u , the operating pressure and temperature, sparger design, gas hold-up distribution, bubble break-up etc. the object of this part improve the efficiency of VOCs removal efficiency with using co-current and counter-current operation system.(Bhaga, 1970)

This experiment can be separated into 2 part. First, Study the effect of continuous operation in ILALR and the second part were studied the effect of simulated VOCs gas absorption by using and plastic media in ILALR. The experiment set up for each part was showed in next section.

6.2 Objectives

- Study the impact of using continuous ILALR system on mass transfer and bubble hydrodynamic parameters.
- The effect of adding plastic media on mass transfer and bubble hydrodynamic parameters in continuous ILALR system.
- Determined the VOCs removal efficiency by using internal loop airlift reactor.

6.3 Literature Review

Tiwari, G. and Bose, P. (2007) studied the continuous flow counter-current bubble type ozone contactor, 3 m in length and 25 mm diameter (Figure), indicated that the gas phase hold-up (ϵ_g) in the contactor increased linearly from 8 to 15% when gas flow rate (Q_g) was increased from 500 to 1000 mL min⁻¹ and focused on mathematically modeled considering the hydrostatic pressure variation along reactor height, and assuming the gas and liquid phases in the reactor to be plug flow and mixed flow. Final compared the data between the experiment and mathematic model. The result showed that the experimental data on evolution of effluent gaseous ozone concentration from the reactor operation under various conditions also matched well with corresponding simulation results, suggesting correctness of the determined $k_L a$ value. Sensitivity analysis indicated that the model simulation results were relatively insensitive to changes in $k_L a$ value in the range of 0.015–0.035 s⁻¹.

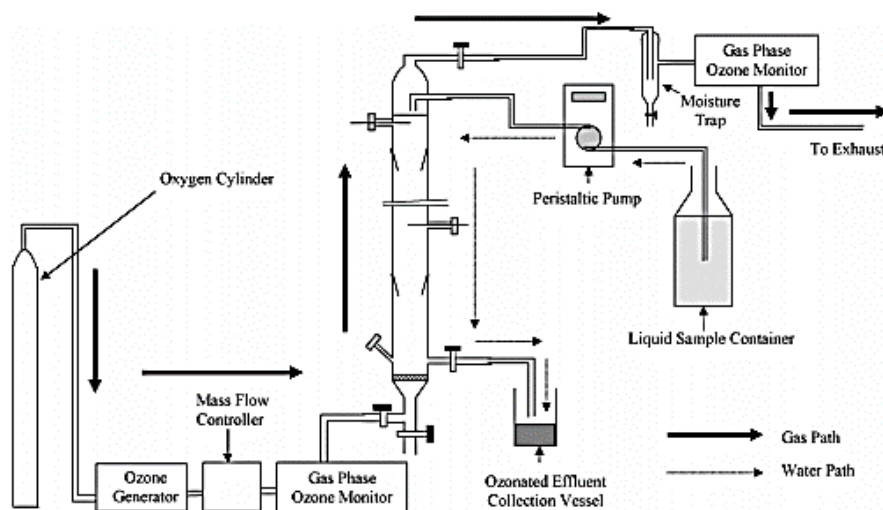


Figure 72 Schematic of the experimental setup.

Gao et al. (2005) studied The gas absorption characteristics of the Karman contactor, The Karman contactor was provided by Reika Kogyo Co., Ltd., Japan. Its volume is 0.7 L and a down-flow static-mixing zone (26 mm i.d.) and an up-flow zone 41 mm inside diameter. The experiment was investigated under various gas and liquid flow rates and mass transfer the volumetric mass transfer coefficient of ozone was compared between the Karman contactor and the other contactors reported. The

result show that the values of $k_L a$ increased with the increase of both gas and liquid flow rates owing to fine bubbles generated by the Karman mixer.

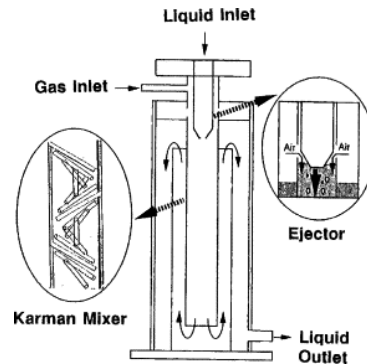


Figure 73 Schematic of Karman contactor.

Farinesa et al. (2003) studied ozone mass transfer and decomposition in a co-current up-flow reactor packed with granular silica. The reactor has 0.05 m diameter column and was carefully packed from the bottom to a given height (0.20, 0.35, 0.50 m) with the granular silica gel. The liquid flow was injected using a peristaltic pump through two inlet points set under and at each side of the gas diffuser at liquid flow rate (20, 30, 40, 60 \pm 0.6 l/h). The result showed that the concentration of dissolved ozone at steady state is found to increase with gas velocity and bed height. Liquid velocity is shown to cause the opposite effect. Whereas ozone decomposition in the presence of silica gel is shown limited to self-decomposition in liquid bulk, the overall mass transfer coefficient is mainly affected by gas velocity.

6.4 Materials and Method

6.4.1 Experimental setup

The airlift reactor (ILALR) with 15 cm in diameter 100 cm in height and add sampling plots every 20 cm for co-counter operation system. The schematic diagrams of experimental set-up for this research work were shown in Figures 74 The equipment used in this study contains: 1) Air pump 2) Ball valve 3) Pressure gage 4) Gas flow meter 5) Rigid orifice gas diffuser 6) Reactor 7) Liquid phase 8) Dissolved oxygen electrode and 9) Plastic media 10) sampling plot 11) liquid inlet 12) liquid inlet

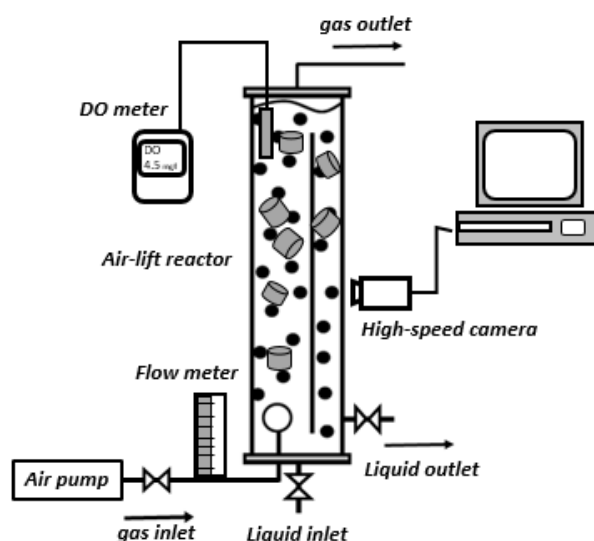


Figure 74 Internal loop airlift reactor (ILALR) in study of continuous system.

- **Benzene generator**

For generating benzene gas in this study, 250 ml of pure benzene was added in a closed Erlenmeyer flask. Then, air was injected into the flask in order to generating benzene gas stream from their volatilization. The schematic diagram of experimental set-up for benzene generation is show in Figure 75. The equipment used for benzene generator contains: 6) Air pump 7) Gas tube 8) Ball valve 9) Glass tube L shape 10) Gas flow meter 11) Rubber stopper 12) Erlenmeyer flask and 13) Pure benzene.

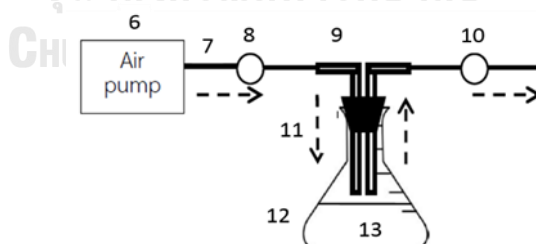


Figure 75 Benzene generator.

- **Preparing of absorbents**

The aim of this part was to generate the absorbents used in this study. Therefore, the aqueous solution of non-ionic and an-ionic surfactant were prepared. Moreover, the different parameters were investigated the Critical Micelle Concentration

(CMC). The summary variables concerning to the preparation of absorbents (tap water, aqueous solution of non-ionic and an-ionic surfactant) can be summarized and shown in Table 12.

Table 12 Characteristics of surfactant and water.

Absorbent	Chemical name	MW (g/mol)	CMC (mg/L)	Concentration		Surface tension (mN/m)
				CMC	mg/L	
Anionic	Sodium 2-ethylhexyl sulfate (SES)	232.27	2879	0.01	28.79	58
				0.1	287.9	37.4
				1.0	2879	33.2
				3.0	8637	31.7
Non-ionic	Polyoxyethylene (5) Lauryl ether (Dehydol LS 5 TH)	406.6	25.21	0.01	0.2521	57.5
				0.1	2.521	48.1
	Polyoxyethylene (20) sorbitan monooleate (Tween 80)	1310	15.7	0.1	0.000012	59.3
				1.0	0.00012	44.2
				3.0	0.00036	43.5
Water	-	18	-	-	-	72

- **Gas Chromatography Detector FID, Agilent Technologies 6890N**

In this study, the Agilent Technologies gas chromatograph 6890N with flame ionization detector (FID) and a split injector, operated in split ratio (10:1) was used for quantification of benzene. The conditions of GC parameters were shown in Table 13.

Table 13 the conditions of GC parameters.

Parameter	Condition
Temperature of injection port and detector	100 - 200 °C
Column Type	HP-1
Column Size	25 m x 0.32 mm i.d., 0.17 μ m film thickness
Detector	FID, 300 °C
Carrier gas	He

- **UV-Visible spectrophotometer**

For this work, the concentration of benzene outlet was measured by using Genesis 10S UV-Vis spectrophotometer. The absorbance of benzene at 254 nm was recorded and the concentration of benzene was calculated using the calibration curve.

- **Method for determining the mass transfer and bubble hydrodynamic parameter**

The volumetric mass transfer coefficient ($k_L a$)

The volumetric mass transfer coefficient ($k_L a$) was determined the efficiency of mass transfer in the system. The mathematic is used to determine $k_L a$ value on the assumption *steady state contract system*, gas phase become plug flow condition and liquid become completely mix flow condition. It can be written as following equation:

$$T = L. (x_{out} - x_{in}) = k_L a. (\Delta x_{ML}). S. Z \quad (6.1)$$

Then Δx_{ML} can be found in equation 5.2

$$\Delta x_{ML} = \frac{(x_{in} - x_{in}^*) - (x_{out} - x_{out}^*)}{\ln \frac{(x_{in} - x_{in}^*)}{(x_{out} - x_{out}^*)}} \quad (6.2)$$

- Benzene removal efficiency (%Eff)

Benzene removal efficiency (%Eff) indicated the performance of the absorption process. Note that the area under curve obtained with gas chromatography was used as the benzene concentration. The %Eff can be determined by the following equation;

$$\%Eff = \frac{C_{inlet} - C_{outlet}}{C_{inlet}} \times 100 = \frac{Area_{inlet} - Area_{outlet}}{Area_{inlet}} \times 100 \quad (6.3)$$

6.4.2 Experimental procedure

- Study the effect of continuous operation in and ILALR.

The objective of this part study the effect of continuous operation in and ILALR with variety of gas flow rates on oxygen mass transfer and bubble hydrodynamic characteristics in BC and ILALR. The outline of this study was presented in Figure 76 and the summary variables concerning to this study can be presented in Table 14.

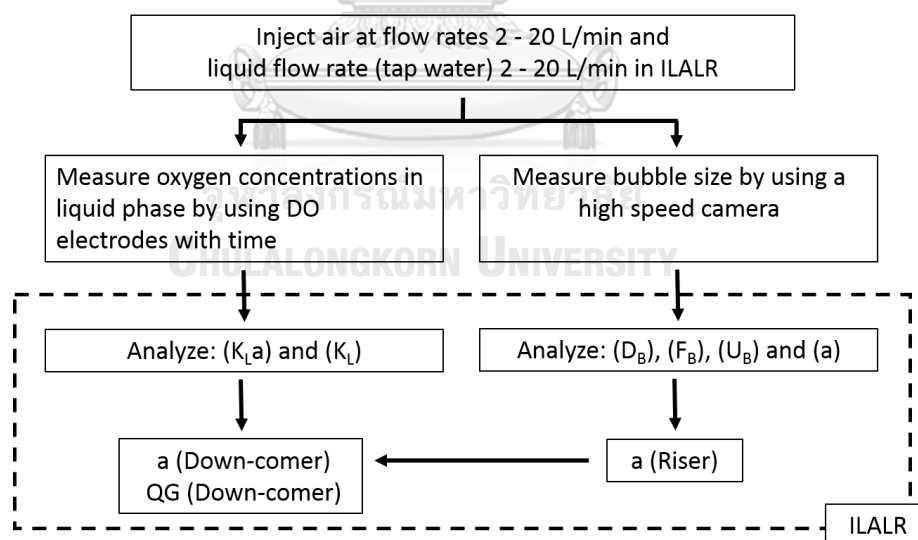


Figure 76 diagram of study the effect of continuous system in ILALR.

Table 14 Variable of study the effect of co-current operation in ILALR.

Fixed Variables	Parameter
Reactor	ILALR
Gas phase (absorbate)	Oxygen
Liquid phase (absorbent)	Tap water
Independent Variables	Parameter
Gas flow rate	2 – 15 l/min
Liquid flow rate	2 – 15 l/min
Dependent Variables	Parameter
Mass transfer parameters	$K_L a$ (Riser and down-comer zone)
Bubble hydrodynamic parameters	U_B , D_B , and a (Riser and down-comer zone)

- Studying application simulated VOCs absorption.

The aim of this study is to combine the best condition of using plastic media and modified absorbent then apply in operation on simulated VOCs absorption in BC and ILALR. The flow diagram and the summary variables in this research are presented in Figure 77 and Table 15, respectively.

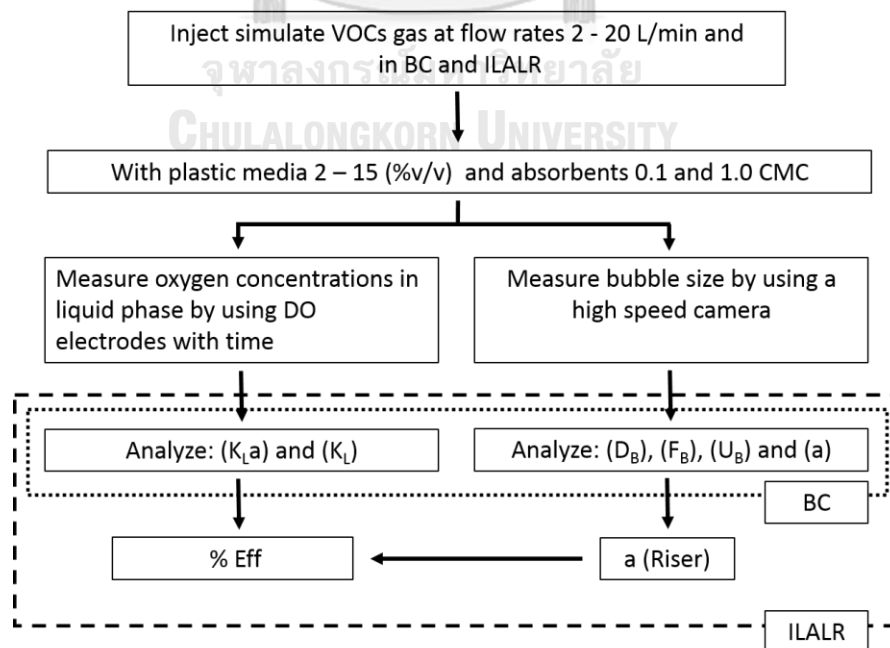


Figure 77 diagram of studying application for simulated VOCs absorption.

Table 15 variable of study the effect of co- current operation on simulated VOCs absorption.

Fixed Variables	Parameter
Reactor	ILALR and BC
Gas phase (absorbate)	Simulate VOCs gas
Independent Variables	Parameter
Liquid flow rate	2.5 - 15 l/min
Gas flow rates.	2.5 - 15 l/min
Media addition	Most practical type and concentration of media and surfactant
Concentration of surfactant	
Dependent Variables	Parameter
Mass transfer parameters	$k_L a$, K_L (Riser and down-comer zone)
Bubble hydrodynamic parameters	
	U_B , D_B , and a (Riser and down-comer zone)

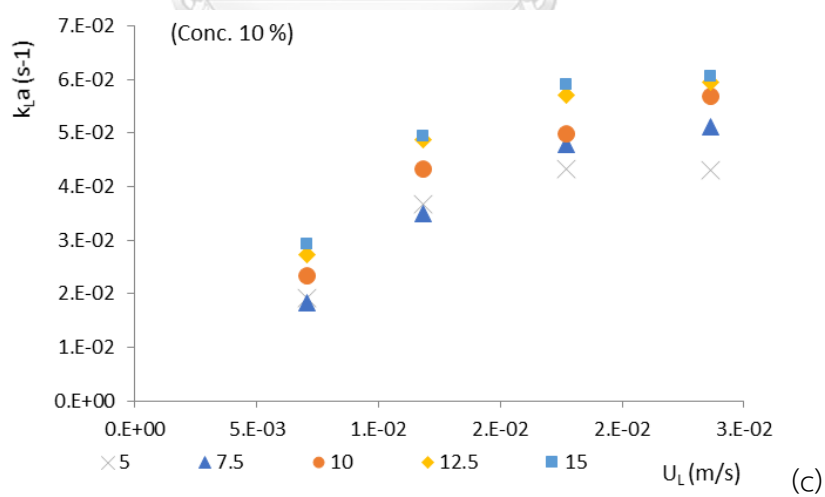
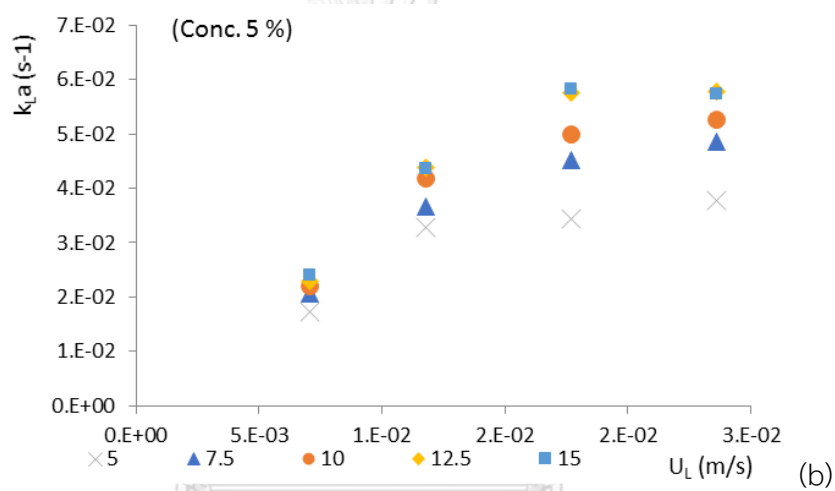
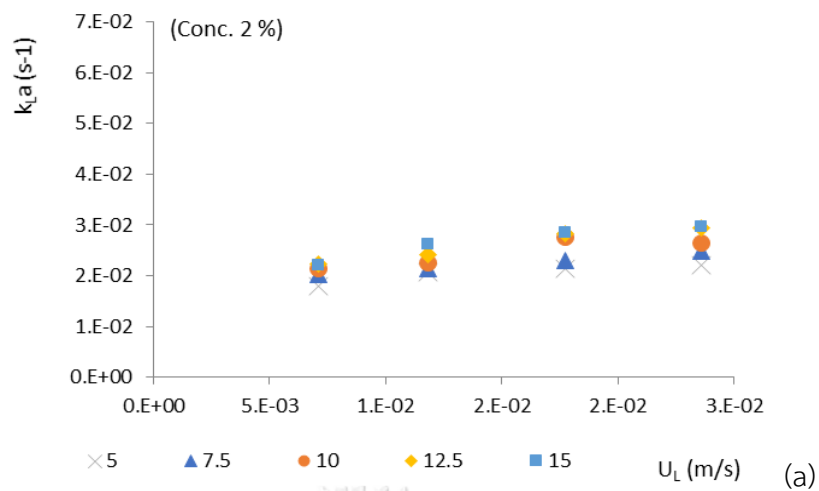
6.5 Results and Discussion

6.5.1 Study the oxygen mass transfer and bubble hydrodynamic parameters in continuous ILALR.

The objective of this part was to study the impact of different types and amounts of plastic media on oxygen mass transfer and bubble hydrodynamic parameters in continuous ILALR. The overall mass transfer coefficient were observed at different gas flow rates and liquid velocity. The methods for analyzed the values of these three parameters were the same as in the ILALR.

- **Effect of plastic media on the overall mass transfer coefficient ($k_L a$) in continuous ILALR**

Figure 78 presents the variation of overall mass transfer coefficient obtained in the ILALR for amount of plastic media and liquid velocity.



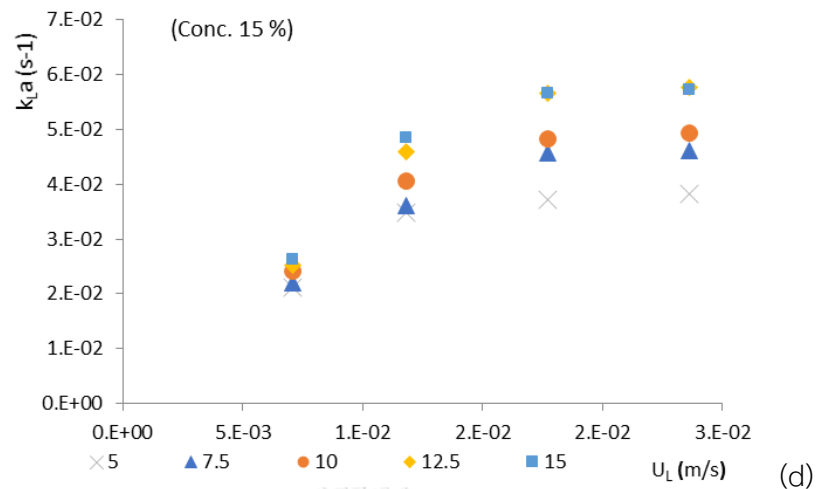


Figure 78 The variation of overall mass transfer coefficient obtained in the ILALR for amount of liquid velocity and plastic media 2%, 5%, 10% and 15% in ILALR respectively.

According to Figure 78 the k_La values obtained with ILALR rose with the gas flow rates. When the gas flow rate varied between 2.5 – 1.5 L/min, the values of k_La coefficient were in range of $0.0072 - 0.0321s^{-1}$ and $0.0084 - 0.0357 s^{-1}$ for the riser zone and the down-comer zone of the ILALR, respectively. Which k_La value in down-comer zone are higher than riser zone, this trend line similar to batch system. Then the effect of liquid velocity in the system, the result show that low liquid velocity (0.007 – 0.018 m/s) k_La value slightly increase and show the highest k_La value with 15% of plastic media loading, 0.018 m/s. When Liquid velocity become higher (0.017 – 0.023 m/s), k_La value slightly decrease.

- The Comparison of experimental and predicted of k_La

In this part of the experiment was rechecked overall mass transfer coefficient (k_La) determination method by using k_La from experiment and k_La equation below; (Chist, 1989)

$$k_La = 0.349(1 + A_d/A_r)^{-1}U_{gr}^{0.837} \quad (6.1)$$

In this study, the predicted $k_L a$ coefficient is calculated as the product of the calculated values from Chist's equation. Figure 79 shows that a relatively good agreement between the experimental and the predicted $k_L a$ coefficient is obtained (average difference about $\pm 20\%$). However, the differences happen at the values of k_L due to the human error and the technical for measuring are probably responsible for the difference value.

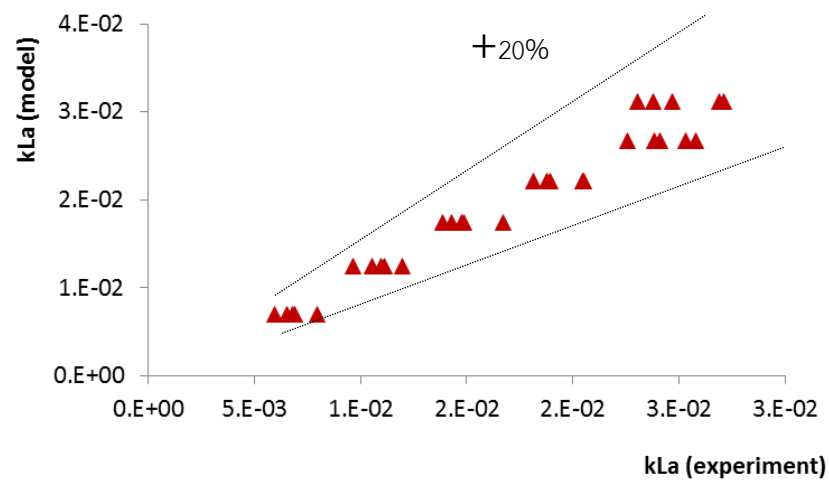


Figure 79 the variation of overall mass transfer coefficient obtained by experiment and model.

6.5.2 Application for benzene gas absorption.

The aim of this part was to study the application of the best condition obtained from the previously part for benzene gas absorption. The effects of surfactant, plastic media addition, and granular activated carbon (GAC) addition on the overall mass transfer coefficient for benzene absorption were investigated in the ILALR.

Benzene gas generator was applied in order to generate the benzene gas at room temperature. The air was injected into the 100 mL of pure benzene in the flask in order to generating benzene gas stream from their volatilization. Due to the low boiling point of benzene (80.1 °C), it proved that the benzene was evaporated. The benzene gas stream was added into the bottom of the BC. and ILALR.

The effect of absorbents and concentrations on hydrophobic VOCs absorption in ILALR

- Bubble diameter (D_B)

Figure 80 shows the variation of the generated bubble diameter with different gas velocity in tap water for different liquid phases (tap water and aqueous solutions with non-ionic surfactant).

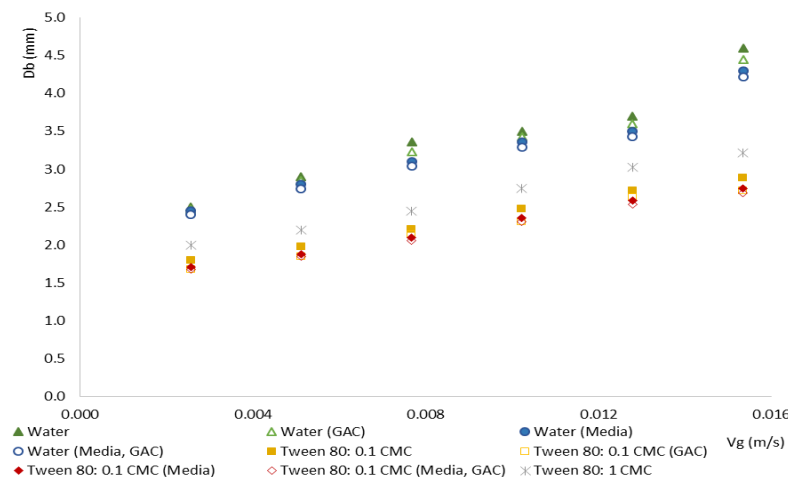


Figure 80 Bubble diameters versus gas velocity for different liquid phases (tap water and surfactant solutions).

According to Figure 80, the bubble diameter obtained from the experiment varies between 1.4 and 4.5 mm, while the superficial gas velocity can change between 2.6×10^{-3} to 2.0×10^{-2} m/s. It can be noted that, at low gas flow rates, the bubble diameters are roughly constant and start to slightly increase at high gas velocity. In this study, the following overall trend is found as follows:

$$D_{B \text{ 1.0 CMC non-ionic}} < D_{B \text{ 0.1 CMC non-ionic}} < D_{B \text{ water}}$$

As proposed by (Loubière & Hébrard, 2003), these results should be due to the differences observed in terms of dynamic surface tensions, and to their consequences on the balance between the surface tension and the buoyancy forces during the bubble growth and detachment. At high gas flow rates, the differences in terms of

bubble diameters are directly linked to static surface tension values. In fact, in this range of gas flow rates, the bubble diameter is no more controlled by the force balance at detachment, but rather by the power dissipated in the liquid, conditioning the bubble break up and coalescence phenomena.

Similar to the previous experiment, the local interfacial area (a) can be determined by using the experimental results of D_B and U_B values.

- **The local interfacial area (a)**

Figure 81 presents the relation between the interfacial area and the superficial gas velocity for different liquid phases applied in these experiments.

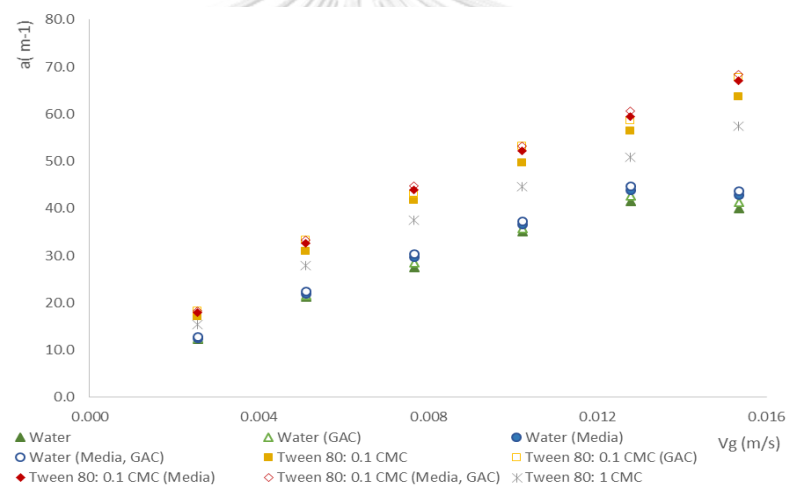


Figure 81 Interfacial area versus superficial gas velocity for different liquid phases.

According to Figure 6.10, regardless of the liquid phases, the interfacial area roughly increases linearly with the superficial gas velocity. Their values vary between 10.0 and 65.0 m^{-1} , whereas the superficial gas velocity change between 2.6×10^{-3} to 2.0×10^{-2} m/s .

Moreover, the highest and lowest of a values can be obtained with anionic 0.1, 1.0 CMC and tap water, respectively. It can be stated that the interfacial area is directly linked to the bubble diameter and thus the static surface tension of liquid phases under the test. Low values of σ_L are associated with high values of a (Sardegna et al.,

2006), (Painmanakul et al., 2005), and (Loubie`re & He´brard, 2004). In this study, the following overall trend is thus found as follows:

$$a_{0.1 \text{ CMC non-ionic}} > a_{1 \text{ CMC non-ionic}} > a_{\text{water}}$$

Furthermore, the difference among the values obtained from tap water and another absorbent can be observed at high gas flow rates. These results may possibly be related to the prevention of bubble coalescence phenomena provided by some contaminant molecules presence in the liquid phase (Deckwer, 1992).

- Overall mass transfer coefficient ($k_L a$) for benzene absorption in ILALR

Figure 82 presents the variation of absorbent with time obtained in the ILALR for benzene absorption with different condition (different liquid phases, media addition, and GAC addition).

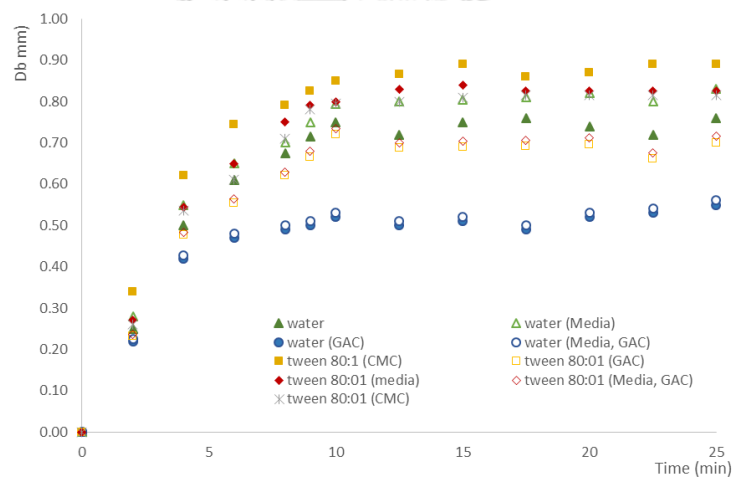


Figure 82 Absorbent versus time for benzene absorption.

Concerning to Figure 82, it can be found that, the benzene concentrations rapidly increased in first step, and then nearly to the constant values (saturated concentration, C_S) with increasing times. From the Figure, it can be stated that the values of saturated benzene concentration were related to types and concentration of liquid phases, and GAC addition.

$$C_{S \text{ Tween } 80:1 \text{ CMC}} > C_{S \text{ Tween } 80:0.1 \text{ CMC}} > C_{S \text{ Water}} > C_{S \text{ Tween } 80:0.1 \text{ CMC (GAC)}} > C_{S \text{ Water (GAC)}}$$

Note that, the effect of plastic media addition on the values of C_S was not observed. The experimental results shown that the addition of GAC.

Table 16 summary of $K_L a$ values for benzene absorption

Condition	$K_L a$ (s^{-1})
Surfactant (No media)	
▪ Water	5.36×10^{-3}
▪ Tween 80: 1 CMC	5.84×10^{-3}
▪ Tween 80: 0.1 CMC	5.54×10^{-3}
Surfactant (Media)	
▪ Water (Media)	6.07×10^{-3}
▪ Tween 80: 0.1 CMC (Media)	6.15×10^{-3}
Surfactant (GAC)	
▪ Water (GAC)	8.38×10^{-3}
▪ Tween 80: 0.1 CMC (GAC)	7.73×10^{-3}
Surfactant (Media, and GAC)	
▪ Water (Media, GAC)	9.15×10^{-3}
▪ Tween 80: 0.1 CMC (Media, GAC)	8.12×10^{-3}

Table 16 presents the values of overall mass transfer coefficient obtained in the ILALR for benzene absorption. From the Table, it can be concluded that:

- Concerning to the different types and concentrations of surfactant (2nd row), it can be shown that the $k_L a$ values depended on the concentration of surfactant: $k_L a$ (1 CMC) > $k_L a$ (0.1 CMC) > $k_L a$ (Water). However, for Tween 80, the $k_L a$ coefficient obtained with 1 CMC was not much higher than those obtained with 0.1 CMC.
- For surfactant with media (3rd row), the $k_L a$ coefficients obtained for both liquid phases with 10% of plastic loading were higher than those obtained with no media. The increase in the $k_L a$ value by adding the plastic media obtained with water (13% increased) was higher than those obtained with

0.1 CMC Tween 80 (11% increased) compared with no media. This was due to large number of bubble foam generated at the surface of the liquid phase (0.1 CMC Tween 80), led the PP particles out of the liquid phase. Therefore, the number of PP particles suspended in the liquid phase was decreased, and related to an increase in U_B values.

- For surfactant with GAC (4th row), the $k_L a$ coefficients obtained for both liquid phases with GAC were higher than those obtained with no media. The increase in the $k_L a$ value by adding GAC obtained with water (56% increased) was higher than those obtained with 0.1 CMC Tween 80 (40% increased) compared with no media. The surfactant reduced the absorption of GAC.
- For surfactant with 10% of PP media and GAC (5th row), the $k_L a$ coefficients obtained for both liquid phases with media and GAC were higher than those obtained with only media and with only GAC. The increase in the $k_L a$ value by adding 10% of plastic loading and GAC obtained with water (71% increased) was higher than those obtained with 0.1 CMC Tween 80 (47% increased) compared with no media.

- **Benzene removal efficiency**

In this section, the inlet and outlet benzene concentrations in the gas phase were sampling and collected at 5 to 5.5 minutes using air bag, and measured by using the GC-FID equipment. The benzene removal efficiency (%Eff) was calculated by using the equation of benzene removal efficiency (%Eff)

Table 16 presents the values of overall mass transfer coefficient obtained in the ILALR for benzene absorption. From the Table 16, it can be concluded that:

- For no GAC addition, for all cases, the addition of Tween 80 into the tap water provide the increased in benzene removal efficiency. By considering the Figure 82, the saturated benzene concentration obtained with Tween 80 was higher than those obtained with tap water. Therefore, at the same

period of time, the benzene gas can absorb in Tween 80 more than in tap water.

- The addition of 10% plastic media media increased the benzene removal efficiency at 5 to 5.5 min. This result was agreeable with the figure 82 and Table 16. According to the Figure 82, the benzene concentration in liquid phase was not reached the saturated benzene concentration. And from the Table 16, the $k_L a$ values obtained with media addition were higher than those obtain with no media. Therefore, the benzene gas can absorption obtained with media addition was higher than those obtained with no media.
- For GAC addition, for all cases, the benzene removal efficiency was higher than those obtained with no GAC addition which mechanism is showed in Figure 83

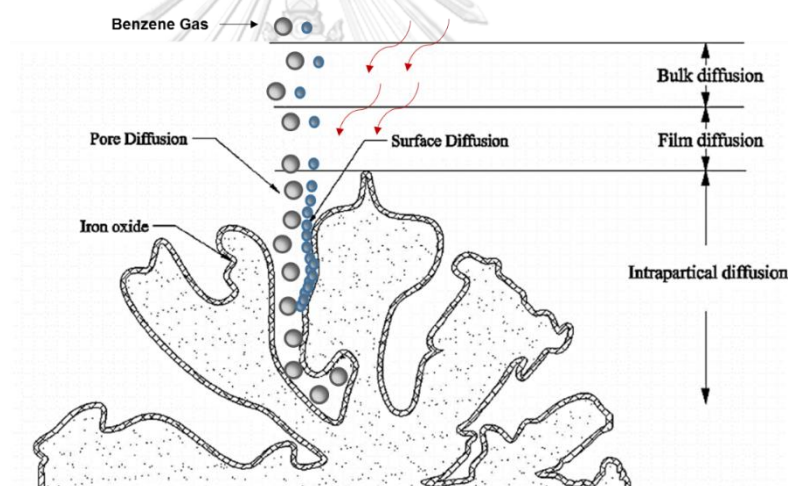


Figure 83 Mechanism for benzene absorption and adsorption.

- Moreover, the %Eff obtained with tap water was higher than those obtained with Tween 80 as showed in figure 84. This result can explained that Tween 80 blocked the benzene gas adsorption into the GAC which the effect of surfactant (non-ionic) on GAC adsorption is showed in figure 6.13.

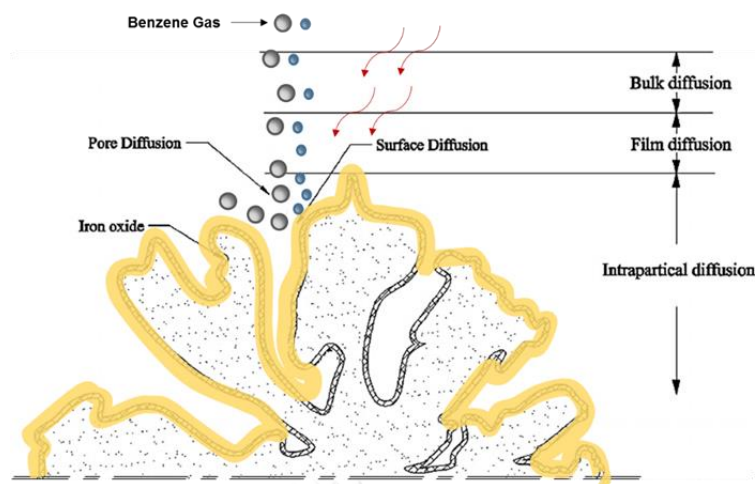


Figure 84 Effect of surfactant (non-ionic) on GAC adsorption.

- The highest value of the %Eff was observed with the addition of 10% of plastic loading media and GAC in tap water. The result show in Figure 85.

In conclusion, it can be expressed that the best condition for hydrophobic VOCs absorption in this work observed with the 10% plastic loading and GAC addition in water within the ILALR.

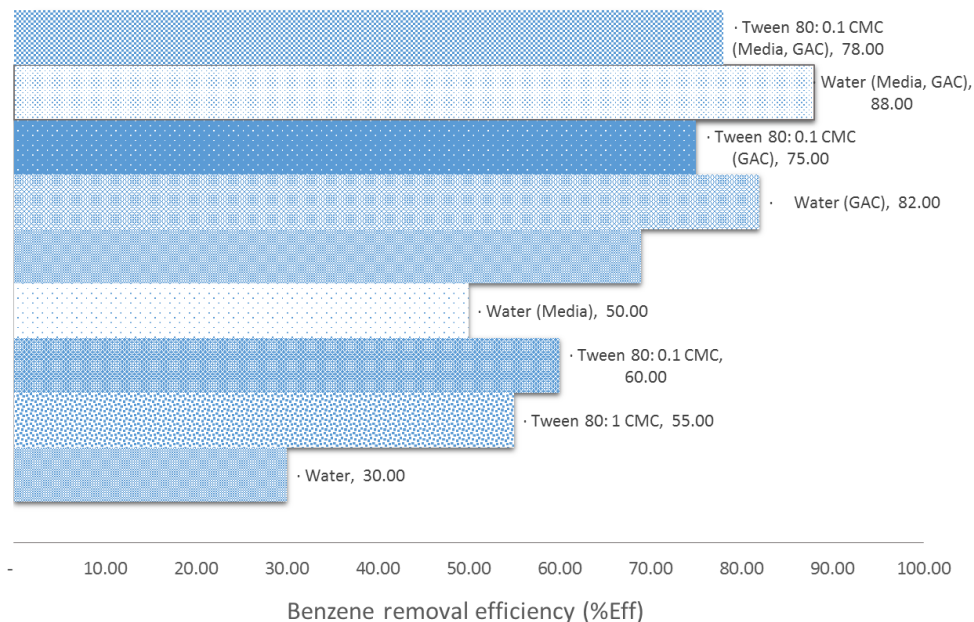


Figure 85 Summary of $k_L a$ benzene removal efficiency.

6.6 Conclusions

The best condition obtained from the oxygen absorption part (10% of PP media addition in ILALR) was applied for benzene absorption part. For the benzene absorption part, the $k_L a$ values and the benzene removal efficiency was analyzed. The operating conditions were as follows: liquid phase is tap water and Tween 80 (0.1 and 1 CMC), liquid height (H_L) = 86.5 cm (13 L), and gas flow rate of 10 L/min. The 100 mL of pure benzene was added in to the benzene gas generator in order to generating benzene gas stream from their volatilization. The 10% of PP was added into the ILALR. Moreover, the granular activated carbon (GAC) was added into the reactor in order to increase the benzene removal efficiency.

In this part, the following results have been obtained;

- The values of saturated benzene concentration were in ranged:

$$C_{S \text{ Tween } 80:1 \text{ CMC}} > C_{S \text{ Tween } 80:0.1 \text{ CMC}} > C_{S \text{ Water}} > C_{S \text{ Tween } 80:0.1 \text{ CMC (GAC)}} > C_{S \text{ Water (GAC)}}$$

- The addition of 10% PP media increased the $k_L a$ values of benzene absorption.
- For no GAC addition, the benzene removal efficiency obtained with Tween 80 was higher than those obtained with tap water.
- For GAC addition, the benzene removal efficiency obtained with tap water was higher than those obtained with Tween 80. This results can be explained that the Tween 80 hindrance the mass transfer of benzene from liquid phase into the GAC.

In conclusion, the best condition for benzene absorption in this work was observed with the 10% PP media and GAC addition into tap water in the ILALR.

The absorption system obtained in this work can be applied for VOCs gas removal and also for water treatment. The advantages of this system over other techniques are simple construction and low operation costs.

CHAPTER 7

CONCLUSIONS AND RECOMMENDATION

7.1 Conclusions

The main objective of this work can be separated in to three main topics. First, study the effect of gas diffuser, bubble column dimensions, operating condition, aqueous solutions with surfactant and type of plastic media on the bubble hydrodynamic and the VOCs mass transfer parameters. Second, find the suitable operation parameters for Batch and Continuous-flow bubble column with co-current system and the last topic, propose the theoretical prediction model for predicting bubble hydrodynamic and mass transfer parameter. To fulfill this purpose, the result have been summarized;

- The membrane with a single orifice, the results related to the physical properties and to the bubble generation have shown that: The hole diameter of rubber membrane in every thickness increase with gas flow rate, the pressure drops slightly increase with the thickness rubber membrane. For rigid diffuser pressure drop directly increase with decreasing of D_o .
- Influences of bubble column dimensions, gas diffuser types, and superficial gas velocities (V_s) on bubble column performance. The following results were obtained: The $k_L a$ coefficients increased with the superficial gas velocity (V_g)
- To enhance the k_L coefficient and absorption efficiency in bubble column, it was unnecessary to generate numerous fine bubbles at high superficial gas velocity for highest interfacial area as this a can be cancelled out by the great decrease of the k_L coefficients as well as the increase of power consumption.
- The effect of small plastic media particles in BC. the following results have been obtained; the operation without using plastic media report the overall mass transfer coefficient ($k_L a$) lower than using plastic media and high amount of plastic loading relate to produce the small size bubbles and increase the interfacial area value in the system.

- The effect of small plastic media particles in BC. the following results have been obtained; The increasing of $k_L a$ value relate with shape and suitable concentration of plastic media (10% plastic media loading) due to the physical properties of ring shape such as, structure and specific surface which obstruct the bubble movement and increasing mass transfer rate in the system. Moreover, air circulation rate (Q_{gr}) determination method suitable for explain the bubble hydrodynamic in the ILALR which k_L value from the experiment showed good agreement with the predicted k_L coefficient is obtained the average difference about $\pm 20\%$.
- The best condition for benzene absorption in this work was observed with the 10% plastic adding and GAC addition into tap water in the ILALR which benzene removal efficiency was showed 88%. Whereas the benzene removal efficiency obtained with tap water was higher than those obtained with Tween 80. This results can be explained that the Tween 80 hindrance the mass transfer of benzene from liquid phase into the GAC.

7.2 Overall suitable operation condition and prediction model

- The prediction model was proposed with the average difference between the experimental and predicted k_L of $\pm 35\%$:

$$k_L a = 0.5643 \times V^{0.7332}$$

- Table 17 the overall suitable operation condition obtained in this experiment.

Table 17 Table the overall suitable operation condition obtained in this experiment.

Topic	Suitable operation condition	Remark
Diffuser with single orifice	Type: D_{or} 0.3 mm rigid diffuser Gas flow rate: 15 ml/min	<ul style="list-style-type: none"> ● The D_B generated from the rigid diffuser depend on D_{or}, whereas the D_B generated from the fixable diffuser depend on the thickness of membrane and gas flow rate
Bubble column	Type: small rigid diffuser Gas flow rate: 10-15 l/min Media adding: 10% (V/V)	<ul style="list-style-type: none"> ● D_B in BC. increase with gas velocity. Moreover, the D_B were become lower by using plastic media and ring shape report the lowest D_B.
Internal loop airlift reactor	Type: small rigid diffuser Gas flow rate: 15 l/min Media adding: 10% (V/V)	<ul style="list-style-type: none"> ● D_B in ILALR increase with gas velocity. Moreover, the D_B were become lower by using plastic media and ring shape report the lowest D_B.
Internal loop airlift reactor with continuous system	Type: small rigid diffuser Gas flow rate: 10-15 l/min Liquid flow rate: 10 l/min Media adding: 10% (V/V)	<ul style="list-style-type: none"> ● The increasing of $k_L a$ vale correspond to liquid vilociry in the system.
VOC absorption	Type: small rigid diffuser Gas flow rate: 10-15 l/min Media adding: 10% (V/V) GAC adding: 195 g	<ul style="list-style-type: none"> ● Tween 80 hindrance the mass transfer of benzene from liquid phase into the GAC. ● GAC with tap water give the highest removal efficiency

7.3 Recommendations for future work

For future research, it is essential to study the effect of various types of Volatile Organic Compounds (VOCs) and also apply VOCs absorption with continuous system in order to provide a better understanding on bubble hydrodynamic phenomena and mass transfer mechanism for absorption process in a internal loop airlift reactor. Moreover, it is analyzed that the results observed in the bubble column, ILALR with batch and ILALR with continuous system have to be validated in industrial unit and higher superficial velocities. Finally, the theoretical models or correlations should be considered to compare the experimental results of bubble hydrodynamic and mass transfer parameters and predict the absorption efficiency obtained in the bubble column and ILALR.



NOTATION

a	interfacial area (m ⁻¹)	Re	Reynolds number
C_1	concentration in the dispersed phase [moles/m ³]	R	unknown concentration of gas at outlet [moles/m ³]
C_2	concentration in the continuous phase [moles/m ³]	R'	unknown concentration of liquid at outlet [moles/m ³]
C_{10}	Known concentration of gas at inlet of sparger [moles/m ³]	SB	bubble surface (m ²)
C_{20}	known concentration of liquid at inlet [moles/m ³]	Sc	Schmidt number
d	column diameter [m]	t_{Frame}	time of bubble spatial displacement (s)
d_c	bubble diameter [m]	u_l	velocity of liquid phase [m/s]
d_b	gas distributor hole diameter [m]	u	slip velocity [m/s]
D_B	bubble diameter (m)	u_g	actual gas velocity ($u_g/\epsilon g$) [m/s]
D_{OR}	orifice diameter (m)	u_{sl}	superficial liquid velocity, [m/s]
D	diffusivity of gas [m ² /s]	u_{sg}	superficial gas velocity, [m/s]
E	enhancement factor	U	ratio of liquid to slip velocity ($=u_l/u$) [-]
f_B	bubble formation frequency (1/s)	U_B	bubble rising velocity (m/s)
h_m	height of gas-liquid mixture in the column [m]	U_G	gas velocity through orifice (m/s)

k_L	liquid-side mass transfer coefficient (m/s)	V_B	bubble volume (m ³)
$k_L a$	volumetric mass transfer coefficient (1/s)	μ_L	liquid viscosity (Pa.s)
k	dimensionless mass transfer coefficient ($k = (K h_m) / \epsilon_L u$) [-]	ρ_L	liquid density (kg/m ³)
K_i	coefficient of mass transfer of the i th substance [m/s]	σ_L	liquid surface tension (N/m)
K_{bi}	coefficient of mass transfer of the i th substance from single bubble [m/s]	y_D	vapor concentration at the top of the column
m_{ei}	equilibrium coefficient of distribution of the substance between phases [-]	v_B	vapor concentration at the top of the column
m_e'	equilibrium distribution coefficient defined as m [m]	ϵ_g	vapor concentration at the top of the column
n	the amount of gas (moles)	ϵ_l	vapor concentration at the top of the column
N_B	generated bubble number	ρ_l	vapor concentration at the top of the column
P	Pressure (Pa)	ρ_g	vapor concentration at the top of the column
p_i	the partial <u>vapor pressure</u> of the component i	σ	vapor concentration at the top of the column
Q_g	gas flow rate (m ³ /s)	μ_l	vapor concentration at the top of the column
R	the gas constant 8.314 J.K ⁻¹ mol ⁻¹	η_{co}	vapor concentration at the top of the column
		η_{count}	vapor concentration at the top of the column

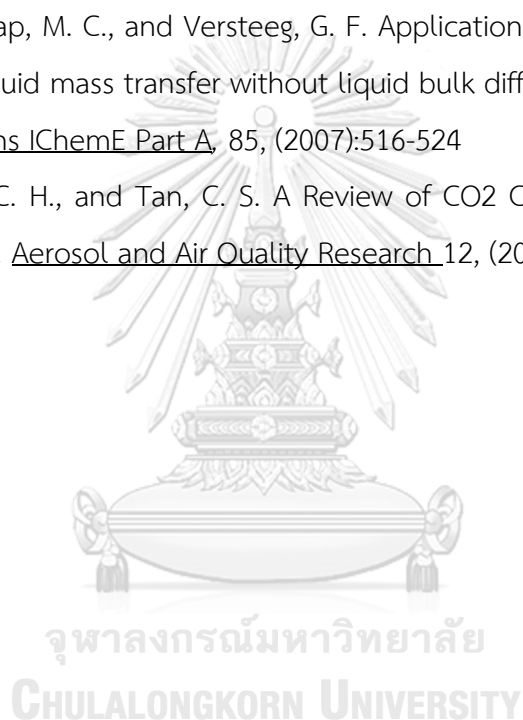
REFERENCE

- Bhaga, D. Hold up and pressure drop in vertical two and three phase Department of Chemical Engineering, (1970)
- Chen, P. C., and Piao, C. C. A Study on CO² Absorption in Bubble Column Using DEEA/EEA Mixed Solvent. International Journal of Engineering Practical Research (IJEPR), Volume 3, (2014)
- Cheng, L., Li, T., Keener, T. C., and Lee, J. Y. A mass transfer model of absorption of carbon dioxide in a bubble column reactor by using magnesium hydroxide slurry. International Journal of greenhouse gas control 17, (2013):240-243
- Chisti, Y., Kasper, M., and Moo-Young. Mass transfer in external-loop airlift bioreactors using static mixer the canadian journal of chemical engineering, 68, (1990)
- ckowiak, J. Model for the prediction of liquid phase mass transfer of random packed columns for gas-liquid systems. Chemical Engineering Research and Design 89, (2011):1308-1320
- Danckwert, P. V., and Kenndy, A. M. Kinetic of liquid-film process in gas absorption part I: Models of the absorption process. Trans IChemE, 75, (1997)
- DANCKWERTS, P. V. The absorption of gases in liquid. (1951)
- Diaz, D. G., Navaza, J. M., Riveiro, L. C. Q., and Sanjurjo, B. Gas absorption in bubble column using a non-Newtonian liquid phase. Chemical Engineering Journal, 146 (2009):16-21
- Farinesa, V., Baigb, S., Albeta, J., Moliniera, J., and Legaya, C. Ozone transfer from gas to water in a co-current upflow packed bed reactor containing silica gel Chemical Engineering Journal 911(2003): 67-73
- Gao, M., Hirata, M., Takanashi, H., and Hano, T. Ozone mass transfer in a new gas-liquid contactor-Karman contactor Separation and Purification Technology, 42, (2005):145-149

- Hossein N., and Gordon A. H. Volatile Organic Chemical Mass Transfer in an External Loop Airlift Bioreactor with a Packed Bed. Biochemical Engineering Journal, 27, 2(2005):138-145
- Kale, C., Górak, A., and Schoenmaker, H. Modelling of the reactive absorption of CO₂ using mono-ethanolamine. International Journal of Greenhouse Gas Control 217, (2013):294-308
- Kantarci, N., Borak, F., and Ulgen, K. O. Review Bubble column reactors. Process Biochemistry 40, (2005):2263-2283
- Kralik, M., and Ilavsky, J. Mathematical Dynamic Model of the Continuous Bubble Column Slurry Reactor. Chem. Eng. Process 28, (1990):127-132
- Levenspiel, O. Department of Chemical Engineering. Chemical Reaction Engineering, (1988).
- Lin, C. Y., Soriano, A. N., and Li, M. H. Kinetics study of carbon dioxide absorption into aqueous solutions containing N-methyldiethanolamine + diethanolamine Journal of the Taiwan Institute of Chemical Engineers 40, (2009):403 - 412,
- Liu, Y., Li, H., Wei, G., Zhang, H., Li, X., and Jia, Y. Mass transfer performance of CO₂ absorption by alkanolamine aqueous solution for biogas purification. Separation and Purification Technology, 113, (2014):476 - 483
- Maceiras, R., Alves, S. S., Cancel, M. A., and Alvarez, E. Effect of bubble contamination on gas-liquid mass transfer coefficient on CO₂ absorption in amine solutions. Chemical Engineering Journal, 137, (2008):422-427
- Mohd, A. A., Hashim, A., and Aroua, M. K. Kinetics of Carbon Dioxide absorption into aqueous MDEA + [bmim][BF₄] solutions from 303 to 333 K. Chemical Engineering Journal, 200-202, (2012):317-328
- Moraveji, M. K., Sajjadi, B., Jafarkhani, M., and Davarnejad, R. Experimental investigation and CFD simulation of turbulence effect on hydrodynamic and mass transfer in a packed bed airlift internal loop reactor. International Communications in Heat and Mass Transfer Volume 38, 4(2011):518-524

- Muroyama K., Imai, K., Oka, Y., and Hayashi, J. Mass transfer properties in a bubble column associated with micro-bubble dispersions. Separation and Purification Technology, 100, (2014):464-473
- Painmanakul, P., and Hebrard, G. Effect of different contaminants on the α - factor: Local experimental method and modeling. chemical engineering research and design 86, (2008):1207-1215
- Painmanakul, P., K. Loubiere, G. Hebrard, M. M. Peuchot, and M.Roustan. Shorter Communication Effect of surfactants on liquid-side mass transfer coefficients. Chemical Engineering Science 60, (2005):6480 - 6491
- Painmanakul, P., K. Loubiere, G. Hebrard, and P. Buffiere. Study of different membrane spargers used in waste water treatment: characterisation and performance. Chemical Engineering and Processing , 43, (2004):1347-1359
- Painmanakul, P., Laoraddecha, S., Chawaloeshonsiya, N., Prajaksoot, P., and Khaodhiar, S. Study of Hydrophobic VOCs Absorption Mechanism in a Bubble Column: Bubble Hydrodynamic Parameters and Mass Transfer Coefficients. Separation Science and Technology, 48:13, (2013):1963-1976
- Razi, N., Bolland, O., and Svendsen, H. Review of design correlations for CO₂ absorption into MEA using structured packings. International journal of greenhouse gas control 9, 193-219(2012)
- Sardeing, R., Painmanakul, P., and Hébrard, G. Effect of surfactants on liquid-side mass transfer coefficients in gas-liquid systems: A first step to modeling Chemical Engineering Science, 616249 - 6260, (2006)
- Shaikh, A., and Al-Dahhan, M. H. A Review on Flow Regime Transition in Bubble Columns. INTERNATIONAL JOURNAL OF CHEMICAL REACTOR ENGINEERING, 5, (2007)
- Singh, M. K., and Majumder, S. K. Co- and counter-current mass transfer in bubble column International Journal of Heat and Mass Transfer, 54, (2011): 2283-2293.
- Sumin, L. U., Youguang, M., Chunying, Z., and Shuhua, S. The enhancement of CO₂ chemical absorption by K₂CO₃ aqueous solution in the presence of activated carbon particles. Chin. J. Chem. Eng 15, (2007):842-846

- Todinca, T., Tanasie, C., Proll T., and Cata, A. Absorption with chemical reaction: evaluation of rate promoters effect on CO₂ absorption in hot potassium carbonate solutions. 17th European Symposium on Computer Aided Process Engineering - ESCAPE, Elsevier B.V., 17, (2007)
- Turney, D., and Banerjee, S. Near surface turbulence and its relationship to air-water gas transfer rates. Kyoto University Press, (2011):51
- USEPA. Control techniques for volatile organic compound emission stationary source United States environmental protection agency, (1992)
- Van Elk, E. P., Knaap, M. C., and Versteeg, G. F. Application of the penetration theory for gas - liquid mass transfer without liquid bulk differences with Systems with a Bulk. Trans IChemE Part A, 85, (2007):516-524
- Yu, C. H., Huang, C. H., and Tan, C. S. A Review of CO₂ Capture by Absorption and Adsorption. Aerosol and Air Quality Research 12, (2012):745-769



REFERENCES



จุฬาลงกรณ์มหาวิทยาลัย
CHULALONGKORN UNIVERSITY

APPENDIX



จุฬาลงกรณ์มหาวิทยาลัย
CHULALONGKORN UNIVERSITY

Appendix A

Small rigid diffuser

(Kla) Overall mass transfer coefficient

Qg (l/min)	No med	PP cir				PP gre				PP squ				PP rin			
		2%	5%	10%	15%	2%	5%	10%	15%	2%	5%	10%	15%	2%	5%	10%	15%
2.50	0.02	0.02	0.02	0.01	0.01	0.01	0.01	0.01	0.01	0.01	0.01	0.01	0.01	0.02	0.02	0.01	0.02
5.00	0.03	0.03	0.02	0.02	0.02	0.02	0.02	0.02	0.02	0.02	0.02	0.02	0.02	0.03	0.03	0.03	0.03
7.50	0.03	0.03	0.03	0.03	0.03	0.03	0.03	0.03	0.03	0.03	0.03	0.02	0.02	0.03	0.03	0.03	0.03
10.00	0.03	0.04	0.04	0.03	0.03	0.03	0.03	0.03	0.03	0.03	0.03	0.03	0.03	0.04	0.04	0.04	0.04
15.00	0.03	0.04	0.04	0.04	0.04	0.03	0.03	0.03	0.04	0.03	0.03	0.03	0.03	0.04	0.04	0.04	0.04

(a) Interfacial area

Qg (l/min)	No med	PP cir				PP gre				PP squ				PP rin			
		2%	5%	10%	15%	2%	5%	10%	15%	2%	5%	10%	15%	2%	5%	10%	15%
2.50	40	64	58	50	52	54	50	36	38	16	22	32	33	90	89	95	102
5.00	62	91	88	79	82	81	83	67	70	321	30	47	49	118	126	91	98
7.50	88	116	125	105	109	100	121	95	99	51	71	76	79	141	149	153	164
10.00	115	145	156	135	141	130	155	125	130	87	103	106	110	166	171	175	188
15.00	146	171	187	170	177	160	290	174	181	121	132	136	142	184	199	201	215

(Db) bubble diameter

Qg (l/min)	No med	PP cir				PP gre				PP squ				PP rin			
		2%	5%	10%	15%	2%	5%	10%	15%	2%	5%	10%	15%	2%	5%	10%	15%
2.50	2.60	2.55	2.45	2.40	2.35	2.70	2.55	2.35	2.30	2.70	2.48	2.45	2.40	2.40	2.30	2.10	2.06
5.00	2.80	2.57	2.57	2.55	2.50	2.60	2.62	2.50	2.45	2.75	2.70	2.55	2.50	2.56	2.55	3.25	3.19
7.50	3.20	2.90	2.81	2.85	2.79	3.10	2.90	2.80	2.74	3.20	2.92	2.85	2.79	2.85	2.70	2.65	2.60
10.00	3.50	3.20	3.10	3.24	3.18	3.40	3.11	3.27	3.20	3.45	3.25	3.25	3.19	3.10	3.10	2.90	2.84
15.00	3.60	3.37	3.37	3.30	3.23	3.50	3.30	3.05	2.99	3.50	3.40	3.30	3.23	3.30	3.20	3.10	3.04

(k_L) Liquid-side mass transfer coefficient

Q _g	PP cir				PP gre				PP squ				PP rin			
l/m in	2%	5%	10%	15%	2%	5%	10%	15%	2%	5%	10%	15%	2%	5%	10%	15%
2.5	2.41E-04	2.73E-04	2.70E-04	2.73E-04	2.22E-04	2.35E-04	2.58E-04	2.61E-04	6.08E-04	3.93E-04	1.84E-04	1.86E-04	1.66E-04	1.70E-04	1.57E-04	1.54E-04
5	2.82E-04	2.68E-04	2.98E-04	3.00E-04	2.72E-04	2.38E-04	2.89E-04	2.92E-04	6.27E-05	5.63E-04	3.43E-04	3.46E-04	2.17E-04	2.05E-04	2.81E-04	2.76E-04
7.5	2.90E-04	2.72E-04	2.85E-04	2.87E-04	3.02E-04	2.48E-04	2.73E-04	2.76E-04	5.49E-04	3.84E-04	2.94E-04	2.96E-04	2.30E-04	2.17E-04	2.09E-04	2.05E-04
10	2.55E-04	2.27E-04	2.44E-04	2.46E-04	2.55E-04	2.13E-04	2.32E-04	2.34E-04	3.54E-04	2.76E-04	2.40E-04	2.42E-04	2.19E-04	2.14E-04	2.03E-04	1.99E-04
15	2.24E-04	2.00E-04	2.20E-04	2.22E-04	2.18E-04	1.20E-04	1.92E-04	1.94E-04	2.71E-04	2.30E-04	2.20E-04	2.21E-04	2.16E-04	1.93E-04	1.91E-04	1.88E-04

Large rigid diffuser

(K_{la}) Overall mass transfer coefficient

Q _g	No med	PP cir				PP gre				PP squ				PP rin			
(l/min)		2%	5%	10%	15%	2%	5%	10%	15%	2%	5%	10%	15%	2%	5%	10%	15%
2.50	0.01	0.01	0.02	0.02	0.02	0.02	0.02	0.02	0.02	0.01	0.01	0.01	0.01	0.02	0.01	0.01	0.01
5.00	0.02	0.02	0.02	0.02	0.03	0.02	0.02	0.02	0.03	0.02	0.02	0.02	0.02	0.02	0.02	0.02	0.02
7.50	0.02	0.03	0.03	0.03	0.03	0.03	0.03	0.03	0.03	0.03	0.03	0.03	0.03	0.03	0.03	0.03	0.03
10.00	0.03	0.03	0.03	0.03	0.04	0.04	0.04	0.03	0.03	0.03	0.03	0.03	0.04	0.03	0.04	0.04	0.04
15.00	0.03	0.04	0.04	0.04	0.04	0.04	0.04	0.04	0.04	0.03	0.04	0.04	0.04	0.04	0.04	0.04	0.04

(a) Interfacial area

Q _g	No med	PP cir				PP gre				PP squ				PP rin			
(l/min)		2%	5%	10%	15%	2%	5%	10%	15%	2%	5%	10%	15%	2%	5%	10%	15%
2.50	22	41	58	60	63	17	40	47	49	21	27	29	30	53	81	76	82
5.00	35	52	66	83	87	44	65	70	73	42	48	44	46	82	103	97	104
7.50	60	82	92	105	109	73	83	87	91	67	26	73	76	108	122	131	141
10.00	87	115	129	148	154	93	96	133	138	98	60	91	95	137	154	163	175
15.00	97	120	145	166	173	118	44	149	155	103	105	108	112	157	178	194	208

(Db) bubble diameter

Q _g	No med	PP cir				PP gre				PP squ				PP rin			
(l/min)		2%	5%	10%	15%	2%	5%	10%	15%	2%	5%	10%	15%	2%	5%	10%	15%
2.50	3.90	3.56	3.00	2.80	2.74	3.70	3.33	2.90	2.84	3.60	3.42	2.70	2.65	3.50	2.90	2.85	2.79
5.00	4.10	3.82	3.30	3.00	2.94	3.72	3.35	3.10	3.04	3.60	3.55	3.15	3.09	3.70	3.10	3.05	2.99
7.50	4.23	3.77	3.50	3.13	3.07	3.75	3.63	3.40	3.33	3.82	3.71	3.50	3.43	3.73	3.30	3.08	3.02
10.00	4.30	3.90	3.62	3.33	3.26	3.80	3.80	3.50	3.43	3.94	3.82	3.70	3.63	3.76	3.45	3.11	3.05
15.00	4.40	4.00	3.75	3.40	3.33	4.00	4.00	3.57	3.50	4.16	4.12	3.90	3.82	3.85	3.58	3.20	3.14

(k_L) Liquid-side mass transfer coefficient

Qg (l/min)	PP cir				PP gre				PP squ				PP rin			
	2%	5%	10%	15%	2%	5%	10%	15%	2%	5%	10%	15%	2%	5%	10%	15%
2.5	3.05E-04	3.11E-04	3.01E-04	3.03E-04	9.46E-04	4.12E-04	3.55E-04	3.58E-04	6.23E-04	5.00E-04	4.66E-04	4.71E-04	3.18E-04	1.76E-04	1.86E-04	1.82E-04
5	3.84E-04	3.72E-04	2.93E-04	2.96E-04	5.59E-04	3.70E-04	3.41E-04	3.44E-04	5.47E-04	4.74E-04	5.12E-04	5.17E-04	2.84E-04	2.15E-04	2.28E-04	2.24E-04
7.5	3.46E-04	3.47E-04	3.04E-04	3.07E-04	4.09E-04	3.79E-04	3.61E-04	3.64E-04	3.70E-04	1.13E-03	3.96E-04	4.00E-04	2.93E-04	2.65E-04	2.45E-04	2.40E-04
10	2.95E-04	2.66E-04	2.31E-04	2.33E-04	3.94E-04	4.08E-04	2.50E-04	2.52E-04	3.24E-04	5.59E-04	3.68E-04	3.71E-04	2.48E-04	2.42E-04	2.29E-04	2.24E-04
15	3.10E-04	2.69E-04	2.34E-04	2.36E-04	3.38E-04	8.76E-04	2.59E-04	2.61E-04	3.22E-04	3.38E-04	3.28E-04	3.31E-04	2.41E-04	2.27E-04	2.07E-04	2.03E-04

Wood rigid diffuser

(K_{La}) Overall mass transfer coefficient

Qg (l/min)	No med	PP cir				PP gre				PP squ				PP rin			
		2%	5%	10%	15%	2%	5%	10%	15%	2%	5%	10%	15%	2%	5%	10%	15%
2.50	0.01	0.01	0.01	0.01	0.01	0.01	0.01	0.01	0.01	0.01	0.01	0.01	0.01	0.01	0.01	0.01	0.01
5.00	0.01	0.01	0.01	0.01	0.01	0.01	0.01	0.01	0.01	0.01	0.01	0.01	0.01	0.01	0.01	0.01	0.01
7.50	0.01	0.01	0.02	0.01	0.01	0.02	0.02	0.02	0.02	0.01	0.01	0.01	0.01	0.02	0.02	0.02	0.02
10.00	0.01	0.02	0.02	0.02	0.02	0.02	0.03	0.02	0.02	0.03	0.02	0.01	0.01	0.02	0.02	0.02	0.03
15.00	0.01	0.02	0.02	0.02	0.02	0.02	0.02	0.02	0.02	0.01	0.02	0.01	0.01	0.02	0.02	0.02	0.02

(a) Interfacial area

Qg (l/min)	No med	PP cir				PP gre				PP squ				PP rin			
		2%	5%	10%	15%	2%	5%	10%	15%	2%	5%	10%	15%	2%	5%	10%	15%
2.50	14	42	52	49	51	28	36	38	40	28	28	27	28	54	64	68	73
5.00	26	54	58	67	70	39	55	57	59	31	38	40	42	65	81	85	67
7.50	39	72	75	85	88	61	68	76	79	47	52	60	63	92	95	101	58
10.00	49	77	101	104	108	60	82	90	94	52	57	56	59	96	114	113	52
15.00	60	96	105	116	121	79	104	92	96	66	70	81	84	109	124	134	50

(Db) bubble diameter

Qg (l/min)	No med	PP cir				PP gre				PP squ				PP rin			
		2%	5%	10%	15%	2%	5%	10%	15%	2%	5%	10%	15%	2%	5%	10%	15%
2.50	3.95	3.50	3.34	3.43	3.36	3.87	3.53	3.53	3.46	3.93	3.59	3.62	3.55	3.70	3.34	3.20	3.14
5.00	4.30	3.90	3.76	3.70	3.63	4.20	3.90	3.70	3.63	4.26	3.86	3.78	3.70	4.10	3.73	3.50	3.43
7.50	4.70	4.40	4.30	3.87	3.79	4.50	4.43	3.90	3.82	4.60	4.49	3.88	3.80	4.35	4.23	4.00	3.92
10.00	5.20	4.57	4.60	4.48	4.39	5.10	4.71	4.83	4.73	5.10	5.00	4.71	4.62	4.70	4.63	4.50	4.41
15.00	6.00	5.00	5.17	4.75	4.66	5.50	4.80	5.50	5.39	5.80	5.70	4.82	4.72	5.20	5.14	4.65	4.56

(k_L) Liquid-side mass transfer coefficient

Qg (l/m in)	No med	PP cir				PP gre				PP squ				PP rin			
		2%	5%	10%	15%	2%	5%	10%	15%	2%	5%	10%	15%	2%	5%	10%	15%
2.5	3.5E-04	1.3E-04	2.1E-04	1.4E-04	1.3E-04	3.4E-04	2.6E-04	2.4E-04	2.3E-04	2.0E-04	2.3E-04	3.0E-04	3.0E-04	1.8E-04	1.1E-04	1.4E-04	1.3E-04
5	3.1E-04	1.7E-04	2.4E-04	1.7E-04	1.6E-04	3.5E-04	2.4E-04	2.1E-04	1.9E-04	3.8E-04	3.2E-04	2.1E-04	2.1E-04	1.9E-04	1.4E-04	1.6E-04	2.1E-04
7.5	2.5E-04	1.9E-04	2.3E-04	1.6E-04	1.5E-04	2.5E-04	2.5E-04	2.6E-04	2.4E-04	3.1E-04	2.8E-04	1.9E-04	1.9E-04	1.8E-04	1.9E-04	2.0E-04	3.5E-04
10	2.6E-04	2.6E-04	2.0E-04	2.1E-04	2.0E-04	3.8E-04	3.1E-04	2.6E-04	2.5E-04	5.4E-04	3.5E-04	2.5E-04	2.5E-04	2.3E-04	2.1E-04	2.2E-04	4.9E-04
15	1.8E-04	1.8E-04	1.8E-04	1.7E-04	1.6E-04	2.5E-04	1.8E-04	2.2E-04	2.1E-04	2.0E-04	2.2E-04	1.5E-04	1.5E-04	1.7E-04	1.7E-04	1.6E-04	4.4E-04

Internal Loop Airlift Reactor

Data result of Ring shape

Qg (l/min)	Conc. (%)	Qr (m ³ /s)	Qg (m ³ /s)	aT2(avg) (m ⁻¹)	ad(avg) (m ⁻¹)	ar(avg) (m ⁻¹)	EgT (-)	dBr (mm)	dBd (mm)	Ubr (m/s)	Ubd (m/s)
2.5	0	0.00E+00	4.17E-05	48.57	0.00	48.57	0.01	3.39	3.32	0.08	0.10
5	0	1.20E-06	8.33E-05	77.43	0.00	77.43	0.01	3.69	3.39	0.09	0.09
7.5	0	3.29E-06	1.25E-04	103.96	2.84	101.12	0.02	3.98	3.49	0.10	0.08
10	0	5.26E-06	1.67E-04	120.04	3.33	116.71	0.03	4.25	4.20	0.12	0.02
12.5	0	6.02E-06	2.08E-04	132.94	5.51	127.43	0.04	4.17	4.46	0.14	0.09
15	0	7.29E-06	2.50E-04	122.67	6.80	115.88	0.05	4.30	4.60	0.18	0.11
Qg (m ³ /s)	Conc. (%)	Qr (m ³ /s)	Qg (m ³ /s)	aT2(avg) (m ⁻¹)	ad(avg) (m ⁻¹)	ar(avg) (m ⁻¹)	EgT (-)	dBr (mm)	dBd (mm)	Ubr (m/s)	Ubd (m/s)
2.5	2	0.00E+00	4.17E-05	59.95	0.00	59.95	0.02	2.97	3.14	0.09	0.10
5	2	1.13E-06	8.33E-05	92.50	2.78	89.72	0.03	3.24	3.20	0.11	0.09
7.5	2	3.33E-06	1.25E-04	124.60	3.26	121.33	0.03	3.20	3.24	0.12	0.08
10	2	4.68E-06	1.67E-04	142.27	5.40	136.86	0.04	3.57	3.67	0.12	0.05
12.5	2	5.35E-06	2.08E-04	126.93	6.66	120.27	0.06	3.71	4.37	0.18	0.09
15	2	7.85E-06	2.50E-04	126.22	8.31	117.91	0.07	3.82	4.50	0.21	0.11
Qg (m ³ /s)	Conc. (%)	Qr (m ³ /s)	Qg (m ³ /s)	aT2(avg) (m ⁻¹)	ad(avg) (m ⁻¹)	ar(avg) (m ⁻¹)	EgT (-)	dBr (mm)	dBd (mm)	Ubr (m/s)	Ubd (m/s)
2.5	5	0.00E+00	4.17E-05	56.39	0.00	56.39	0.01	3.19	3.15	0.08	0.07
5	5	1.09E-06	8.33E-05	101.21	2.78	98.43	0.02	3.22	3.22	0.09	0.06
7.5	5	2.93E-06	1.25E-04	126.05	3.77	122.28	0.04	3.50	3.50	0.10	0.06
10	5	3.47E-06	1.67E-04	133.06	5.20	127.86	0.05	3.53	3.74	0.14	0.03
12.5	5	5.77E-06	2.08E-04	134.16	5.34	128.82	0.06	3.79	4.27	0.16	0.09
15	5	8.82E-06	2.50E-04	140.80	7.47	133.33	0.07	3.91	4.40	0.18	0.10

Qg	Conc.	Qr	Qg	aT2(avg)	ad(avg)	ar(avg)	EgT	dBr	dBd	Ubr	Ubd
(m3/s)	(%)	(m3/s)	(m3/s)	(m-1)	(m-1)	(m-1)	(-)	(mm)	(mm)	(m/s)	(m/s)
2.5	10	0.00E+00	4.17E-05	85.26	0.00	85.26	0.02	2.92	2.87	0.06	0.06
5	10	1.76E-06	8.33E-05	125.24	2.79	122.46	0.03	3.27	2.93	0.08	0.05
7.5	10	3.47E-06	1.25E-04	167.30	5.74	161.56	0.04	3.30	3.27	0.08	0.05
10	10	5.25E-06	1.67E-04	177.10	7.94	169.17	0.05	3.29	3.30	0.12	0.01
12.5	10	7.92E-06	2.08E-04	179.85	8.40	171.45	0.06	3.30	3.35	0.14	0.06
15	10	9.17E-06	2.50E-04	190.00	9.64	180.35	0.07	3.40	3.45	0.15	0.07
Qg	Conc.	Qr	Qg	aT2(avg)	ad(avg)	ar(avg)	EgT	dBr	dBd	Ubr	Ubd
(m3/s)	(%)	(m3/s)	(m3/s)	(m-1)	(m-1)	(m-1)	(-)	(mm)	(mm)	(m/s)	(m/s)
2.5	15	0.00E+00	4.17E-05	110.94	0.00	110.94	0.03	3.02	2.93	0.05	0.06
5	15	1.61E-06	8.33E-05	169.66	3.08	166.58	0.05	3.37	2.99	0.05	0.05
7.5	15	4.01E-06	1.25E-04	177.79	5.20	172.59	0.06	3.40	3.33	0.06	0.05
10	15	6.40E-06	1.67E-04	203.26	6.89	196.37	0.06	3.39	3.36	0.11	0.01
12.5	15	7.45E-06	2.08E-04	223.08	7.57	215.50	0.06	3.40	3.42	0.12	0.06
15	15	9.01E-06	2.50E-04	226.05	9.36	216.70	0.07	3.50	3.52	0.12	0.06



Data of Summary of $K_L a$ benzene removal efficiency.

Condition	Average peak area	Benzene removal efficiency (%Eff)
Benzene gas inlet	40419.97	-
Benzene gas outlet		
Surfactant (No media)		
• Water	28248.00	30
• Tween 80: 1 CMC	18249.80	55
• Tween 80: 0.1 CMC	16297.60	60
Surfactant (Media)		
• Water (Media)	20307.80	50
• Tween 80: 0.1 CMC (Media)	12422.90	69
Surfactant (GAC)		
• Water (GAC)	7263.30	82
• Tween 80: 0.1 CMC (GAC)	10175.36	75
Surfactant (Media, and GAC)		
• Water (Media, GAC)	4790.07	88
• Tween 80: 0.1 CMC (Media, GAC)	8954.40	78

VITA

Name: Prajak Sastaravet

Date of Birth: June 30, 1983

University Education:

Bachelor of Science Program in Environmental Chemistry, King Mongkut's Institute of Technology Ladkrabang.

Master of Engineering Program in Environmental Engineering, Chulalongkorn University.





จุฬาลงกรณ์มหาวิทยาลัย
CHULALONGKORN UNIVERSITY